TURUN
YLIOPISTO
UNIVERSITY
OF TURKU

# BASAL GANGLIA FUNCTION IN PARKINSONISM AND DYSTONIA

Emma Honkanen

TURUN YLIOPISTON JULKAISUJA – ANNALES UNIVERSITATIS TURKUENSIS
SARJA – SER. D OSA – TOM. 1611 | MEDICA – ODONTOLOGICA | TURKU 2022

TURUN
YLIOPISTO
UNIVERSITY
OF TURKU

# BASAL GANGLIA FUNCTION IN PARKINSONISM AND DYSTONIA

Emma Honkanen

TURUN YLIOPISTON JULKAISUJA – ANNALES UNIVERSITATIS TURKUENSIS
SARJA – SER. D OSA – TOM. 1611 | MEDICA – ODONTOLOGICA | TURKU 2022

## University of Turku

University of Turku, Faculty of Medicine
Clinical Neurosciences, Neurology
Doctoral programme in Clinical Research
Turku University Hospital, Neurocenter
Turku PET Centre

## Supervised by

Assistant Professor Juho Joutsa
Turku Brain and Mind Center
University of Turku and
Turku University Hospital
Turku, Finland

Professor Valtteri Kaasinen
Clinical Neurosciences
University of Turku and
Turku University Hospital
Turku, Finland

## Reviewed by

Associate Professor Harith Akram
UCL Queen Square Institute of Neurology
and The National Hospital for Neurology
and Neurosurgery
London, UK

Adjunct Professor Mikko Kuoppamäki
Chief Neurologist, Orion Corporation
Orion Pharma
University of Turku
Turku, Finland

## Opponent

Adjunct Professor Aki Hietaharju
Department of Neurology
University of Tampere and
Tampere University Hospital
Tampere, Finland

The originality of this thesis has been checked in accordance with the University of Turku quality assurance system using the Turnitin OriginalityCheck service.

ISBN 978-951-29-8777-1 (PRINT)
ISBN 978-951-29-8778-8 (PDF)
ISSN 0355-9483 (Print)
ISSN 2343-3213 (Online)
Painosalama, Turku, Finland 2022

*To Joonas*

UNIVERSITY OF TURKU
Faculty of Medicine, Clinical Neurosciences, Neurology
EMMA HONKANEN: Basal Ganglia Function in Parkinsonism and Dystonia
Doctoral Dissertation, 139 pp.
Doctoral Programme in Clinical Research
January 2022

## ABSTRACT

Parkinsonism and dystonia are movement disorders linked with abnormal function of the basal ganglia. The most common cause of parkinsonism, Parkinson's disease (PD), is caused by loss of dopaminergic neurons in the nigrostriatal tract, leading to dopamine depletion in the striatum. The pathophysiology in dystonia is largely unknown, although a major role of the basal ganglia has been suspected. Both syndromes can be treated with deep brain stimulation (DBS) in specific targets in the basal ganglia. The aim of this thesis was to study the function of the basal ganglia in parkinsonism and dystonia using single-photon emission computed tomography (SPECT) and positron emission tomography (PET).

The work in this thesis was broadly divided into two sets of experiments. The basal ganglia function of patients with PD, non-degenerative parkinsonism and healthy controls were evaluated using dopamine transporter (DAT) imaging. In the other experiment, basal ganglia function in dystonia was investigated in patients with cervical dystonia undergoing globus pallidus interna (GPi) DBS using 18F-fluoro-deoxyglucose-positron emission tomography (FDG-PET).

The results of this thesis showed that DAT binding does not predict the number of preserved neurons in the striatum in PD. Moreover, patients with a non-degenerative condition seemed to have higher DAT binding compared to healthy controls. Bupropion, even with a recommended wash-out time, caused clearly abnormal DAT binding in a patient without a neurodegenerative disorder affecting the dopamine system. In cervical dystonia, GPi-DBS increased glucose metabolism at the stimulation site and in other basal ganglia structures as well as in the primary sensorimotor cortex. Metabolic changes in the cortical regions, including the primary sensorimotor cortex and the supplementary motor area (SMA), correlated with acute and long-term therapeutic benefits, respectively. The symptoms returned gradually to the preoperative level after cessation of treatment.

The results of this thesis indicate that DAT imaging reflects dopamine function of the striatum rather than neuron count. Moreover, DAT binding is affected by several factors that should be controlled for in both clinical work and in research settings. The findings also suggest that dystonia involves brain regions outside the basal ganglia, which may play a critical role in motor symptoms of dystonia and contribute to slow neuroplastic changes associated with DBS.

KEYWORDS: parkinsonism, dystonia, basal ganglia, deep brain stimulation, brain imaging, SPECT, PET, dopamine transporter, brain glucose metabolism

TURUN YLIOPISTO
Lääketieteellinen tiedekunta, Kliiniset neurotieteet, Neurologia
EMMA HONKANEN: Tyvitumakkeiden toiminta parkinsonismissa ja dystoniassa
Väitöskirja, 139 s.
Turun kliininen tohtoriohjelma
Tammikuu 2022

## TIIVISTELMÄ

Parkinsonismi ja dystonia ovat neurologisia liikehäiriösairauksia, jotka yhdistetään tyvitumakkeiden eli aivojen liikehäiriökeskuksen toimintahäiriöihin. Yleisimmässä parkinsonismissa, Parkinsonin taudissa, aivojen striatumin ja mustatumakkeen dopamiinisolut tuhoutuvat. Dystonian etiologia on sen sijaan edelleen epäselvä, mutta sen on epäilty johtuvan tyvitumakkeiden poikkeavasta toiminnasta. Molempien sairauksien vaikeita muotoja voidaan hoitaa tyvitumakealueelle kohdennettavalla syväaivostimulaattorilla. Tässä tutkimuksessa tyvitumakkeiden toimintaa tutkittiin isotooppikuvantamisella parkinsonismissa ja dystoniassa.

Väitöskirjassa tutkittiin Parkinsonin tautia sairastavia henkilöitä, oireisia ja dopamiinitoiminnaltaan terveitä henkilöitä sekä terveitä ja oireettomia henkilöitä dopamiinitransportterikuvantamisella. Lisäksi syväaivostimulaatiohoitoa saavia dystoniapotilaita tutkittiin aivojen sokeriaineenvaihduntaa kuvaavalla PET-tutkimuksella.

Tulokset osoittivat, että aivojen dopamiinitransportterisitoutuminen ei ennusta säilyneiden hermosolujen määrää. Sitoutumisarvot saattavat myös olla korkeampia dopamiinitoiminnallaan terveillä, mutta oireisilla potilailla kuin terveillä ja oireettomilla henkilöillä. Lisäksi bupropion saattaa aiheuttaa virheellisiä tuloksia dopamiinikuvantamiseen. Syväaivostimulaattori lisää dystoniapotilalla aivojen sokeriaineenvaihduntaa stimulaatiokohdassa ja lisäksi viereisissä rakenteissa tyvitumakealueella sekä aivokuorella tunto- ja liikeaivokuorella. Oirekuvan nopea korjaantuminen korreloi aineenvaihdunnan lisääntymiseen tunto- ja liikeaivokuorella ja pitkäaikainen hoitovaste lisääntymiseen suplementaarisella motorisella aivokuorella. Oirekuvan hitaampaa palautumista kahden vuorokauden hoitotauon aikana ennusti nuori ikä.

Tulokset osoittavat, että tyvitumakkeiden dopamiinikuvantamisessa tulosten tulkinta kliinisessä työssä ja tutkimuksessa ei ole johtopäätösten kannalta yksiselitteistä ja tulee tehdä mahdolliset virhelähteet huomioiden. Dystoniassa myös tyvitumakkeen ulkopuoliset aivoalueet saattavat olla tärkeitä oirekuvan synnyssä sekä hoitovasteen kehittymisessä syväaivostimulaatiohoidossa.

AVAINSANAT: parkinsonismi, dystonia, tyvitumakkeet, syväaivostimulaatio, aivokuvantaminen, SPECT, PET, dopamiinitransportteri, sokeriaineenvaihdunta

# Table of Contents

# Abbreviations

| | |
|---|---|
| ALS | amyotrophic lateral sclerosis |
| AMPA | α-amino-3-hyroxy-5-methyl-4-isoxazolepropionic acid |
| BAI | Beck Anxiety Inventory |
| BDI | Beck Depression Inventory |
| BIS-11 | Barratt Impulsiveness Scale |
| BFMDRS | Burke-Fahn-Marsden Dystonia Rating Scale |
| CBD | corticobasal degeneration |
| CD | cervical dystonia |
| CNS | central nervous system |
| CT | computed tomography |
| D1 receptor | dopamine receptor subtype 1 |
| D2 receptor | dopamine receptor subtype 2 |
| DAT | dopamine transporter |
| DBS | deep brain stimulation |
| DIP | drug-induced parkinsonism |
| DLB | dementia with Lewy bodies |
| ET | essential tremor |
| FDG | 18F-fluoro-deoxyglucose |
| FTD | frontotemporal dementia |
| GABA | gamma-aminobutyric acid |
| GBA | glucocerebrosidase |
| GP | globus pallidus |
| GPe | globus pallidus externa |
| GPi | globus pallidus interna |
| 123I-FP-CIT | N-ω-fluoropropyl-2β-carbomethoxy-3β-(4 iodophenyl)nortropane |
| M1 | primary motor cortex |
| MDS | Movement Disorders Society |
| MMSE | Mini-Mental State Examination |
| MPTP | 1-methyl-4-phenyl-1,2,3,6-tetrahydropyridine |
| MRI | magnetic resonance imaging |
| MSA | multiple system atrophy |

| | |
|---|---|
| NMDA | N-methyl-D-aspartate |
| NMS | non-motor symptom |
| NMSS | Non-Motor Symptoms Scale |
| PD | Parkinson's disease |
| PET | positron emission tomography |
| PIGD | postural instability gait difficulty |
| PSP | progressive supranuclear palsy |
| RBD | REM sleep behaviour disorder |
| rCBF | regional cerebral blood flow |
| REM | rapid eye movement |
| SBR | specific binding ratio |
| SMA | supplementary motor area |
| SN | substantia nigra |
| SNc | substantia nigra pars compacta |
| SNr | substantia nigra pars reticulata |
| SNRI | serotonin-norepinephrine reuptake inhibitor |
| SPECT | single-photon emission tomography |
| SPM | Statistical Parametric Mapping software |
| SSRI | selective serotonin reuptake inhibitor |
| STN | subthalamic nucleus |
| TMS | transcranial magnetic stimulation |
| TWSTRS | Toronto Western Spasmodic Torticollis Rating Scale |
| UPDRS | Unified Parkinson's Disease Rating Scale |
| VIM | ventral intermediate nucleus of thalamus |
| VMAT | vesicular monoamine transporter |
| VP | vascular parkinsonism |

# List of Original Publications

This dissertation is based on the following original publications, which are referred to in the text by their Roman numerals:

I Honkanen EA, Saari L, Orte K, Gardberg M, Noponen T, Joutsa J, Kaasinen V. No link between striatal dopaminergic axons and dopamine transporter imaging in Parkinson's disease. *Mov Disord*, 2019; 34(10): 1562–1566.

II Honkanen EA, Kemppainen N, Noponen T, Seppänen M, Joutsa J, Kaasinen V. Bupropion causes misdiagnosis in brain dopamine transporter imaging for parkinsonism. *Clin Neuropharmacol*, 2019; 42(5): 181–183.

III Honkanen EA, Eklund M, Nuuttila S, Jaakkola E, Mäkinen E, Hirvilammi R, Noponen T, Seppänen M, Lindholm K, Scheperjans F, Parkkola R, Joutsa J, Varrone A, Kaasinen V. Dopamine transporter binding in symptomatic controls and healthy volunteers: Considerations for neuroimaging trials. *Neuroimage Clin*. 2021; 30;32:102807.

IV Honkanen EA, Korpela J, Pekkonen E, Kaasinen V, Reich MM, Joutsa J. Reappearance of symptoms after GPi-DBS discontinuation in cervical dystonia. *Mov Disord Clin Pract*, 2021; 26;8(3): 406–411.

V Honkanen EA, Korpela J, Pekkonen E, Aaltonen J, Koivu M, Eskola O, Eldebakey H, Kaasinen V, Reich MM, Joutsa J. GPi-DBS induced brain metabolic activation in cervical dystonia. *[manuscript]*

The original publications have been reproduced with the permission of the copyright holders.

# 1 Introduction

Parkinsonism and dystonia are common movement disorder syndromes. Parkinsonism refers to clinical presentation of motor symptoms such as bradykinesia, rigidity, and resting tremor, although other motor and non-motor symptoms may also be present. The most common cause of parkinsonism is Parkinson's disease (PD), a typically sporadic neurodegenerative disorder (Balestrino & Schapira, 2020). However, parkinsonism can also be caused by other neurodegenerative (atypical parkinsonism) or secondary (e.g., drug-induced, vascular) reasons. Dystonia is characterized by repetitive, twisting movements or abnormal postures caused by excessive muscle contractions. Etiology of dystonia can be acquired, inherited or idiopathic. Dystonic symptoms can appear in one or several muscular regions leading to a broad variety of clinical features (Albanese et al., 2013). Cervical dystonia (CD), affecting muscles in the neck and upper shoulder regions, is the most common adult-onset, idiopathic dystonia.

Dopaminergic degeneration in the nigrostriatal tract together with Lewy body pathology have been established to be the key neuropathological features of PD (Dickson, 2018). These processes are known to lead to basal ganglia dysfunction causing the cardinal symptoms. Basal ganglia dysfunction in dystonia was originally considered to play a major role in the pathogenesis of symptoms, although the symptoms are currently known to emerge from the wider brain network (Lehéricy et al., 2013). However, the neuropathological features of dystonia remain unknown. Considering the good therapeutic responses of deep brain stimulation (DBS) targeted to basal ganglia nuclei in both PD and dystonia (Mansouri et al., 2018; Moro et al., 2017), these nuclei seem also relevant in the treatment of these disorders.

Molecular imaging, including positron emission tomography (PET) and single-photon emission computed tomography (SPECT), has improved the understanding of the basic molecular mechanisms and pathophysiological processes underlying movement disorders. Brain dopamine transporter (DAT) imaging is an established diagnostic tool in the differential diagnostics in parkinsonism (T. S. Benamer et al., 2000), while there is no corresponding imaging technique to assist the clinical diagnosis in dystonia. The deficit seen in DAT imaging is usually related to

neurodegenerative parkinsonism, but it still remains unclear what the tracer binding deficiency truly reflects at the neural level (Palermo & Ceravolo, 2019).

This thesis focuses on the basal ganglia functions investigated with DAT imaging in parkinsonism, and the basal ganglia stimulation-induced changes in brain glucose metabolism and in the clinical features in cervical dystonia.

# 2 Review of the Literature

## 2.1 Clinical aspects of parkinsonism and dystonia

### 2.1.1 Parkinsonism

#### 2.1.1.1 Parkinson's disease

Parkinson's disease (PD) is the most frequent neurodegenerative movement disorder. The single most important clinical risk factor for PD is age (Jankovic & Tan, 2020), and the prevalence in industrialized countries is 0.3% in the general population, which increases to 3% in those aged 80 years or older (Lee & Gilbert, 2016). Prevalence and incidence are estimated to range between 6 and 12500 cases per 100 000 and between 5 and 346 per 100 000 person-years respectively in Europe (von Campenhausen et al., 2005). The clinical and environmental risk factors for PD include age, male gender, a family history of PD, rural living, exposure to pesticides and use of β2-adrenoreceptor antagonists (Balestrino & Schapira, 2020). Moreover, several monogenic forms of PD have been described and over 100 genetic loci have been identified as risk factors for PD (Jankovic & Tan, 2020). The single most important genetic risk factor of PD is mutations in the glucocerebrosidase (GBA) gene that increases the risk of PD more than five times (Jankovic & Tan, 2020).

The most typical symptoms of PD, referred to as cardinal motor symptoms, are bradykinesia, resting tremor and rigidity (Kalia & Lang, 2015). The presence of these cardinal symptoms, together with supportive features such as unilateral motor symptom onset, a progressive nature of the symptoms or beneficial response to dopaminergic medication, increases the probability of PD diagnosis. Postural instability, which is considered as a fourth cardinal feature, occurs generally later in the course of the disease (Kalia & Lang, 2015). Other motor symptoms that may also be present include gait disturbances, hypomimia, disturbances of speech and alteration in eye movements. PD is also associated with important non-motor symptoms (NMSs), such as autonomic, gastrointestinal, sleep, cognitive and neuropsychiatric disturbances, that have a major impact on patients' quality of life

(Schapira et al., 2017). Some of these NMSs, such as hyposmia, rapid eye movement (REM) sleep behaviour disorder (RBD) and constipation, are symptoms that may also anticipate the development of PD even years prior to motor symptoms and are called prodromal symptoms (Berg et al., 2015; Heinzel et al., 2019).

Diagnosis of PD is based on typical symptoms and signs in a clinical examination (Postuma et al., 2015), although the absolute confirmation for PD diagnosis is only acquired by a neuropathological examination at autopsy (Rizzo et al., 2016). Presynaptic dopaminergic imaging such as dopamine transporter (DAT) imaging can improve the accuracy of diagnosis; on the contrary, a normal finding in DAT imaging is considered as an absolute exclusion criterion for PD (Postuma et al., 2015). According to the Movement Disorders Society's (MDS's) PD criteria, a patient should have parkinsonism without any absolute exclusion criteria and an equal number of red flags (maximum 2) or fewer than the number of supportive criteria (Table 1).

**Table 1.** Diagnostic criteria for PD by the MDS. The table was modified from the table by Postuma et al., 2015.

| |
|---|
| Clinically Established PD |
| • essential criterion<br>• absence of absolute exclusion criteria<br>• at least two supportive criteria<br>• no red flags |
| Clinically Probable PD |
| • essential criterion<br>• absence of absolute exclusion criteria<br>• presence of red flags counterbalanced by supportive criterion<br>• maximum 2 red flags |
| Essential Criterion: Parkinsonism |
| • bradykinesia<br>• at least 1 of resting tremor or rigidity |
| Supportive criteria |
| • beneficial response to dopaminergic therapy<br>• presence of levodopa-induced dyskinesia<br>• rest tremor of a limb<br>• olfactory loss or cardiac sympathetic denervation (on MIBG) |
| Absolute exclusion criteria |
| • unequivocal cerebellar abnormalities<br>• downward vertical supranuclear gaze palsy or selective slowing of downward vertical saccades<br>• diagnosis of probable behavioral variant frontotemporal dementia or primary progressive aphasia within the 5 years of disease<br>• parkinsonian features restricted to the lower limbs for more than 3 years |

- treatment with a dopamine receptor blocker or a dopamine-depleting agent in a dose and time-course consistent with drug-induced parkinsonism
- absence of observable response to high-dose levodopa at least moderate severity of disease
- unequivocal cortical sensory loss, clear limb ideomotor apraxia or progressive aphasia
- normal functional neuroimaging of the presynaptic dopaminergic system
- alternative condition known to produce parkinsonism or the expert evaluating physician feel that an alternative syndrome is more likely than PD

Red flags

- rapid progression of gait impairment within 5 years of onset
- a complete absence of progression of motor symptoms over 5 or more years (unless related to treatment)
- early bulbar dysfunction (severe dysphonia, dysarthria or dysphagia) within the first 5 years
- inspiratory respiratory dysfunction
- severe autonomic failure in the first 5 years of disease (severe orthostatic hypotension or severe urinary retention/incontinence)
- recurrent falls because of impaired balance within 3 years of onset
- disproportionate anterocollis (dystonic) or contractures of hand or feet within the first 10 years
- absence of any of the common nonmotor features of disease despite 5 years disease duration
- otherwise-unexplained pyramidal track signs, defined as pyramidal weakness or clear pathologic hyperreflexia
- bilateral symmetric parkinsonism

PD is very heterogeneous at presentation and over the disease course, which is why several different categorizations of PD subtypes have been proposed. PD has recently been categorized in both motor and nonmotor subtypes (De Pablo-Fernández et al., 2019; Fereshtehnejad et al., 2017). This approach considers that the mild motor predominant subtype starts at a younger age and has milder motor and nonmotor symptoms, slower progression, and a good response to medication. The diffuse malignant subtype has, instead, more severe baseline symptoms, including motor symptoms, RBD, mild cognitive impairment and orthostatic hypotension, and it progresses rapidly and responds poorly to levodopa. There are also more prominent dopaminergic defects on DAT imaging in the diffuse malignant subtype. The intermediate subtype has intermediate symptoms and a moderate response to medications, and a prognosis is between previous subtypes (De Pablo-Fernández et al., 2019; Fereshtehnejad et al., 2017). Another option for subtyping PD is by motor phenotypes, that is, to tremor-dominant, postural instability gait difficulty (PIGD) or akinetic-rigid phenotypes (Fereshtehnejad et al., 2017). Substantial heterogeneity exists in prognosis as well as in the clinical presentation and disease course. However, a meta-analysis of postmortem studies revealed that mean survival after diagnosis ranged between 6.9 and 14.3 years (Macleod et al., 2014).

To date, treatment of PD is still symptomatic because no therapy has been shown to prevent or delay the disease progression. Treatment options to alleviate the symptoms include pharmacological agents, physical interventions and invasive therapies such as deep brain stimulation (DBS), stereotactic lesioning, levodopa-carbidopa enteral suspension and subcutaneous apomorphine infusion. (Fox et al., 2018)

#### 2.1.1.2 Other parkinsonism

Other neurodegenerative parkinsonisms than PD include the atypical parkinsonism syndromes: multiple system atrophy (MSA), progressive supranuclear palsy (PSP), dementia with Lewy bodies (DLB) and corticobasal degeneration (CBD). Non-degenerative causes for parkinsonism include, for instance, drug-induced parkinsonism (DIP) and vascular parkinsonism (VP).

Atypical parkinsonian disorders are conditions of a mix of pathologies: PSP and CBD are tauopathies, and MSA and DLB are synucleinopathies (Dickson, 2012). They have overlapping symptoms with PD and each other. Expert consensus has suggested diagnostic criteria to guide to clinicians (Armstrong et al., 2013; Gilman et al., 2008; Höglinger et al., 2017; McKeith et al., 2017), but the diagnostic accuracy is still insufficient (Joutsa et al., 2014; Rizzo et al., 2016). This is why the final diagnosis can only be confirmed at the autopsy. In addition to parkinsonism, atypical parkinsonisms have characteristic symptoms such as autonomic dysfunction and a cerebellar syndrome in MSA-C (Gilman et al., 2008), ocular motor dysfunction, progressive gait freezing and postural instability in PSP (Höglinger et al., 2017), visual hallucinations, fluctuating cognition and RBD in DLB (McKeith et al., 2017) and asymmetric limb akinesia/dystonia/myoclonus/apraxia together with frontal behavioral-spatial, agrammatic or PSP-like symptoms in CBD (Armstrong et al., 2013). These disorders are usually characterized by a more rapid progression and poorer prognosis than PD (Stoker & Greenland, 2018).

Vascular parkinsonism (VP) is caused by a cerebrovascular disease. Typical risk factors are age, in addition to the well-known vascular risk factors such as high blood pressure, high blood cholesterol, diabetes mellitus, smoking and a family history of vascular incidents. VP has also been referred to as lower-body parkinsonism due to a typical involvement of the lower limbs, proceeding to gait disorder, shorts steps, postural instability and falls. The resting tremor and visual hallucinations are usually rare in VP compared to PD (Glass et al., 2012). A response to levodopa is usually poor or absent (Benítez-Rivero et al., 2013). However, because of the disorders' similarities, clinical differentiation of VP from PD is usually challenging and is completed by structural brain imaging (computed tomography (CT) or magnetic resonance imaging (MRI)), which typically shows

cerebrovascular lesions such as white matter changes and lacunar infarcts in the basal ganglia in VP.

Drugs such as neuroleptic or dopamine receptor blocking agents, may induce parkinsonism. The prevalence of drug-induced parkinsonism (DIP) has been estimated to vary from 10 to 33 cases per 100 000 (Wisidagama et al., 2021). Older age, female gender and exposure to first generation antipsychotics or a high dosage of antipsychotics are the main risk factors for DIP (Wisidagama et al., 2021). The time interval between the development of parkinsonian symptoms and intaking the drugs may vary greatly, and the amelioration of the symptoms after the discontinuation of the drug may also require several months. Distinguishing DIP from PD is challenging, but the typical clinical characteristics of DIP are more bilateral involvement compared to PD, upper limbs are affected more often than lower limbs and usually only mild gait disturbances and no freezing of gait are presented (Hassin-Baer et al., 2001).

## 2.1.2 Dystonia

### 2.1.2.1 Cervical dystonia

Cervical dystonia (CD) is among the most common forms of dystonia. It is classified as a focal dystonia and is almost always an adult-onset and idiopathic condition. Prevalence estimates of dystonia have varied between 5 and 40 persons per 100 000 (Group, 2000; Ortiz et al., 2018; Steeves et al., 2012). Dystonia is more common in women, and the prevalence increases with age (LaHue et al., 2020; Soland et al., 1996).

CD affects the muscles in the cervical region, causing abnormal and patterned head and neck movements or postures or both. Symptoms can present spontaneously or be triggered by motor tasks (Defazio et al., 2019). There are no established diagnostic criteria, and the diagnosis is based on the clinical evaluation. There also are no reliable diagnostic biomarkers, and laboratory tests or brain imaging are used mainly to identify the etiology of dystonia in selected cases. Clinical features supporting the diagnosis of dystonia include, for example, the geste antagoniste (Defazio et al., 2019). This highly specific maneuver, also called a sensory trick, alleviates the dystonic symptoms transiently by touching the affected body region (Ramos et al., 2014). On the contrary, fixed involuntary head posture, weakness of neck muscles antagonizing the abnormal posture, and an ability to mentally suppress the symptoms or diplopia induced by voluntary correction of the abnormal posture, are features usually not presented in CD and suggest alternative diagnoses (Defazio et al., 2019).

Non-motor symptoms (NMSs), in addition to motor symptoms, for example, pain, sleep problems, anxiety, and depression, have also been described in CD patients (Kuyper et al., 2011). Although it seems that these NMSs may be an independent part of cervical dystonia (Conte et al., 2019), but this hypothesis remains unconfirmed. Regardless of whether the NMSs are independent dystonia symptoms or comorbidities, these symptoms are associated with reduced quality of life (Han et al., 2020). CD is not associated with reduced life expectancy, yet it reduces working ability, and CD patients with anxiety or depression were more likely to retire earlier than patients without these NMSs (Ortiz et al., 2019).

Botulinum toxin is an efficient and safe first-line treatment for cervical dystonia Several drugs, such as benzodiazepines and muscle relaxants, are used in the treatment of CD, but there are no well-designed and reported trials to assess their benefit (Jankovic, 2006). In botulinum toxin-refractory and medication-refractory CD, DBS has been proved highly efficacious in improving motor symptoms, disability, and pain in CD patients (Tsuboi et al., 2020).

#### 2.1.2.2 Other dystonia

Different forms of dystonia can be manifested by a broad variety of presentations depending on dystonia's clinical characteristics and etiology (Albanese et al., 2013). The prevalence of dystonia is estimated altogether to be 15–30 cases per 100 000 (Group, 2000; Steeves et al., 2012), although this is probably underestimated, because the prevalence of isolated dystonia was 732 per 100 000 when a random sample of the population over 50 years was studied (Müller et al., 2002). Women are affected more often than men, and a positive family history is reported in about 20% cases, although the confirmed genetic causes are still considered rare, especially among the focal dystonias (Albanese et al., 2019).

Dystonia symptoms are defined as repetitive, abnormal movements, postures or both. They are caused by sustained or intermittent muscle contractions due to overflow muscle activation. Movements are usually patterned and twisting, and tremor may be present. Voluntary action often initiates or worsens the dystonic symptoms (Albanese et al., 2013). Similar to CD, dystonia diagnosis is based on clinical observations, but laboratory tests, including gene tests and imaging, may provide diagnostic support (Albanese et al., 2019). Dystonia can occur at any age, affect one or several body regions, have different temporal patterns and occur with or without associated features. The etiology of dystonia can be inherited, acquired or idiopathic. Table 2 presents the classification of dystonia based on clinical characteristics and etiology.

**Table 2.** Proposed classification of dystonia by Albanese et al 2013. The table was modified from the table of the original article.

| Clinical characteristics | |
|---|---|
| Clinical characteristics of dystonia | |
| | • Age at onset: infancy (birth to 2 years), childhood (3–12 years), adolescence (13-20 years), early adulthood (21–40 years), late adulthood (>40 years) |
| | • Body distribution: focal, segmental, multifocal, generalized (with or without leg involvement), hemidystonia |
| | • Temporal pattern: disease course (static, progressive), variability (persistent, action-specific, diurnal, paroxysmal) |
| Associated features | |
| | • Isolated dystonia or combined with another movement disorder |
| | • Occurrence of other neurological or systemic manifestations |
| **Etiology** | |
| Nervous system pathology | |
| | • evidence of neurodegeneration, evidence of structural lesions, no evidence of degeneration or structural lesions |
| Inherited or acquired | |
| | • Inherited: autosomal dominant, autosomal recessive, X-linked recessive, mitochondrial |
| | • Acquired: perinatal brain injury, infection, drug, toxic, vascular, neoplastic, brain injury, psychogenic |
| | • Idiopathic: sporadic, familial |

Non-motor features are also present in other forms of dystonia in addition to CD. Sensory abnormalities such as pain are also common in isolated dystonia and may even present prior to the typical motor symptoms (Patel et al., 2014). Neuropsychiatric symptoms such as depression are also part of NMS of isolated dystonia, whether idiopathic or inherited. However, no cognitive abnormalities are usually found in idiopathic or inherited dystonia patients, whereas they are often seen in patients with combined dystonia syndromes (Albanese et al., 2019).

Treatment of dystonia depends on the form of the dystonia. Focal dystonias affecting only one body region or segmental dystonia affecting 2 or more contiguous body regions can be treated efficiently with botulinum toxin. Generalized dystonia, involving at least the trunk and 2 other body sites, usually responds instead to medical treatments such as anticholinergic medication or baclofen (Jankovic, 2013).

Some combined dystonias, such as dopa-responsive dystonia, can also be responsive to medications such as levodopa. As an invasive treatment, DBS has proven efficacious, particularly in medication-refractory inherited and idiopathic dystonia, whereas more evidence is needed for combined and acquired dystonia (Cury et al., 2018).

## 2.2 Basal ganglia circuit

### 2.2.1 Anatomy

The basal ganglia are subcortical nuclei first distinguished from the cortex and white matter in the 16th century by Vesalius and Piccolomini (Lanska, 2010). Located beneath the cerebral cortex the core nuclei of the basal ganglia are the caudate, the putamen, the globus pallidus (GP), the subthalamic nucleus (STN) and the substantia nigra (SN) (Figure 1).

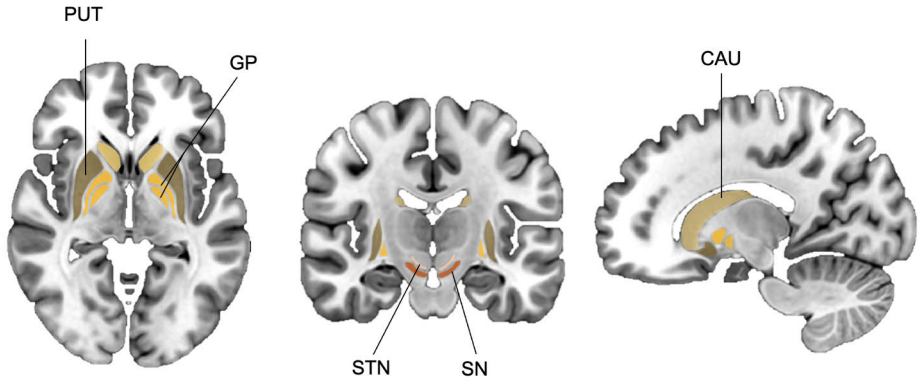


**Figure 1.** Anatomical structures of basal ganglia include putamen (PUT), caudate (CAU), globus pallidus (GP), subthalamic nucleus (STN) and substantia nigra (SN).

The striatum consists of the caudate nucleus and the putamen. Striatum, together with the nucleus accumbens and olfactory tubercle, are categorized as input nuclei of the basal ganglia and receive afferents from the cerebral cortex, thalamus and substantia nigra par compacta (SNc). Efferent projections are directed to the GP and the substantia nigra pars reticulata (SNr) (Crossman & D, 2010). 90% of striatal neurons are gamma-aminobutyric acid (GABA)ergic medium spiny neurons. Medium spiny neurons projecting directly to the globus pallidus interna (GPi) and the SNr contain the dopamine receptor subtype 1 (D1 receptors), while neurons projecting to the globus pallidus externa (GPe) express the dopamine receptor subtype 2 (D2 receptors) (Fazl et al. 2017(Strange, 1993). The remaining 10% of the

striatal neurons are interneurons, which are mainly cholinergic (Fazl & Fleisher, 2018). Striatum can further be divided into the dorsal striatum and ventral striatum based on connections and functions described further in section 2.2.4. The nucleus accumbens and the olfactory tubercle are considered ventral extensions of the ventral striatum and receive their dopaminergic modulation from the mesolimbic dopaminergic system (Fazl & Fleisher, 2018).

The GP and the putamen are together termed the lentiformis nucleus mainly for anatomical purposes, because they are located relatively close to each other (Figure 1). The GP alone can be divided into an internal (GPi) and an external part (GPe). Both segments have similar afferent connections arising from striatum and STN. On the contrary, efferent projections differ between the two segments. GABAergic fibres from the GPe projects principally to STN, while efferent projections from the GPi go to the thalamus or to the tegmentum in the brain stem.

The SN is located dorsal to the cerebral peduncles and comprises two distinct parts: inhibitory SNr and dopaminergic SNc. The healthy SN in the neuropathologic sample is composed of dark pigment that is produced as a by-product of dopamine synthesis. Similar to GPi, SNr can be referred to as the output nucleus of the basal ganglia because it receives inputs from the striatum and STN and projects to the ventral thalamus, superior colliculus, pedunculopontine nucleus and medullary reticular formation. The dopaminergic SNc synapses on the striatum.

The STN is a small nucleus located superior to the cerebral peduncle, beneath the thalamus and against the medial border of the internal capsule. Afferent neurons from wide areas of the cortex, GPe and pontine reticular formation project to the STN. Glutamatergic projections from the STN terminate in both segments of the GP and SNr.

### 2.2.2 Neurotransmitters

Dopamine, 3,4-dihydroxytyramine, is a brain neurotransmitter produced by dopaminergic neurons (Speranza et al., 2021). Dopamine is synthesized by the tyrosine hydroxylase enzyme and carried to the vesicles by the synaptic vesicle protein, vesicular monoamine transporter (VMAT2). After its release into the synaptic cleft, dopamine binds to the dopamine receptors, which either activates or inhibits on the target neurons. Five dopamine receptors (D1, D2, D3, D4 and D5) altogether can be divided into two dopamine receptor families (D1-like and D2-like), but D1 and D2 receptors play the major role in the basal ganglia context (Strange, 1993). DAT collects the released dopamine back up into the presynaptic terminals. Dopamine is the main neurotransmitter in three neural circuits in the basal ganglia: the nigrostriatal, the mesolimbic and the mesocortical. The nigrostriatal pathway projects from the SNc to the dorsal striatum, the mesolimbic pathway from the

ventral tegmental area to the ventral striatum and the nucleus accumbens and the mesocortical pathway from the ventral tegmental area to the prefrontal cortex (Speranza et al., 2021).

Glutamate, the ionic form of glutamic acid, is an excitatory neurotransmitter in the central nervous system (CNS). It acts via inotropic receptors such as N-methyl-D-aspartate (NMDA) or α-amino-3-hyroxy-5-methyl-4-isoxazolepropionic acid (AMPA) (Jamwal & Kumar, 2019). Glutamate is a principal excitatory neurotransmitter in the basal ganglia. It is released by corticostriatal afferents to the striatal neurones, and it also transmits the excitatory signals from the STN to the GPe and the basal ganglia output nuclei and from the thalamus to the motor cortex (Fazl & Fleisher, 2018).

GABA, as a primary inhibitory neurotransmitter of the CNS, mediates its action by acting upon ionotropic (GABA-A and GABA-C) and metabotropic (GABA-B) receptors. GABA transmits the inhibitory transmission from the striatum to the output nuclei (GPi/SNr) in the basal ganglia and further transmits to the thalamus as a part of a direct pathway and from the striatum to the GPe and then the STN as a part of the indirect pathway (Jamwal & Kumar, 2019).

Other neurotransmitters, such as adenosine, cannabinoids, acetylcholine and serotonin, are also presented in the basal ganglia (Jamwal & Kumar, 2019). Adenosine regulates post-synaptic glutamatergic actions mainly by enhancing the synaptic plasticity in the striato-pallidal pathway. Cannabinoid receptors CB1 are expressed both in the striatal efferent and afferent medium spiny neurons. Endocannabinoids modulate the activity of both GABAergic and glutamate neurons. Acetylcholine is presented in nuclei such as the striatum, nucleus accumbens and olfactory tubercle, which are also highly innervated by dopamine. Acetylcholine, acting via nicotinic acetylcholine receptors (nAChR), alters the dopaminergic signalling. Serotonin is a neurotransmitter utilised by the raphe nuclei in the brain stem and is transmitted to the striatum.

### 2.2.3 Pathways

Two classic pathways (direct and indirect pathways) were originally described in the early 1990s (Albin et al., 1989; DeLong, 1990). The third pathway, called the hyperdirect pathway, was later described to complete the basal ganglia pathways (Nambu et al., 2002). Model of these pathways is presented in Figure 2.

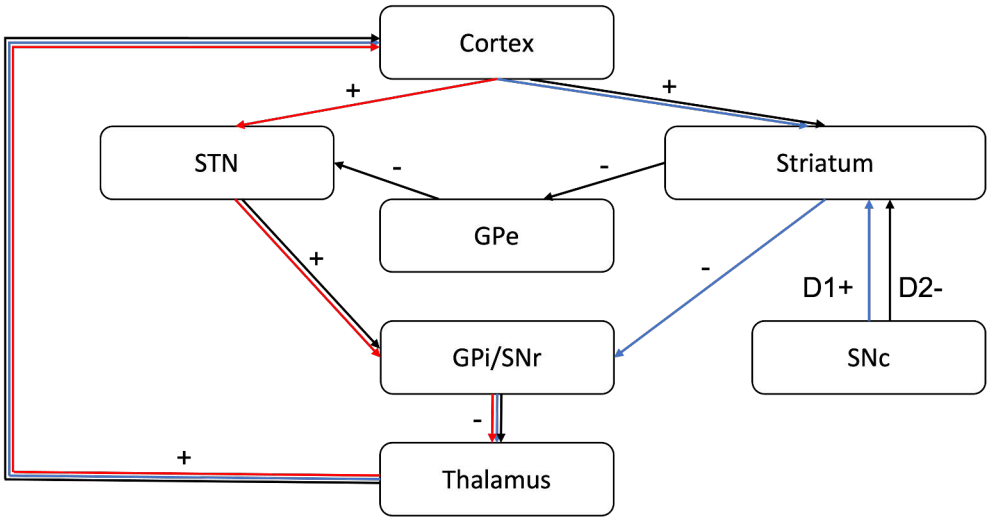


**Figure 2.** Direct (blue line), indirect (black line) and hyperdirect (red line) pathways of the basal ganglia. The main neurotransmitters are glutamate (excitatory, marked with plus sign), GABA (inhibitory, marked with minus sign) and dopamine (excitatory, marked as D1+ or inhibitory, marked as D2-). STN = subthalamic nucleus, GPe = globus pallidus externa, GPi = globus pallidus interna, SNr = substantia nigra pars reticulata, SNc = substantia nigra pars compacta.

The direct pathway projects from the cortex to the striatum, continuing straight to the output nuclei (GPi/SNr). Fig 2 shows that the GABAergic neurons inhibit the inhibitory output from GPi/SNr in the direct pathway, leading to less inhibition of the thalamus and thereby stimulating the cortex and the movement. The indirect pathway projects from the striatum to the GPe, then to the STN and then finally to the GPi/SNr, whereas the hyperdirect pathway projects directly from the cortex to the STN and then to the output structures. Both of these pathways lead to increasing the inhibition of the basal ganglia's output to the thalamus, thereby suppressing the cortex and the movement. The SNc provides the dopaminergic input to the striatum and modulates the effects of the pathways. The dopaminergic input leads to excitation of the direct pathway by activating the excitatory D1-receptors of the striatal medium spiny neurons, whereas it leads to inhibition of the indirect pathway by activating the inhibitory D2-receptors. Dopamine facilitates the solution between competing direct and indirect pathways by tipping the balance toward the winning direct pathway to accomplish the appropriate movement (Fazl & Fleisher, 2018).

The basal ganglia can be divided into motor, associative and limbic circuits in the functional organization (Obeso et al., 2008). The dorsal parts of the striatum are connected to the motor and premotor cortices and are primarily responsible for motor execution. This motor cortex – basal ganglia – thalamic projection is called the motor circuit. The motor circuit has a somatotopic organization, including a hand loop, leg

loop, etc., according to the afferent track's location in the motor cortex (Obeso et al., 2008). The cingulate and orbitofrontal cortices project to the ventral parts of the striatum to form the limbic circuit of the basal ganglia. The prefrontal and orbitofrontal cortices project to the medial parts of the striatum and form the associative circuit.

However, primarily relatively simple motor circuit of the basal ganglia has expanded to a complex integration of different structures and functions. The cerebellar connections with the basal ganglia have lately received attention. The cerebellum, together with the basal ganglia, seems to be involved in the same brain networks regulating both motor and nonmotor functions (Bostan et al., 2013).

### 2.2.4 Function

The traditional role of the basal ganglia has been considered to be motor control and motor learning by effectively choosing which actions to allow or to inhibit. The understanding of the basal ganglia function to date has extended to also encompass reward-related and goal-directed behaviors, emotional processing, implicit learning and habit formation, attention and time estimation and conflict monitoring (Obeso et al., 2008).

Conscious motor functions are mainly executed by projection from the posterior, sensorimotor putamen (Lanciego et al., 2012). Efferents to GPi are responsible for limb movements and to SNr for eye movements. Preparatory activation and finger movement have been considered to be located in the anterior putamen, while the caudate nucleus is involved in the active planning of a novel action (Monchi et al., 2006). The ventral striatum and its major component, nucleus accumbens, are considered to be part of the emotional responses, decision making and reward-related behaviour.

The regulation of the basal ganglia functions occurs via the pathways described in the previous section. The direct pathway supports the action plan, while the indirect pathway inhibits or stops it. The hyperdirect pathway enables the action planning to quickly stop by inhibiting the pallidal output and provide more time for rational action. The failure of the main structure of the hyperdirect pathway, STN, may lead to impulsive decisions (Rossi et al., 2015).

### 2.2.5 Dysfunction in parkinsonism and dystonia

#### 2.2.5.1 Parkinsonism

The neuropathologic feature of PD is dopaminergic neuronal loss in the nigrostriatal track together with α-synuclein deposition in Lewy bodies or neurites found in

residual neurons (Dickson, 2018). According to hypothesis of Braak et al., the neuropathology of PD starts in the medulla and the olfactory bulb (stages 1 and 2) and then progresses to the substantia nigra pars compacta and other basal ganglia structures (stage 3 and 4) (Braak et al., 2004). It has been shown that the axons, not the somas, are the first damaged in the nigrostriatal track, meaning that the retrograde ("dying back") degeneration affects the striatal neurons first and only then the nigral ones (Kordower et al., 2013; Tagliaferro & Burke, 2016).

Dopaminergic depletion in the SNc leads to hyperactivity of the indirect pathway because the direct pathway loses its dopaminergic support. This results in an ultimately increased inhibitory output of the basal ganglia and this pathological inhibition has been considered to cause the decrease of movements known as bradykinesia or akinesia. If this was this simple, removing or lesioning the inhibitory output nuclei of basal ganglia should result in movement facilitation or disinhibition. However, pallidotomy does not, paradoxically, induce involuntary movement; it ameliorates dyskinesias, and lesions of the STN, GPi or thalamus improve motor function (Lanciego et al., 2012).

In addition to these paradoxes associated with hypokinesia and the basal ganglia circuits, two other cardinal symptoms, tremor and rigidity, cannot be explained by the classic model. The role of the cerebellum and the pedunculopontine nucleus behind these symptoms has been debated (Fazl & Fleisher, 2018). Dopamine is only one neurotransmitter modulating the basal ganglia function, and glutamate, GABA and acetylcholine have particularly also been known to be altered in PD (Jamwal & Kumar, 2019). These and other still unknown explanations may lie behind the basal ganglia dysfunction in PD.

#### 2.2.5.2 Dystonia

No typical neuropathological abnormalities have been confirmed in dystonia and a wide range of different genotypes and phenotypes with limited data available complicates the interpretation of current studies (Sharma, 2019). Dystonia has classically been considered to be manifested by a decreased inhibitory basal ganglia output, resulting in the overactivity of thalamus and cortex that leads to dystonic movements. Results supporting this hypothesis have shown reduced firing rates in the GPi in dystonia in electrophysiologic studies (Starr et al., 2005) and abnormal function in the basal ganglia in imaging studies (Neychev et al., 2011). Lesions of the putamen and globus pallidus have been identified as causes of acquired dystonias (Sharma, 2019).

However, there is a growing body of evidence against the hypothesis of dystonia originating purely from the basal ganglia. Dystonia imaging studies have shown abnormalities in cortical regions, the cerebellum, thalamus, midbrain and brainstem.

Moreover, electrophysiological studies have provided evidence of loss of inhibition, impaired sensorimotor integration and maladaptive neural plasticity in dystonia (Neychev et al., 2011). Lesions causing acquired dystonias have also been described in many brain regions outside the basal ganglia, including the cortex, thalamus, brainstem and cerebellum (Jinnah et al., 2017). Different forms of dystonia may also be linked with dysfunctions in different brain regions (Jinnah et al., 2017).

Dystonias can be effectively treated with deep brain stimulation or lesioning targeted to basal ganglia structures, but the accumulating evidence suggests that dystonia is a network-wide problem involving the cerebellum, basal ganglia and cortex, and plasticity changes rather than a pure basal ganglia disorder (Conte et al., 2019; Corp et al., 2019; Sharma, 2019). This would also explain why the treatment effect of DBS in dystonia appears slower than in other movement disorders (Fazl & Fleisher, 2018). It should also be noted that it's possible that pathophysiological differences between idiopathic, inherited and acquired forms of dystonia may explain the heterogeneity of the current results (Conte et al., 2019).

## 2.3 Deep brain stimulation of the basal ganglia

### 2.3.1 Mechanisms

Deep brain stimulation (DBS) is an invasive treatment technique based on high-frequency electric impulses from electrodes implanted into specific targets within deep regions in the brain. Since the first implantation in movement disorders in the 1980s in a PD patient, DBS has expanded to several neurological and neuropsychiatric disorders such as PD, essential tremor (ET), dystonia and obsessive compulsive disorder. An estimated 208 000 deep brain stimulators have been implanted (Vedam-Mai et al., 2021). The effect of DBS is usually considered to be reversible, adaptable and titratable; thus, due to these qualities and ability to bilateral implantation without significant side effects, DBS has almost replaced the lesioning techniques.

The exact underlying mechanism of the DBS is still undetermined, despite its broad use. The main targets have been established by the experiences of lesion treatments, so the DBS mechanism was first considered as a lesion-like inhibition of the target region (Deniau et al., 2010). However, a recent hypothesis on the DBS mechanism suggests that DBS modulates a connected brain network in addition to the local stimulation effect (Deniau et al., 2010; Gonzalez-Escamilla et al., 2020; Gonzalez-Escamilla et al., 2019; Horn, 2019; Lozano & Lipsman, 2013). Electric stimulation has been described as eliciting neural responses that result in excitative or inhibitive synaptic events, depending on the pathway being reached (Herrington et al., 2016). These responses have been found to spread across the brain networks

(Horn et al., 2017; Lozano & Lipsman, 2013) and potentially even affect the neuroplasticity of the brain (Jakobs et al., 2019).

Most of the research on DBS mechanism in humans has been performed using imaging or electrophysiological methods (Gonzalez-Escamilla et al., 2020). In imaging studies, individual volume of tissue activated modelling has enabled the evaluation of regional brain activation by a DBS electrode. Furthermore, a comparison of stimulation site volumes and clinical responses has helped to identify the optimal sweets spots, e.g. for STN in Parkinson's disease and for GPi in dystonia (Akram et al., 2017; Bot et al., 2018; Reich et al., 2019). These results have also emphasized the importance of the accurate lead implantation (Gonzalez-Escamilla et al., 2020). However, there is a broad variance in postoperative outcomes after DBS implantation even with optimal lead location; thus, correct localization of the electrode is probably only part of the explanation for a good outcome (Gonzalez-Escamilla et al., 2020). Functional resting connectivity maps associated to the location of electrodes have presented the brain networks connected to stimulation site (volume of tissue activated) (Boes et al., 2015; Fox, 2018). Stimulation-induced changes in these connectivity patterns are also considered to affect the clinical improvement (Horn et al., 2017). For example in PD, the connectivity profile from the STN to the supplementary motor area (SMA) is thought to ameliorate bradykinesia, while electrode connectivity to the primary motor cortex (M1) is thought to explain tremor improvement (Akram et al., 2017).

Electrophysiologic studies have offered extended information on electrophysiological changes in the basal ganglia and enabled the utilization of the microelectrode recordings in the correct lead positioning (Gonzalez-Escamilla et al., 2020). Increased subthalamic oscillatory beta activity seems to be associated with bradykinetic motor symptoms in PD, and DBS can suppress this overactivity locally (Kühn et al., 2008) but also in STN-cortical networks such as SMA and premotor regions (Gonzalez-Escamilla et al., 2020). However, this suppression effect on STN disappears in 6 months follow-up but not in repetitive overstimulation over minutes, reflecting potentially more changes in neural plasticity than habituation (Chen et al., 2020). Even so, the role of the beta oscillatory function of DBS and the basal ganglia is still an unresolved area and further investigations are needed (Vedam-Mai et al., 2021).

There are still several uncertainties involving the effects of DBS. Some patients do not show a good response despite optimal lead placement. Absent or poor responses have also been described for certain symptoms such as freezing of gait in PD or swallowing problems in dystonia. DBS effects may differ between the disorders, and DBS can paradoxically cause dystonic symptoms in PD and parkinsonism in dystonia. Then, the response of DBS in PD is almost immediate after the implantation, whereas it usually takes several weeks to months to see

improvement in dystonia(Gonzalez-Escamilla et al., 2020). Finally, after discontinuation of DBS, symptoms appear immediately in PD, whereas sustained response has been reported in generalized dystonia (Ruge et al., 2014). On the contrary, possible fatal rebound phenomena have been described after sudden DBS cessation in both PD and dystonia (Azar et al., 2019; Lumsden et al., 2017).

### 2.3.2 Targets in Parkinson's disease and dystonia

Depending on the disorder, the appropriate brain target is chosen to alleviate the cardinal symptoms. The main targets of DBS are STN and GPi in Parkinson's disease (Figure 3), the ventral intermediate nucleus of thalamus (VIM) in PD tremor, GPi and STN in dystonia and VIM in ET, while no consensus of optimal DBS targets has yet been achieved in other neurologic and psychiatric disorders (Gonzalez-Escamilla et al., 2020). In order to ease to motor symptoms, electrodes are targeted motor parts of the nuclei, which are the posteroventral part in GPi and and the superolateral part in STN.

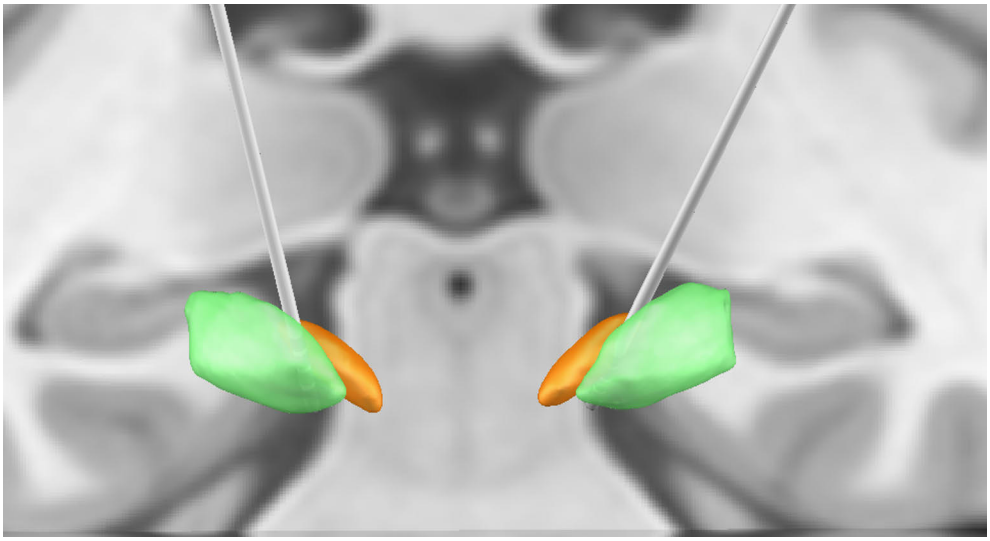

**Figure 3.** Visualization of the DBS electrodes targeted to the STN (in orange). GPi is another target option in PD (in green). The DBS electrodes were localized and visualized using Lead-DBS software (http://www.lead-dbs.org) (Horn et al., 2019). Atlas was used for 3D visualization: DISTAL Minimal Atlas (Ewert et al., 2018).

The most common target of the DBS is the STN in PD, but the DBS can also be targeted to the GPi instead of the STN or to the VIM in tremor-dominant PD. Both STN and GPi targeted DBSs improve motor symptoms including tremor and quality of life equally, although the off-medication state may be better with patients with STN-DBS

(Ramirez-Zamora & Ostrem, 2018; Wong et al., 2019). STN-DBS usually allows a greater reduction of dopaminergic medications. GPi-DBS may be more beneficial with patients who suffered hallucinations or diminished cognitive capacity preoperatively, compared to STN. However, target selection of DBS should be based on individual characteristics and the surgery's goals (Ramirez-Zamora & Ostrem, 2018).

The GPi is the established and the most used target in dystonia. STN is also reported as an optional target nucleus. No randomized control trials have compared the efficacy of these targets. Although the meta-analysis of isolated dystonia suggested that STN may be an optimized stimulation target, it should be noted that number of dystonia patients with STN-DBS are still quite small and the baseline scores were lower in patients with STN-DBS compared to patients with GPi-DBS (Wu et al., 2019). In the other study, these targets seem to have similar efficacy in cervical dystonia (mean 58.8% improvement in Toronto Western Spasmodic Torticollis Rating Scale (TWSTRS) total scores) with different adverse effect profiles (Tsuboi et al., 2020).

There is no consensus of neuromodulatory effects of STN-DBS and GPi-DBS. In fMRI study, STN was shown to induce activation in a circuit that includes the GPi, thalamus and deep cerebellar nuclei while inhibiting a circuit involving M1, putamen and cerebellum (Shen et al., 2020). Motor cortex inhibition was also induced by GPi-DBS in an electrophysiological study (Ni et al., 2018). The DBS-induced effects found in molecular imaging studies are described in the next section of this review of the literature (section 2.4).

The VIM is the target used to suppress tremor in ET, PD and dystonia. It has proven to be an effective treatment for ET and tremor in PD even for the long-term (10 years), while the effects on dystonic tremor were modest and transient (Cury et al., 2017). The effect of VIM stimulation has been thought to derive from its placement on a cerebello-thalamo-cortical network connecting the primary cortex and to the dentate nucleus of contralateral cerebellum (Akram et al., 2018).

## 2.4 Molecular imaging of the basal ganglia

### 2.4.1 Parkinsonism

Imaging of the basal ganglia in parkinsonism is usually targeted to the altered function of the nigrostriatal dopaminergic nerve terminals (Strafella et al., 2017). There are several SPECT and PET ligands available to target either presynaptic or postsynaptic dopaminergic terminal (Table 3). In addition to dopamine, brain glucose metabolism, blood flow, serotonergic function and neuroinflammation in the basal ganglia region have also been investigated with PET and SPECT imaging in PD (Strafella et al., 2017).

**Table 3.** Some PET and SPECT tracers targeted to the dopaminergic nerve terminal. The table was modified and completed from the Fig 2 in Strafella et al., 2017.

| | PET/SPECT target | [$^{11}$C] | [$^{18}$F] | [$^{123}$I] | [$^{99}$mTC] |
|---|---|---|---|---|---|
| Presynaptic | VMAT2 | DTBZ | DTBZ | | |
| | DAT | CFT<br>RTI 32<br>methylphenidate | CFT<br>PE2I<br>FE-PE21 | altropane<br>beta-CIT<br>FP-CIT | TRODAT |
| | Dopamine synthesis | beta-DOPA<br>methyl-m-tyrosine | FDOPA<br>FMT | | |
| Postsynaptic | D1 | NNC 112<br>SCH 23390 | | | |
| | D2/D3 | Raclopride<br>FLB457<br>NMSP<br>PHNO | Fallypride | IBZM<br>Epidepride | |

Abbreviations:
B-CIT, (–)-2β-Carbomethoxy-3β-(4-iodophenyl)tropane
CFT,(-)-2β-Carbomethoxy-3β-(4fluorophenyl)tropane
DAT, dopamine transporter
DOPA, L-3,4-dihydroxyphenylalanine
DTBZ, Dihydrotetrabenazine
FE-PE21,(E)-N-(3-iodoprop-2-enyl)-2-beta-carbofluoroethoxy-3-beta-(4′-methyl-phenyl)nortropane
FLB457, (S)-5-bromo-N-[(1-ethyl-2-pyrrolidinyl)methyl]-2,3-dimethoxybenzamide
FMT, Fluoro-m-tyrosine
FP-CIT, N-ω-fluoropropyl- 2β-carbomethoxy- 3β-(4-iodophenyl) nortropane
IBZM, Iodobenzamide.
NMSP, 3-N-[11C]Methylspiperone
NNC112,(+)-8-chloro-5-(7-benzofuranyl)-7-hydroxy-3-methyl-2,3,4,5-tetrahydro-1H-3benzazepine
PE21, (E)-N-(3-iodoprop-2-enyl)-2-beta-carbomethoxy-3-beta-(4′-methyl-phenyl)nortropane
PHNO, (+)-4-propyl-9-hydroxynaphthoxazine
RTI, (–)-2β-Carbomethoxy-3β-(4-tolyl)tropane
SCH23390,R(+)-7-chloro-8-hydroxy-3-methyl-1-phenyl-2,3,4,5-tetrahydro-1H-3-benzazepine hydrochloride
TRODAT, tropane derivative
VMAT2, vesicular monoamine transporter 2

Striatal DAT imaging with N-ω-fluoropropyl- 2β-carbomethoxy- 3β-(4-iodophenyl) nortropane ([123I]FP-CIT) SPECT is one of the most commonly used imaging methods to detect the dopaminergic defect in the basal ganglia in neurodegenerative parkinsonism. It can be used to differentiate neurodegenerative parkinsonism from non-neurodegenerative conditions (T. S. Benamer et al., 2000). It is also a useful tool in the differential diagnostics between dementia with Lewy bodies (DLB) and Alzheimer's disease (McKeith et al., 2007). To date, the value of DAT imaging in distinguishing PD from atypical parkinsonism still remains unclear, although differences in DAT binding between the disorders have been evaluated (Kaasinen et al., 2019).

[123I]FP-CIT SPECT has been proven to have 97% sensitivity for the clinical diagnosis of neurodegenerative parkinsonism and 100% specificity for ET (T. S. Benamer et al., 2000). Striatal DAT loss has been estimated to be an average 50–60% in early to moderate PD compared to healthy controls (Kaasinen & Vahlberg, 2017). Abnormal DAT uptake is first seen in the putamen in PD, usually posterior part and later in the caudate nucleus. In the healthy controls, the DAT bindind is usually described as a comma-shaped structure and in PD, the typical pattern is the tail of comma (putamen) starting to disappear. Moreover, the side of the DAT defect also correlates with the disease severity of the contralateral side and, the progression of abnormal DAT binding has shown to be associated with the disease's duration (H. T. Benamer et al., 2000). Interestingly, bradykinesia and rigidity are associated with the abnormal DAT binding, but a similar relationship has not been found with tremor severity (H. T. Benamer et al., 2000; Rossi et al., 2010).

Striatal or nigral DAT uptake has been considered to be a possible imaging biomarker of preservation of the nigrostriatal dopaminergic neurons (Strafella et al., 2017). However, the evidence has been controversial (Palermo & Ceravolo, 2019). Striatal DAT binding correlated with nigral neurons only when nigral loss was below 50% in parkinsonian macaques (Karimi et al., 2013). In vivo human studies combining DAT imaging and neuropathological data are scarce for obvious reasons. The postmortem study of neurodegenerative PD patients found no association between nigral (tyrosine hydroxylase positive or neuromelanin-containing) neurons and antemortem DAT binding, but the interval between the study points was 5.2 years (Saari et al., 2017). Nevertheless, those findings question the use of DAT as a marker of disease progression because the DAT may reflect the dopaminergic activity rather than a number of viable neurons (Palermo & Ceravolo, 2019).

The DAT uptake in VP and DIP is supposed to be normal (Gerschlager et al., 2002; Tolosa et al., 2003) and these groups are usually included in the reference groups, when non-degenerative conditions are compared to degenerative conditions. However, the uptake in vascular parkinsonism can be relatively abnormal but still higher in all regions compared to PD. Unlike in PD, vascular parkinsonism has usually symmetrical findings in DAT imaging (Benítez-Rivero et al., 2013). Up to 50% of drug-induced parkinsonism showed abnormal DAT binding values when compared to healthy controls, but greater differences were observed in the caudate nuclei which are usually affected last in PD (Lorberboym et al., 2006). Parkinsonian cardinal symptoms can occasionally be observed in patients with essential tremor (ET), and in this PD-ET phenotype, DAT uptake has been showed to be more decreased when more clinical features were observed (Waln et al., 2015). However, DAT binding may also be reduced in ET patients with or without mild parkinsonian features but in this case the pattern may differ from PD (Waln et al., 2015). Therefore, the interpretation of imaging results in the case of these atypical findings

should be carried out carefully, especially in clinically uncertain cases, to avoid a false diagnosis.

DBS is mainly targeted to the basal ganglia structures and much of the knowledge of its role and networks has been gained through the imaging studies in DBS patients. There are several studies investigating the glucose metabolism, rCBF and dopaminergic activation. Interestingly, considering the reduced need of levodopa medication after DBS implantation, STN-DBS did not seem to modulate dopaminergic activity in PD patients (Hilker et al., 2003; Strafella et al., 2003). However, the majority of the studies evaluated the metabolism changes with FGD-PET or rCBF changes with PET or SPECT. The most common target of DBS was the STN, but a few studies included patients with VIM or GPi DBS (Fukuda et al., 2004; Fukuda et al., 2001; Payoux et al., 2009; Wielepp et al., 2001). The results of the effect of STN stimulation were very heterogenous, but, in brief, mainly stimulation-induced increased activation was seen in the stimulation site, globus pallidus and thalamus, while decreased activation was seen in the M1, SMA and cerebellum (Asanuma et al., 2006; Bradberry et al., 2012; Ceballos-Baumann et al., 1999; Garraux et al., 2011; Geday et al., 2009; Haslinger et al., 2005; Hershey et al., 2003; Herzog et al., 2006; Herzog et al., 2008; Hilker et al., 2004; Karimi et al., 2008; Nagaoka et al., 2007; Park et al., 2015; Trost et al., 2006; Wang et al., 2010).

### 2.4.2 Dystonia

Imaging studies in dystonia are scarce compared to studies in PD. As described in section 2.2.5.2, dystonia has recently been linked to network-wide dysfunction, such as abnormalities in the basal ganglia-thalamo-cortical and cerebello-thalamo-cortical pathways. The most used molecular imaging methods have been investigating the brain glucose metabolism with 18F-fluoro-deoxyglucose (FDG)-PET or regional cerebral blood flow (rCBF), although there are also a few neurotransmitter studies investigating dopamine, GABA-receptor availability, serotonin transporter and acetylcholine transporter (Zoons et al., 2011).

There are different findings in focal dystonias, depending on the symptoms' locations. Glucose metabolism has been shown to be increased in the lentiform nucleus in CD compared to healthy controls (Magyar-Lehmann et al., 1997). There is evidence of hypermetabolism in the cerebellum and the pons in blepharospasm (Zoons et al., 2011). rCBF has been described to be decreased by a sensory trick in motor areas (SMA, PCM, M1) contralaterally to the direction of head deviation in CD. Sensory trick also led to hypermetabolism in the ipsilateral parietal cortex and bilateral occipital cortex (Naumann et al., 2000). Dopaminergic studies of dystonia have mainly failed to show any dopaminergic differences between the dystonia patients and healthy controls (Leenders et al., 1993; Playford et al., 1993), except for

one study showing a decrease of dopamine D2-like binding in the putamen in patients with writer's cramp or facial dystonia (Perlmutter et al., 1997).

Different types of dystonia have been shown to be associated with different patterns in FDG-PET imaging. Increased metabolism was found in the basal ganglia, cerebellum and SMA in DYT1 patients in inherited dystonias (Eidelberg et al., 1998), while uptake was decreased in the putamen in DYT6 dystonia (Carbon et al., 2004), and the increased activity was noted in the posterior thalamus and inferior pons in DYT11 myoclonus dystonia (Carbon et al., 2013). However, the role of these patterns still remains to be confirmed because they have not proven to be totally genotype specific (Trost et al., 2002).

There are only very few molecular imaging studies with DBS in dystonia patients. All of the studies, involving the imaging during the active stimulation and after stimulation was switched off, investigated stimulation induced changes in rCBF (Detante et al., 2004; Greuel et al., 2020; Katsakiori et al., 2009; Thobois et al., 2008; Yianni et al., 2005). In generalized dystonia, GPi-DBS has shown to increase the perfusion in the stimulation site, caudate, thalamus, cerebellum and several cortical regions (frontal gyrus, cingulate cortex, dorsal lateral prefrontal cortex, temporal and parietal cortex), while to decrease the perfusion in primary motor cortex (Detante et al., 2004). However, another study found decreased perfusion in the cerebellum, pons, midbrain, lentiform nucleus and thalamus and anterior cingulate induced by GPi-stimulation in a heterogenous group of dystonias (Yianni et al., 2005). Brain perfusion in focal or segmental dystonia patients was recently evaluated using rCBF imaging and GPi-stimulation (Greuel et al., 2020). No stimulation induced metabolic changes were detected within GPi-DBS patients, but patients with GPi-DBS showed reduced perfusion in a prefrontal network at rest and reduced sensorimotor cortex activity during the motor task compared to patients without DBS (Greuel et al., 2020).

# 3 Aims

The aims of this study were to investigate the basal ganglia function and its correlation with clinical features using molecular imaging in parkinsonism and dystonia.

The specific objectives of the each sub study were:

I To evaluate the relationship between the putaminal dopaminergic axons and DAT binding in Parkinson's disease.

II To present a case report of the sustained effect of bupropion causing an abnormal finding in striatal DAT imaging in a patient without dopamine neuronal loss

III To examine the potential differences in striatal DAT binding between healthy controls and patients with non-degenerative parkinsonism

IV To investigate the temporal pattern of the reappearance of symptoms after discontinuation of GPi-DBS in cervical dystonia

V To study the effects of GPi-DBS on brain glucose metabolism and the relationship between motor symptom improvement and GPi-DBS induced metabolic changes in cervical dystonia

# 4 Materials and Methods

## 4.1 Study I

### 4.1.1 Subjects

Fourteen patients with neurodegenerative parkinsonism (10 PD and 4 atypical parkinsonism) were enrolled in this study. This was a retrospective study of patients who underwent the DAT imaging *antemortem* and the neuropathologic examination *postmortem*. First, cases with neuropathologically confirmed PD or atypical parkinsonism were identified from the records of the Department of Pathology at Turku University Hospital between 2004 and 2015. Then patients scanned with DAT SPECT due to diagnostic purposes were selected. Clinical information, including sex, age at the time of diagnosis, motor symptom duration and time interval between scanning and death were extracted from the hospital records of these patients. This was a partial subsample of a previous study of 18 patients (Saari et al., 2017). Six patients, included in the previous study were excluded from this study due to unavailable putamen samples. Two patients excluded from the previous study because of the lack of nigra samples were included in this study.

### 4.1.2 Neuropathological examination

Neuropathological samples were obtained at the autopsy as part of a routine examination by the neuropathologist. Putamen samples were selected by the neuropathologist on the basis of the representativeness of the postcommissural striatum including the putamen, GPi and GPe (Fig 4A). Formalin-fixed, paraffin-embedded tissue from the putamen were sectioned at 8um and stained for tyroxine hydroxylase (TH) to quantify the dopaminergic axons, as previously described (Kraemmer et al., 2014). After scanning the slides with a Pannoramic P25 Flash slide scanner, they were analyzed with CaseViewer software version 1.4.0.50094 (3DHISTECH Ltd, Budapest, Hungary). Margins of the putamen were drawn, and included area were divided into nine subregions (Fig 4A). In each subregion, three standardized area of visual field (20x magnification) were annotated by two independent examiners. TH-positive fibers were calculated in these standardized areas, (Fig 4B).

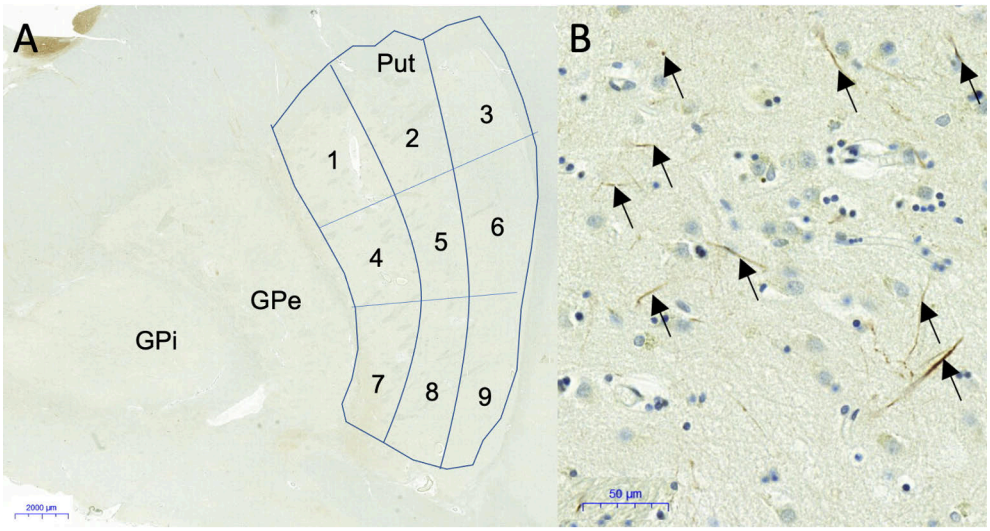


**Figure 4.** Illustration of the quantifying of the dopaminergic axons. **A**. The putamen was divided in nine subregions in the postcommissural samples presenting GPi and GPe besides the putamen. **B**. The dopaminergic axons (clearly visible brown lines or brown cross-sections of fibers) marked with arrows were calculated. GPi = globus pallidus interna, GPe = globus pallidus externa, Put = putamen.

### 4.1.3 DAT imaging

DAT imaging was performed according to the prevailing protocol of the Department of Nuclear Medicine between the years 1999–2013. Twelve patients had been scanned with [$^{123}$I]FP-CIT SPECT and 2 patients (both PD) with [$^{123}$I]β-CIT SPECT. Patients had been scanned with either a Picker Irix gamma camera (Picker International Inc, Highland Heights, OH) (n = 8), with 2 different GE Infinia II Hawkeye SPECT/CT cameras (GEMedical Systems,Waukesha, WI) (n = 3) or with an ADAC Vertex V60 gamma camera (ADAC Laboratories, Milpitas, Canada) (n = 1) (missing data for two patients). Details of the scanning protocol have been published previously (Saari et al., 2017).

Reconstruction of the SPECT images was conducted using HybridRecon Neurology, version 1.0F (Hermes Medical Solutions AB, Stockholm, Sweden). A three-dimensional (3D) ordered-subsets expectation maximization (OSEM) reconstruction algorithm was used. Image analysis was performed with BRASS automated semi-quantitative analysis software version 3.6 (study I) or version 2.6 (study III) (Hermes Medical Solutions, Stockholm, Sweden). The system-specific calibration coefficients were implemented into the BRASS software. Regions of interest (ROIs) were automatically segmented with BRASS. In study II, specific binding ratios (SBRs) for striatal DAT were calculated for four ROIs (left and right putamen, left and right caudate), while they were calculated for six striatal ROIs (the

right and left anterior putamen, the right and left posterior putamen, the right and left caudate nucleus) in studies I and III. The occipital cortex was used as a reference region, and SBRs were calculated according to the following formula: (ROI – ROIoccipital) / ROIoccipital (Varrone et al., 2013).

Images presented in the figures were co-registered using statistical parametric mapping software (SPM12; The Wellcome Centre for Human Neuroimaging, London, UK, https://www.fil.ion.ucl.ac.uk/spm/) implemented on MATLAB (MathWorks Inc., Sherborn, MA, USA).

## 4.2 Study II

### 4.2.1 Subject

This is a case report of a 52-year-old male patient referred to a neurologist by his psychiatrist due to problems with cognition, balance, and verbal communication. His medical history consisted of atrial fibrillation and severe depression for several years. He was taking venlafaxine and bupropion daily for depression. He had no family history of PD or other neurodegenerative disorders. All the clinical information presented in the case report was acquired from patient's hospital record.

### 4.2.2 DAT imaging

The patient was scanned with [$^{123}$I]FP-CIT SPECT due to unknown parkinsonism according to the protocol of Department of Nuclear Medicine in 2017. The patient was using bupropion, which potentially interferes with DAT SPECT interpretation due its affinity to DAT (Booij & Kemp, 2008), so scanning was performed 7 days after the patient had paused the bupropion intake. A follow-up scan with an identical scanning protocol was performed 11 months after the first scan, but the patient was instructed to discontinue bupropion 1 month prior the scanning. Image analysis and presentation was performed as described in the study I.

## 4.3 Study III

### 4.3.1 Subjects

Forty healthy controls were scanned with [123I]FP-CIT SPECT as a part of a neuroimaging study of gambling in older population (GAMDAT) in 2019–2020. Age between 50–85 years, no prior neurological or psychiatric diseases, no neurological symptoms and no medications affecting the central nervous system

were the inclusion criteria for healthy controls. The structural brain MRI was performed on the same day with SPECT imaging.

69 age- and sex-matched symptomatic parkinsonism or tremor patients without dopaminergic degeneration were selected from a sample of the cross-sectional clinical and imaging study of parkinsonism (NMDAT) scanned in Turku University Hospital between 2014 and 2019. All patients with neurodegenerative parkinsonism (PD, PSP, MSA, CBD), dementia (DLB, AD, frontotemporal dementia (FTD)) or undetermined diagnosis were excluded from the study. All patients underwent structural brain imaging (CT or MRI) prior to the SPECT imaging. For sub-analyses, the subjects were divided into the subgroups according to the family history of PD, diagnosis of ET, VP or DIP or the use of selective serotonin reuptake inhibitors (SSRIs) or serotonin-norepinephrine reuptake inhibitors (SNRIs).

The flowchart of included samples and patient selection is presented in Figure 5.

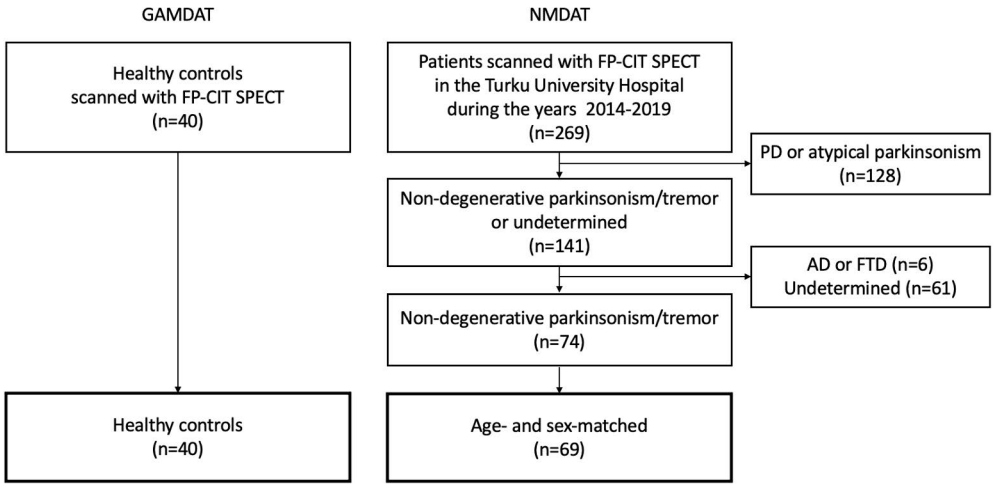


**Figure 5.** Flowchart of the studied samples and patient selection of symptomatic controls.

### 4.3.2 Clinical examination and questionnaires

Clinical examination of the healthy and symptomatic subjects was performed 2–4 hours prior to the SPECT scanning. In addition to a clinical interview, motor symptom severity was evaluated with the Unified Parkinson's Disease Rating Scale (MDS-UDPRS) part III (Goetz et al., 2008), cognition with the Mini-Mental State Examination (MMSE) (Folstein et al., 1975), RBD with the single-question screen for rapid eye movement (REM) sleep behavior disorder (Postuma et al., 2012) and NMSs with the Non-Motor Symptoms Scale (NMSS) (Chaudhuri et al., 2007). Moreover, each subject was asked to fulfil the following questionnaires: the

Beck Depression Inventory (BDI) (BECK et al., 1961), the Beck Anxiety Inventory (BAI) (Beck et al., 1988) and the Barratt Impulsiveness Scale (BIS-11) (Patton et al., 1995).

### 4.3.3 DAT imaging

Healthy controls were scanned with DAT SPECT as part of a GAMDAT project, while symptomatic subjects were referred to DAT imaging due to uncertain parkinsonism or tremor by their treating neurologists and recruited to the NMDAT study upon their arrival for the scanning visit in the Department of Nuclear Medicine in Turku University Hospital. However, both groups were scanned with [$^{123}$I]FP-CIT SPECT with identical scanning protocols. The subjects received 250–300 mg of potassium perchlorate or Jodix™ (potassium iodide) 130 mg tablet 30–60 min before the tracer injection to prevent thyroid gland uptake. A tracer bolus of [$^{123}$I]FP-CIT (185 MBq) was administered intravenously with a slow 20-second injection. Imaging started 3 hours after injection.

Scanning of all healthy controls was performed with Siemens Symbia T6 SPECT/CT (Siemens Healthineers, Erlangen, Germany). Symptomatic patients were scanned with Siemens Symbia T6 or one of two GE Infinia II Hawkeye SPECT/CT systems (GE Healthcare, Tirat Hacarmel, Israel). All SPECT/CTs are dual-head systems with low-energy, high-resolution collimators. Subjects were lying in a supine position. The energy window was 159 keV±5% for the Symbia and 159 keV±10% for the GE Infinia. The acquisition matrix size was 128x128 and the rotation arc was 180° in step-and-shoot mode for all systems. The angular step was 3°, which resulted in 60 projections for each camera head and a total of 120 projections. The acquisition zoom was 1.23–1.28, and the time per projection was 35 s.

Image analysis and presentation were performed as described in the study I. Reconstruction of the SPECT images was conducted using HybridRecon Neurology, version 1.3, Hermes Medical Solutions AB, Stockholm, Sweden). In addition, occipital counts-per-voxel values were also calculated for each subject.

## 4.4 Studies IV-V

### 4.4.1 Subjects

Twelve patients diagnosed with cervical dystonia and treated with GPi-DBS participated in the study. Inclusion criteria were age over 18 years, diagnosed cervical dystonia, implanted bilateral GPi-DBS, a best DBS treatment response of at least 25% (Vidailhet et al., 2005), stable DBS parameters, ability to temporarily

switch the DBS off and no medical contraindication to PET imaging. Patients were recruited by their treating neurologists in the University Hospital Turku and in the Helsinki University Hospital. Data collection was performed between 2019 and 2020.

At the time of the study, 10 patients had only cervical symptoms, whereas the symptoms were also spread and involving other body parts in two patients. This spread is known to frequently happen in focal dystonia (Berman et al., 2020), and one of our two patients had developed segmental dystonia affecting their neck, mouth and eyes and another generalized dystonia affecting their neck, mouth, vocal cords, trunk, left upper and lower limb. The patient with segmental dystonia had a sudden and severe worsening of symptoms after switching DBS off, which required DBS to be reinitiated within 10 minutes as requested by the patient. This patient was unable to complete the whole study as a result and was only included in study IV in this thesis. Eleven patients completed the whole study.

Parameters of bilateral GPi-DBS (Medtronic Activa PC, n=8; Abbott St. Jude Infinity, n=3; or Boston Scientific Vercise, n=1) were collected during the study visits. Voltages (V) in devices that used current mode (Abbott), were calculated using current (mA) and resistance (ohms). These details were not available for the Boston Scientific device (n=1).

### 4.4.2 Clinical examination and questionnaires

Clinical assessments were performed during the GPi-DBS stimulation (ON), acutely (10–30 minutes) after DBS was switched off (OFFacute) and two days after the stimulation was discontinued (OFFchronic). In all three visits, clinical state was followed for approximately two hours after the evaluation. The severity of the cervical dystonia symptoms was evaluated with the Toronto Western Spasmodic Torticollis Rating Scale (TWSTRS) (Comella et al., 1997) and the Burke-Fahn-Marsden Dystonia Rating Scale (BFMDRS) movement part (Burke et al., 1985). TWSTRS (total 0–85 points) is developed for the evaluation of cervical dystonia and comprises three parts: severity scale (0–35 points), disability scale (0–30 points) and pain scale (0–20 points). BFMDRS movement part measures dystonia in nine body regions (0–120 points) and is also used to evaluate other forms of dystonia. Cognitive impairment was excluded with MMSE during the stimulation with a cut-off lower than 26 points. Information of presurgical symptom severity, best postoperative treatment response, interval to best treatment response as well as dominant preoperative symptom type (phasic/tonic as described by (Grips et al., 2007)) was extracted from the patients' hospital records.

### 4.4.3 FDG-PET (study V)

#### 4.4.3.1 Scanning protocol

PET imaging with 18F-FDG was performed during the stimulation (FDG-ON) and after the stimulation was switched off (FDG-OFF) with respect to the clinical examinations at ON and OFFacute. DBS was discontinued on average 101 (SD 11, range 73–115) minutes before the tracer injection.

A brain $^{18}$F-FDG-PET/CT imaging was performed on GE Discovery MI PET/TT (Milwaukee WI, USA) at Turku PET Centre. Patients fasted at least 4 hours prior to the study to ensure normoglycemia. Mean blood glucose was 5.7 mmol/l (SD 0.7, range 4.6–7.7) before the injection. The mean injected dose of $^{18}$F-FDG was 199 MBq (range 188–214). Patients were lying still in a supine position during and after the injection with their eyes open and earmuffs on both ears. A brain CT was obtained before the emission. The PET emission began 35 minutes after the injection, and four 5-minute frames were acquired. Patients were instructed to not to move and to stay awake during the scanning. The head was placed in a head holder, and no head tremor was detected during the PET scanning in any of the patients.

#### 4.4.3.2 Image preprocessing

DICOM files were first converted to the NIfTI format using MRIcron software (version 2010, https://www.nitrc.org/projects/mricron). The preprocessing of the PET images was performed with FSL software (6.0.4, https://fsl.fmrib.ox.ac.uk/fsl/fslwiki/). Realignment was conducted frame-by-frame. All four frames were then summed in a sum image and images were warped to the Montreal Neurological Institute (MNI152) space using an in-house $^{18}$F-FDG template created from an age-matched group of healthy volunteers (Joutsa et al., 2017). Normalization to the average whole brain uptake was conducted for the voxelwise $^{18}$F-FDG uptakes. A standardized uptake value (SUV) for the whole brain was calculated with the following formula: ratio of tissue radioactivity concentration at time T / (administered dose / weight). Finally, the images were smoothed with a 6mm Gaussian kernel at full width half-maximum, and the FDG-OFF uptake was subtracted from the FDG-ON uptake (ON-OFFratio images) using statistical parametric mapping software (SPM12; The Wellcome Centre for Human Neuroimaging, London, UK, https://www.fil.ion.ucl.ac.uk/spm/) implemented on MATLAB (version R2020b, MathWorks Inc., Sherborn, MA, USA).

Volumes of tissue activated were defined using preoperative MRI images together with postoperative CT images as described previously by Reich et al (Reich et al., 2019). One patient with directional DBS was excluded from this analysis. The

group-level volume of tissue activated hot spot was defined as voxels with volumes of tissue activated overlap in at least 50% of the patients. These resulting bilateral regions were used as regions-of-interest (ROI). 3D vector distances (mm) from the individual volumes of tissue activated to the group-level hot spot were calculated between the ROI and individual volume of tissue activated centers of gravity for both sides separately and then averaged.

## 4.5 Statistical analysis

SPSS Statistics (IBM, SPSS Inc., Chicago, IL, USA) was used for statistical analyses in studies I (version 24), III (version 26), IV (version 26) and V (version 27). The level of significance was set at $P<0.05$. In study V, voxelwise analyses were performed with SPM. Cluster-level false discovery rate (FDR)-corrected p-values of less than 0.05 were considered significant.

*Study I*. Mean and standard deviation (SD) were calculated to describe the data. Correlation analyses were performed with Spearman's rank-correlation coefficients or Pearson's partial correlation coefficients, as appropriate.

*Study III*. Data were described as mean (SD) or n. The Shapiro-Wilk test together with histograms was used to test the assumption of normality. Differences between the groups were tested with independent samples t-test, Mann-Whitney U-test, Chi-square test or Fisher's exact test as appropriate. Bonferroni corrections was used to correct for three comparisons (brain regions) and for nine comparisons (symptom scales and comparisons). One-way ANOVA with Tukey's HSD test to correct for multiple comparisons was used to investigate the differences between three different SPECT systems. Levene's test was used to test equality of variances. Differences in occipital binding between VP patients, other patients and healthy controls were also studied with the Kruskal-Wallis test. Correlations were analyzed with Spearman's rank-correlation coefficients or Pearson's correlation coefficients.

*Study IV*. Demographic data was described as a mean and SD or range. Comparisons in TWSTRS scores and BFMRDS movement scores between the time points within the group was conducted using paired samples t-test. In addition, percentage changes of TWSTRS points were calculated to illustrate the changes. Effects of assessment order and characteristics between the subgroups were analyzed with Mann-Whitney U test or Fisher's exact test, as appropriate. Correlations were also analyzed with Spearman rank order correlation or a point-biserial correlation coefficients.

*Study V*. Statistical analyses of demographic data and comparisons of clinical evaluations were performed similar to study IV. Correlation analyses were conducted with Pearson correlation coefficients. Voxelwise analyses were performed with SPM. Voxels with an average 18F-FDG ratio >/= 0.5 within the

standard FSL brain mask were used to create a whole brain analysis mask. One-sample t-test with ON-OFFratio images was used to study the effects of DBS FDG-ON vs FDG-OFF without covariate and when age, dystonia age of onset, age at DBS surgery, dystonia duration, delay from surgery to the best clinical response or acute change in motor symptom severity were also used as a covariate. Voxelwise linear regression was used to study the associations between the changes in regional brain glucose metabolism and acute motor symptom improvement and the overall best treatment response. Moreover, voxelwise linear regression was also used to study the associations between brain metabolism during the stimulation (FDG-ON images) and symptom severity during the stimulation (ON). The significant clusters resulting from the linear regression analyses were used as ROIs to extract regional 18F-FDG ratios to illustrate the magnitudes and directions of the effects (not for statistical testing of any hypothesis).

## 4.6 Ethics

The studies were conducted according to the principles of the Declaration of Helsinki. The studies were approved by the Ethics Committee of the Hospital District of the Southwest Finland (permission numbers 86/1803/2018 for study I, 15/1801/2019 (GAMDAT) and 145/1801/2013 (NMDAT) for study III, 135/1801/2018 for studies IV–V) except for study II because ethical approval is not required for clinical case reports according to the institutional policies and current legislation. All participants in studies III–V gave written informed consent upon the participation in the study. Written informed consent is not required for retrospective studies or clinical case reports in our institution.

# 5 Results

## 5.1 Putaminal axons and DAT binding in Parkinson's disease (study I)

The demographic and clinical characteristic of the patients are shown in Table 4. The mean interval between scanning and death was 5.2 (SD 3.4) years in all patients (n=14) and in PD patients (n=10). Results were also separately analyzed for the patients with a shorter interval (3.2 (1.6) years, n=9).

**Table 4.** Demographical and clinical characteristics of all patients, PD patients and patients with shorter interval between scanning and death. Values are mean (SD) or n.

| Variable | All patients (n=14) | PD patients (n=10) | Patients with shorter interval (n=9) |
|---|---|---|---|
| Sex (m/f) | 12/2 | 9/1 | 8/1 |
| Diagnosis (PD/MSA/PSP/CBD) | 10/1/2/1 | 10/0/0/0 | 6/1/1/1 |
| Age at death (years) | 71 (9.4) | 74 (6.7) | 70 (9.6) |
| Motor symptom duration at scanning (years) | 1.5 (1.3) | 1.7 (1.5) | 1.6 (1.6) |
| Interval between scan and death (years) | 5.2 (3.4) | 5.2 (3.7) | 3.2 (1.6) |
| Interval between death and autopsy (days) | 5.1 (2.2) | 5.2 (2.5) | 4.2 (2.2) |
| Interval between autopsy and neuropathological examination (days) | 30.1 (9.6) | 32.9 (9.3) | 29.7 (10.9) |
| Putamen SBR | 1.82 (0.62) | 1.84 (0.66) | 1.67 (0.72) |
| Anterior putamen SBR | 2.30 (0.80) | 2.40 (0.89) | 2.15 (0.91) |
| Posterior putamen SBR | 1.27 (0.49) | 1.21 (0.48) | 1.19 (0.60) |
| Number of putamen TH+ fibers | 417 (193) | 466 (209) | 483 (173) |

No correlation was found between the putamen SBRs and the total putamen TH+ fiber counts in all patients (r=0.00, p=1.0, Figure 6A), in PD patients (r=0.07, p=0.86, n=10) or in patients with a shorter interval between death and autopsy (r=0.21,

p=0.62, n=9). Neither mean, anterior or posterior putamen SBRs correlated with fiber counts in any of the six putaminal subregions in all patients (r=-0.24–0.11, p>0.42), in PD patients (r=-0.29–0.23, p>0.43) or in patients with a shorter interval (r=-0.28–0.33, p>0.38). Correlations remained non-significant between the putamen SBRs and the total putamen fiber counts when the time intervals between scanning and death, death and autopsy or autopsy and neuropathology were used as covariates (r=-0.02–0.27, p>0.37 in all patients, r=-0.29–0.6, p>0.09 in PD patients and r=0.21–0.44, p>0.28 in patients with shorter interval). The results also remained similar when symptom duration at the time of the scan or the scanner or the tracer was used as a covariate (r=0.06–0.34, p>0.31, r=-0.09–0.31, p>0.45 and r=0.23–0.5, p>0.20, respectively).

The number of nigral TH-positive neurons (counted from 12 out of 14 patients in Saari et al. 2017) correlated with the medial and central putamen fiber count in all patients (central in craniocaudal direction: r=0.65, p=0.02, Figure 6B) and in PD patients (medial, r=0.68; P=0.04; central in craniocaudal direction: r=0.80, p=0.01).

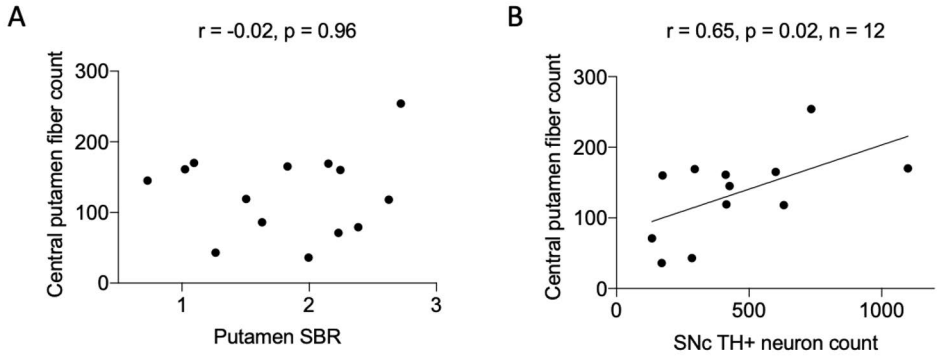


**Figure 6.** Scatter plots demonstrating **A**) the non-significant correlation between the putamen SBR and central putamen fiber count and **B**) the significant correlation between the SNc and central putamen TH-positive neuron counts.

## 5.2 Effect of bupropion on DAT binding (study II)

Clinical examination of the patient showed mild bradykinesia in the left hand, mild slowness in his foot-tapping rate and reduced stride length. The patient underwent brain MRI, brain FDG-PET and blood and urine tests, which all were evaluated as normal. Neuropsychological tests showed loss in memory functions and problems with concentration. Due to mild but uncertain symptoms of parkinsonism, especially asymmetric bradykinesia, the patient was scanned with [123I]FP-CIT SPECT. As instructed in clinical routine, bupropion was discontinued 7 days prior to scanning due its affinity to the dopamine transporter. DAT binding was found to be reduced bilaterally but especially in the left putamen (left putamen SBR 1.99 [standard

deviation from the reference value mean (SD) −2.40], right putamen SBR 2.27 [SD −1.84], left caudate SBR 2.33 [SD −2.26], right caudate SBR 2.29 [SD −2.18]) (Fig 7A).

Levodopa treatment with 450mg/d was initiated without a response after scanning. Considering this lack of levodopa response and previously used bupropion, DAT SPECT imaging was performed again 11 months after the first scan. This time, bupropion was discontinued 4 weeks before the scanning and replaced by agomelatine (25 mg/d) because of the long discontinuation. The follow-up scan was analyzed with identical methods with the first scan. Both the visual analysis and SBRs of the follow-up scan were interpreted as normal (left putamen SBR 2.62 [SD −1.09], right putamen SBR 2.50 [SD −1.37], left caudate SBR 2.45 [SD −2.01], right caudate SBR 2.57 [SD −1.62]) (Fig. 7B). SBRs increased in the follow-up scan by 31.7% in left putamen, 10,1% in right putamen, 5,2% in left caudate and 12,2% in right caudate. Between the two scans, there were no differences in the Montgomery Asberg Depression Rating Scale (1. scan: 37/60 vs follow-up scan: 39/60) or in non-specific background binding of scanning (117,26 counts/voxels and 117,26, respectively).

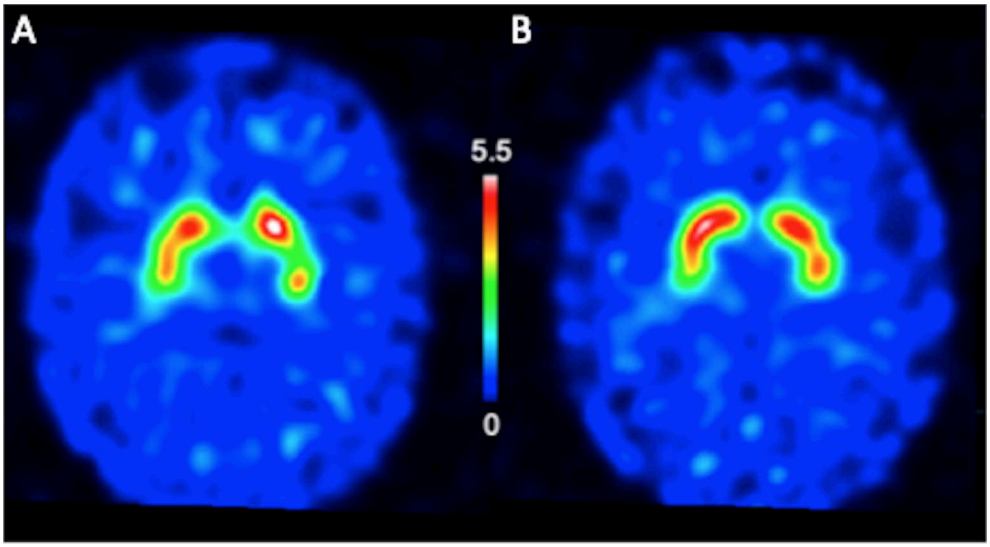


**Figure 7.** Representative images of first scan (**A**) with abnormal results and follow-up scan with normal results (**B**).

## 5.3 Comparison of DAT binding between healthy controls and patients with symptomatic parkinsonism (study III)

All the demographic and clinical data of the patients is presented in Table 5. Symptomatic patients had higher DAT binding in the posterior putamen (p=0.01, Bonferroni corrected p=0.03, Table 5, Fig 8A). Similar trend was also found in the caudate and anterior putamen (caudate p=0.05, anterior putamen p = 0.03, Table 5, Fig 8A) although the difference was not significant after multiple corrections (Bonferroni corrected p-values 0.13 and 0.08 respectively). Symptomatic patients had significantly higher scores on the motor and non-motor symptom scales and on the depression and anxiety scales, and they scored lower on the MMSE compared to healthy individuals (Table 5, Fig 8B–E).

**Table 5.** Demographical and clinical characteristics of the subjects.

| | **Healthy subjects (n=40)** | **Symptomatic patients (n=69)** | **P value[1]** | **Corrected P value[2]** |
|---|---|---|---|---|
| Age (years) | 65.5 (10.7) | 66.8 (9.0) | 0.99 | |
| Sex (male/female) | 34/35 | 21/19 | 0.75 | |
| MDS-UPDRS-motor score | 37.1 (15.0) | 6.6 (5.5) | <0.001 | <0.001 |
| NMSS total score | 67.8 (53.9) | 16.2 (16.5) | <0.001 | <0.001 |
| RBD (yes/no) | 13/51 | 5/35 | 0.31 | 1.00 |
| Constipation | 1.4 (3.2) | 0.5 (1.5) | 0.22 | 1.00 |
| Hyposmia | 2.2 (3.7) | 0.3 (1.4) | 0.002 | 0.02 |
| MMSE | 26.3 (2.6) | 28.0 (2.1) | <0.001 | <0.001 |
| BDI | 8.5 (8.1) | 2.6 (3.9) | <0.001 | <0.001 |
| BAI | 11.8 (7.6) | 4.2 (4.4) | <0.001 | <0.001 |
| BIS-11 total | 60.4 (7.5) | 56.8 (6.0) | 0.02 | 0.14 |
| Caudate SBR | 2.74 (0.43) | 2.58 (0.32) | 0.04 | 0.13 |
| Anterior putamen SBR | 2.65 (0.39) | 2.49 (0.33) | 0.03 | 0.08 |
| Posterior putamen SBR | 2.37 (0.38) | 2.18 (0.32) | 0.01 | 0.03 |

[1]Mann-Whitney U-test, independent samples t-test or Chi-Square test. [2]Bonferroni correction for nine (UPDRS, NMSS, RBD, Constipation, Hyposmia, MMSE, BDI, BAI, BIS-11 total) or 3 (SBRs) comparisons. Values are means (SD) or n. Numbers of missing values: UPDRS=1, RBD=5, NMSS total score=2, Constipation=2, Hyposmia=2, MMSE=1, BDI=7, BAI=18, BIS11-total=20.

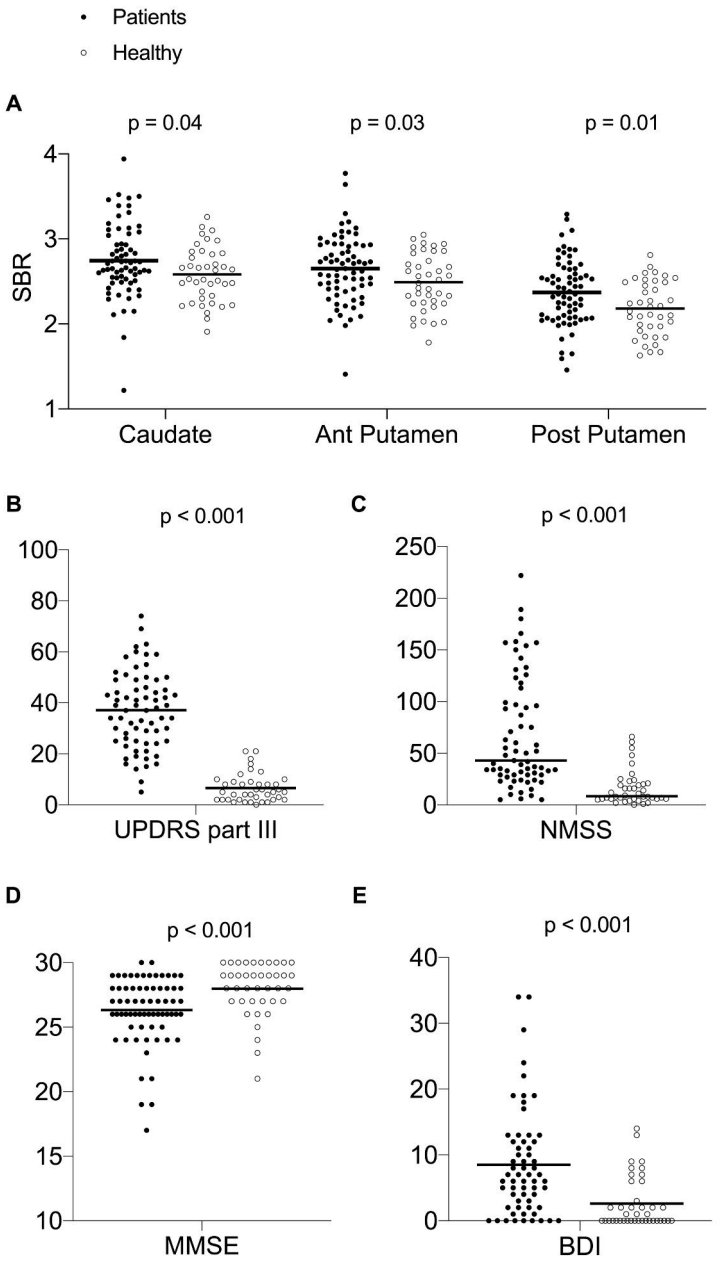


**Figure 8.** Differences between symptomatic patients and healthy controls in DAT binding (**A**), motor symptoms (**B**), non-motor symptoms (**C**), cognitive function (**D**) or depression points (**E**).

DAT binding was negatively associated with age in the posterior putamen in healthy controls and in all regions in patients (Table 6). DAT binding did not correlate with the MDS-UPDRS score, MMSE or BDI in either group (Table 6). The results remained non-significant when age was used as a covariate (healthy r=-0.06 to 0.27, p>0.10; patients r=-0.01 to 0.16, p>0.22).

**Table 6.** Correlations between mean regional DAT binding and age, MDS-UPDRS motor scores, NMSS, MMSE, BDI in healthy controls and symptomatic patients. * p-value<0.05

| | | **Healthy controls** | | **Symptomatic patients** | |
|---|---|---|---|---|---|
| | | r | P value | r | P value |
| Caudate | Age | -0.25 | 0.11 | -0.39 | <0.001* |
| | MDS-UPDRS motor | 0.07 | 0.67 | -0.04 | 0.72 |
| | MMSE | 0.05 | 0.78 | 0.09 | 0.49 |
| | BDI | 0.16 | 0.34 | 0.20 | 0.12 |
| Anterior | Age | -0.17 | 0.30 | -0.36 | 0.003* |
| Putamen | MDS-UPDRS motor | 0.14 | 0.38 | 0.03 | 0.78 |
| | MMSE | 0.15 | 0.37 | -0.04 | 0.78 |
| | BDI | 0.22 | 0.17 | 0.20 | 0.12 |
| Posterior | Age | -0.33 | 0.04* | -0.29 | 0.02* |
| Putamen | MDS-UPDRS motor | 0.01 | 0.97 | -0.06 | 0.61 |
| | MMSE | 0.15 | 0.37 | 0.05 | 0.70 |
| | BDI | 0.20 | 0.21 | 0.08 | 0.54 |

The final diagnoses of symptomatic patients after mean follow-up time of 43.5 (SD 19.3) months were ET (n=27), DIP (n=12), VP (n=7) and other non-degenerative diagnosis such as dystonia, functional movement disorder and depression (total n=23). Comparisons between three main subgroups (ET, DIP, VT) and healthy controls revealed that ET patients had a higher DAT binding in posterior putamen (p=0.009), while no other differences in DAT binding were found (p>0.06). The differences in DAT binding remained similar or even increased between the healthy controls and the symptomatic patients when the healthy controls with a positive family history of PD (n=6) were excluded (11.3% difference in the posterior putamen, p=0.002, Bonferroni corrected p=0.006) or when patients with SSRI/SNRI medication (n=10), VP (n=7) and DIP (n=12) were excluded (8.7% difference in the posterior putamen, p=0.008, Bonferroni corrected p=0.02). No differences were seen in occipital binding values between healthy controls and symptomatic patients (p=0.24) or SBRs obtained with different SPECT systems (p>0.06).

## 5.4 Motor symptom severity after the discontinuation of GPi-DBS in cervical dystonia (study IV)

Table 7 presents the main demographic features of all the studied patients and patients with only cervical symptoms (n=10).

**Table 7.** Demographical and clinical data of all the studied patients and patients with only cervical symptoms (CD only). The table is modified from study IV.

| | **All patients (n=12)** | **CD only (n=10)** |
|---|---|---|
| Sex (male/female) | 6/6 | 4/6 |
| Age (years) (mean (SD)) | 52.8 (8.1) | 53.1 (8.6) |
| Age of onset | 40.7 (6.5) | 41.0 (6.3) |
| Age at the surgery | 50.1 (7.3) | 50.3 (8.0) |
| Dystonia duration (years) | 12.2 (6.5) | 12.1 (7.1) |
| Duration of DBS treatment (years) | 2.8 (1.7) | 2.8 (1.7) |
| Best DBS response (%) | 82.3 (21.8) | 78.7 (22.3) |
| Delay to best DBS response (months) | 5.6 (4.4) | 6.5 (4.3) |
| Deep brain stimulation: Amplitude (V) | 2.7 (0.7) | 2.6 (0.8) |
| Pulse Width (us) | 208 (85) | 220 (88) |
| Frequency (Hz) | 83 (42) | 82 (41) |

At the time of the study, DBS treatment response was maintained at 67 (SD 39)% from the preoperative symptom severity and did not differ from the best postoperative DBS response (mean (SD) TWSTRS severity scale postop 3.6 (4.7) vs TWSTRS severity scale ON 4.9 (5.6) points, p=0.47). Immediately after DBS was switched off, treatment response reduced to 27 (53)% (ON 4.9 (5.6) vs OFFacute 10.2 (7.7) points, P=0.046). After 2 days stimulation off, treatment response further worsened to 4 (56)% (OFFacute 8.5 (5.6) vs. OFFchronic 13.7 (7.4) points, P=0.01, n=11) and was similar to preoperative symptom severity (OFFchronic 13.7 (7.4) vs preop 15.8 (8.0) points, P=0.42) (Figure 9A).

The results remained similar in patients with cervical symptoms only (n=10). Treatment response at the time of the investigation (79 (22)%) did not differ from the best postoperative response (TWSTRS postop 4.9 (1.5) vs ON 5.4 (1.7), p=0.87). This response was lost to 39 (42)% immediately after the discontinuation (ON 4.6 (5.4) vs OFFacute 8.5 (5.9) points, P=0.004) and was reduced to 10 (54)% after two days (OFFacute 8.5 (5.9) vs OFFchronic 13.3 (7.6) points, P=0.02). Symptom severity at 2 days follow-up did not differ from presurgical level (OFFchronic 13.3 (7.6) vs preop 16.3 (8.3) points, P=0.27) (Figure 9A).

In addition to TWSTRS severity scale, TWSTRS total scores increased significantly after switching DBS off, but no significant differences were found in disability or pain scales between ON, OFFacute and OFFchronic evaluations (Figure 9B). The results remained similar for patients with cervical symptoms only (n=10), except the difference in total scores between the OFFacute and OFFchronic just failed to reach significance (p=0.06).

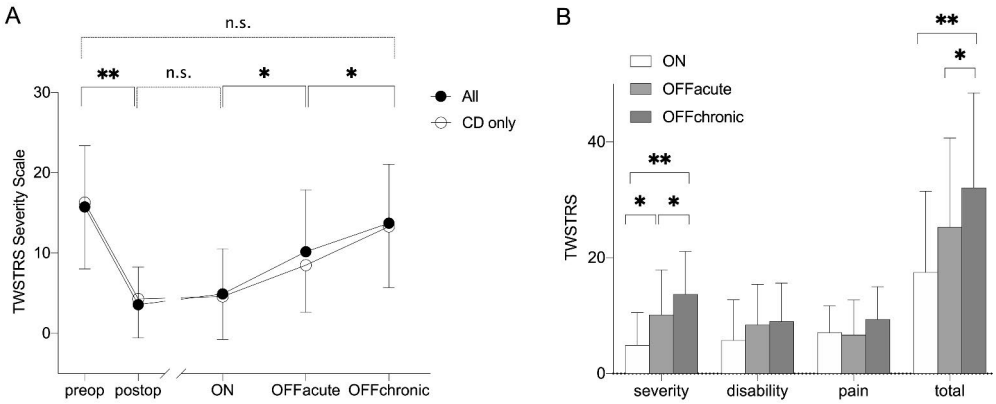


**Figure 9.** Toronto Western Spasmodic Torticollis Rating Scale (TWSTRS) severity scale increased to the preoperative level after 2 days discontinuation of DBS (**A**). Disability scale, pain scale and total scores increased during the 2 day follow-up in all patients (**B**). The figure is modified from study IV.

BFMDRS movement scores were significantly higher in OFFchronic compared to ON (mean (SD) BFMDRS OFFchronic 4.5 (3.4) vs ON 1.4 (1.9), p=0.003, n=11) and to OFFacute (OFFchronic 4.5 (3.4) vs OFFacute 1.8 (2.3), p=0.005, n=11). Similar to patients with cervical symptoms only, BFMDRS movement scores were higher in OFFchronic compared to ON (OFFchronic 3.9 (3.0) vs ON 1.3 (1.9), p=0.006) and to OFFacute (OFFchronic 3.9 (3.0) vs OFFacute 1.7 (2.4), p=0.008).

In the additional analyses, milder acute symptom worsening was associated with younger dystonia age of onset (r=0.71, p=0.01), younger age at the time of surgery (r=0.60, p=0.04) and at the study r=0.63, p=0.03). Instead, no other association were found between TWSTRS changes and demographic or clinical features such as presurgical symptom severity, symptom type (phasic vs tonic), DBS parameters, treatment duration or treatment response.

The order of the ON and OFFacute evaluations did not affect the TWSTRS or BFMDRS raw scores (p>0.2) or the relative or total changes in TWSTRS scores (p>0.1).

## 5.5 Effect of GPi-DBS on brain glucose metabolism in cervical dystonia (study V)

All volumes of tissue activated located in GPi showing correct lead positions (Figure 10A). A higher amplitude correlated with the larger stimulation-induced increase in brain glucose metabolism at the stimulation site (r=0.70, p=0.03, Figure 10B). However, there were no correlations between the change in local glucose metabolism and lead distance from the group level stimulation site (r=0.22, p=0.54), acute motor symptom improvement (r=-0.06, p=0.9) or overall treatment response (r=0.02, p=0.9).

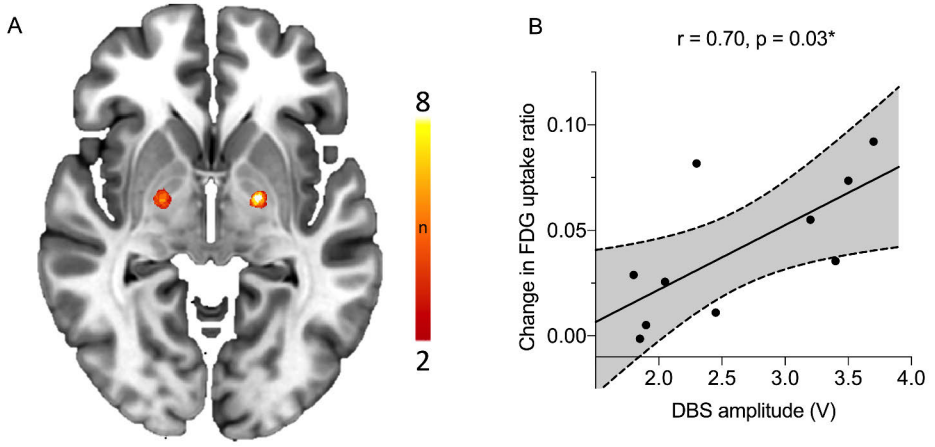


**Figure 10.** Volumes of activated tissue. **A**. red-yellow color scale sum image of all patients showing the lead positioning. **B**. Greater local change in glucose metabolism was associated with higher DBS amplitude.

Standardized uptake values (SUVs) did not differ between the FDG-ON and FDG-OFF (p=0.14). In voxelwise whole brain analyses, DBS induced an increase in regional glucose metabolism bilaterally at the stimulation sites (Figure 11). Increased glucose metabolism was also observed in the STN, putamen, insula, primary motor cortex and primary somatosensory cortex (Figure 11). When age at the study, dystonia age of onset, age at DBS surgery, dystonia duration, delays to best DBS response or acute motor symptom improvement was used as a covariate, results remained similar. No significant decrease in regional brain glucose metabolism was found.

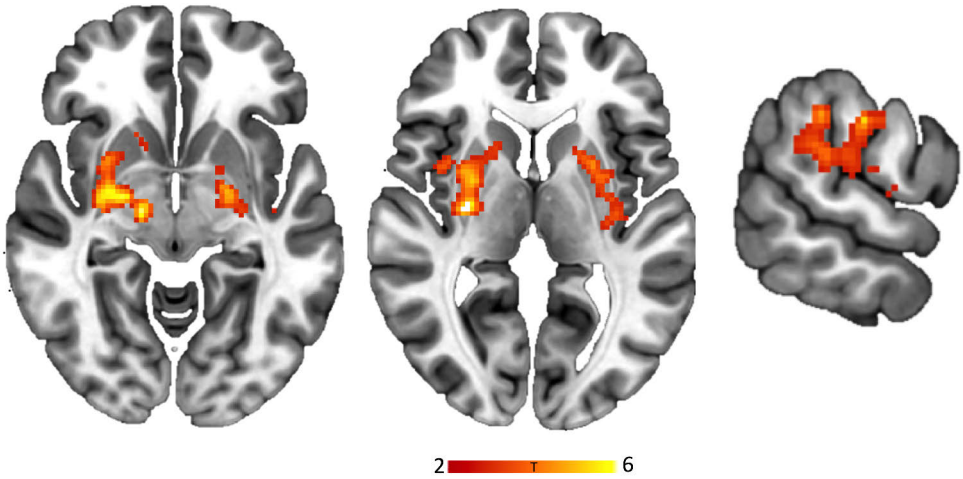


**Figure 11.** Regions with significant increase in glucose metabolism induced by GPI-DBS. Subcortical clusters covered bilaterally the stimulation site and extended to STN, putamen and insula. Cortical clusters covered primary motor and somatosensory cortices.

Significant correlation was found between the acute motor symptom improvement (TWSTRS severity scale OFFacute vs ON) and DBS-induced increased regional metabolism in the left sensorimotor cortex (Figure 12A). The better overall treatment response instead predicted a greater increase in metabolism in SMA (Figure 12B).

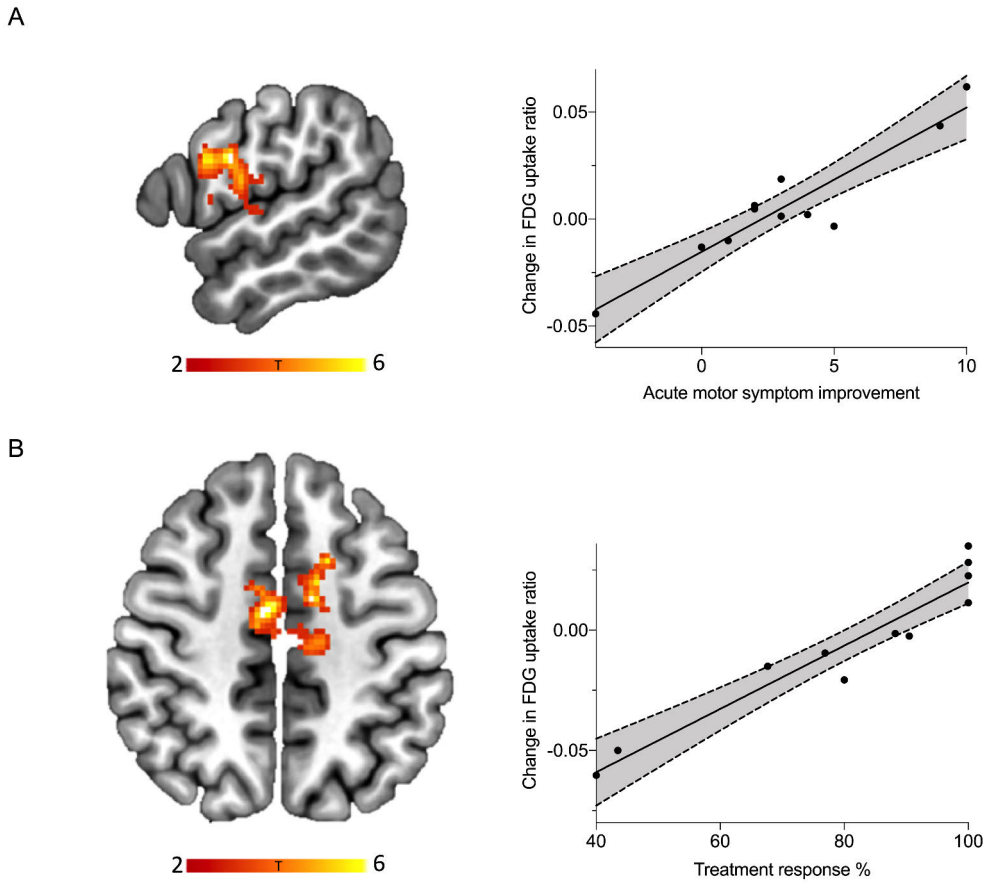


**Figure 12.** Correlations between symptom improvement and DBS-induced change in regional brain glucose metabolism. **A**. Acute motor symptom improvement correlated positively with an increase in metabolism in S1/M1 (r=0.94). **B**. Best overall treatment response was associated with increased glucose metabolism in SMA (r=0.96).

# 6 Discussion

## 6.1 Striatal dopamine transporter binding in parkinsonism

### 6.1.1 Neuropathological correlates of dopamine transporter imaging (study I)

This study showed no correlation between the number of putaminal dopaminergic axons and putaminal DAT binding in PD. This represents the first study to investigate the association between the number of putaminal axons and putaminal DAT binding in humans. A previous study showed a lack of correlation between the nigral cell counts and striatal DAT binding (Saari et al., 2017). However, the striatal DAT binding may not be associated with the nigral neurons due to the retrograde degeneration damaging the striatal terminals prior the nigral somas, so this study could have detected a possible correlation (Kordower et al., 2013; Tagliaferro & Burke, 2016). A correlation between putaminal fibers and putamen DAT binding would have proved the role of DAT as a reflection of viable putaminal axons. However, these findings now suggest that DAT binding preferably reflects more dopaminergic activity or synaptic dopamine levels rather than the number of neurons in PD patients with motor symptoms of mean 1.5 years at the time of the scanning and approximately 50% loss in DAT binding compared to healthy subjects (Kaasinen & Vahlberg, 2017).

Animal studies with 1-methyl-4-phenyl-1,2,3,6-tetrahydropyridine (MPTP) treated monkeys are in line with the results as they have found no correlations between striatal fibers and striatal PET measures (Shimony et al., 2018; Tian et al., 2014). An association between the number of nigral cells and striatal DAT binding has been found (Tian et al., 2014), but this correlation disappeared when the nigral loss exceeded 50% (Karimi et al., 2013). Clinicopathological imaging studies in humans are rare. Only three previous studies evaluated the correlation between the nigral neurons and striatal dopaminergic imaging (Colloby et al., 2012; Kraemmer et al., 2014; Snow et al., 1993). Contrary to non-significant nigral findings (Saari et al., 2017), these previous studies showed significant associations between nigral neuronal counts and striatal dopamine synthesis capacity (Snow et al., 1993) or

striatal DAT binding (Colloby et al., 2012; Kraemmer et al., 2014). However, those studies included a rather small but a specifically very heterogenous sample of different pathologic conditions such as PD, PSP, MSA, CBD, AD, LBD, amyotrophic lateral sclerosis (ALS) and Creutzfeldt-Jakob disease. In fact, patients with normal dopaminergic function in the imaging were also included, which might influence the results.

Taking all this into consideration, it could be argued that DAT is probably not an essential biomarker of the viable nigrostriatal track, at least after a certain level of nigrostriatal damage. However, further data are required to confirm these findings.

### 6.1.2 Effect of bupropion on DAT imaging interpretation (study II)

Bupropion interfered with the DAT binding even after the recommended break in medication and caused an abnormal result in DAT binding imaging in this case report. A four-times longer bupropion wash-out time normalized the results in the follow-up scan.

According to Medicine Agencies of Europe and US, several drugs, including, for example sertraline, bupropion, amphetamine, benztrotropine, cocaine, methylphenidate and phentermine, can influence the [123I]FP-CIT tracer binding (*Highlights of prescribing information for DatScan ioflupane I 123 injection*, Revised 2015; *Product information for DatScan ioflupane I 123 injection.* , Updated 2017). These potentially interfering medications are recommended to be stopped at least 5 plasma clearance half-lives before scanning (Booij & Kemp, 2008). Bupropion is a norepinephrine-dopamine reuptake inhibitor and nicotinic receptor antagonist used to treat depression or to support smoking cessation (Foley et al., 2006). Its plasma clearance half-life is approximately 20 hours (Foley et al., 2006), suggesting that only a 5-day washout should be sufficient to reduce the potential interference with DAT imaging. However, the recommended wash-out time in many imaging centers is from 7 to 10 days, and in this case, the patient was instructed to discontinue his daily 150 mg dose of bupropion 7 days prior to the first scanning.

A case report recently described a 45–50% decline in DAT binding throughout the striatum during an active bupropion medication, but it normalized after an 8-day discontinuation of bupropion (Milenkovic et al., 2021). On the contrary and in line with the case of this thesis, Lin and Lane have previously described the sustained effect of bupropion on another dopamine transporter tracer, Tc-99m TRODAT-1, even after 14 days of stopping the medication (Lin & Lane, 2017). However, in all these cases, including the present case, a deficit of DAT binding was not typical for neurodegenerative disorder (PD or LBD) as it presented bilaterally (Lin & Lane,

2017), throughout the whole striatum (Milenkovic et al., 2021) or in anterior putamen (our study).

The potential drug effects on DAT binding should be taken into consideration as it reduces the likelihood of DAT imaging leading to a false positive diagnosis of neurodegenerative disease. Even though there seems to be individual variability in the affinity of DAT in the patients using bupropion, a relation between the medication and the interference seems to be clear and therefore the sufficient wash-out, even one month, is recommended to avoid a misdiagnosis.

### 6.1.3 Differences in DAT binding between symptomatic patients with non-degenerative parkinsonism and healthy subjects (study III)

In this study, symptomatic patients had higher striatal DAT binding than healthy individuals. This finding may be explained by selection bias, self-selection bias or upregulation of DAT. However, the findings emphasize the importance of a careful selection of the controls in neuroimaging trials to avoid errors in conclusions.

Neuroimaging trials with DAT imaging have regularly used symptomatic patients with non-degenerative conditions as a control group. Diagnoses may be directed by DAT imaging in these cases, because normal presynaptic dopaminergic imaging is considered as an absolute exclusion criterion for PD by MDS (Mirpour et al., 2018; Postuma et al., 2015). This can lead to a selection bias as these symptomatic controls may represent dopaminergically overly healthy individuals, while healthy individuals are unselected and also include the borderline results in DAT binding.

However, due to self-selection bias, healthy controls might have volunteered more actively if they represented hypodopaminergic conditions (Hernán et al., 2004). It has been previously shown that individuals with novelty- seeking personality traits volunteer more actively in PET imaging studies (Oswald et al., 2013), and young men are the most willing to participate in brain MRI studies (Ganguli et al., 2015). Moreover, educated women were the most interested in participating in the study focusing on aging and cognition (Ganguli et al., 1998). However, there were no associations with the lowest binding values and highest motor, non-motor, prodromal or premotor symptoms or impulsivity-related test in the present healthy control group, this is why it is unlikely that these individuals represent prodromal PD patients.

There is evidence suggesting that DAT can be upregulated or downregulated in different conditions. DAT upregulation is seen during the short-term amphetamine exposure, while DAT is found to be downregulated after longer use of amphetamine and in conditions such as PD, attention deficit hyperactivity disorder (ADHD) and

bipolar disorder.(Vaughan & Foster, 2013) Taking into consideration the heterogeneity of diagnoses of our symptomatic controls, upregulation of DAT in all these conditions seems unlikely, but this possibility cannot be excluded.

### 6.1.4 Limitations

*Study I.* Main limitation of this study is the small number of patients, although the clinicopathological data are rare. Nevertheless, the sample was comparable to previous studies in humans (Colloby et al., 2012; Kraemmer et al., 2014; Snow et al., 1993). It should also be stressed that the fiber counting was not performed with an unbiased stereological method. The counting was conducted manually, yet there was good to excellent inter-rater reliability of the measurement by two independent investigators. Putaminal fibers were also associated with the nigral neurons, suggesting that the method and the sample size were sufficient to detect correlations. Finally, the limitation of clinicopathological data in human is the time interval between the measurement, which limits the interpretation of this study. Nevertheless, it was used as a covariate in the analyses, and analyses were also conducted separately in the patients with shorter and longer intervals. However, studies with a shorter interval and with patients in the early stages of PD are greatly needed.

*Study II.* Case report has its limitations as it presents the anecdotal evidence of an individual patient with no statistical sampling. However, in this case, the same patient was scanned twice with identical methods only 11 months apart and only clear change between the scans was the wash-out time of bupropion. It can be argued, considering this, that this case report plays its role as representing a novel and useful finding. However, it cannot be excluded that there were some unrecognized factors that may have influenced the results.

*Study III.* The subjects were scanned with 3 different SPECT systems. There were no differences in DAT binding in this study or in previous similar studies with the same scanners (Jaakkola et al., 2017; Jaakkola et al., 2019; Kaasinen et al., 2014; Mäkinen et al., 2019; Mäkinen et al., 2016), but this should be considered a limitation. More studies are needed to confirm these findings, preferably scanned with one SPECT system and recruiting bigger samples.

Section 6.2.3 presents the limitations of studies IV–V.

## 6.2 Pallidal stimulation in cervical dystonia

### 6.2.1 Motor symptom severity after GPi-DBS discontinuation (study IV)

This study showed a two-phased reappearance of symptoms in cervical dystonia after GPi-DBS was switched off. First, part of the symptoms reappeared immediately after the discontinuation. Second, there was also a slower component that worsened the symptoms, and the preoperative level of symptoms was reached within two days after DBS discontinuation. Symptoms seemed to reappear slower in younger patients, but there were no other demographic or clinical characteristics or DBS settings that predicted the slower worsening. Eleven out of 12 patients tolerated well the discontinuation of DBS.

This is the first study to investigate the reappearance of the symptoms after discontinuation of GPi-DBS in cervical dystonia with more than 5 hours of follow-up. Levin et al. previously reported a well-designed, controlled and double-blind study of the reappearance of cervical dystonia symptoms in a 5-hour timeframe and showed that symptoms worsen within 10 minutes with no further worsening during the next 5 hours (Levin et al., 2014). This is in line with the results of this thesis because no worsening was seen after the immediate reappearance during the next two hours. The evidence of the symptom worsening after discontinuing DBS in other forms of dystonia is mixed and varied from the severe and fast worsening of symptoms to sustained benefit of DBS (Cif et al., 2013; Grabli et al., 2009; Grips et al., 2007; Ruge et al., 2014; Ruge et al., 2011; Vidailhet et al., 2005). (Cif et al., 2013; Grabli et al., 2009; Grips et al., 2007; Ruge et al., 2014; Ruge et al., 2011; Vidailhet et al., 2005). It is noteworthy that the study of segmental dystonia showed rapid symptom reappearance to the preoperative level after DBS was switched off (Grips et al., 2007). This is consistent with this study's finding, because only the segmental dystonia patient had an abrupt worsening of symptoms and did not tolerate the stimulation off. These differences between focal, segmental and generalized dystonia may reflect the different underlying pathophysiology of the conditions (Conte et al., 2019), which highlights the importance of the study focusing on one form of dystonia at the time.

Patients of a younger age at the time of the study, DBS implantation and dystonia onset had a slower symptom reappearance compared to older patients. Younger age in this study seems to predict a sustained effect of DBS after discontinuation; a similar finding was previously described in patients with primary generalized dystonia (Cheung et al., 2013). This may be due to higher plasticity, which has been shown to correlate to the better treatment response of GPi-DBS (Kroneberg et al., 2018) and also to the sustained effect of DBS after cessation (Ruge et al., 2011).

Secondary dystonia due to a brain lesion may also take months to years to develop, indicating that the slow neuroplastic changes tend to play a role in pathophysiology of dystonia (Corp et al., 2019). These slowly occurring neuroplastic changes may also be one potential explanations of the slow treatment response of GPi-DBS.

### 6.2.2 Stimulation-induced changes in regional brain glucose metabolism (study V)

Main findings of the study showed that GPi-DBS in cervical dystonia induces an increased brain glucose metabolism at the stimulation site and additionally in the subthalamic nucleus, putamen and primary sensorimotor face/neck representation area in the cortex. No reduced metabolism was induced by GPi-DBS. The increased metabolism at the stimulation site was associated with the level of stimulation amplitude but not with the therapeutic response either acutely or long-term. The acute motor symptom improvement was related instead to increased metabolism in the sensorimotor cortex and the best treatment response in the SMA.

This is the first study to investigate the stimulation-induced changes in brain glucose metabolism in dystonia. Only molecular imaging study of DBS in focal dystonia was conducted by Greuel et al, who did not find stimulation-linked effects on brain regional blood flow in 6 patients with GPi-DBS (Greuel et al., 2020). Other studies reported variable changes in rCBF due to stimulation in patients with generalized, secondary, tardive, or mixed forms of dystonia (4 studies, n=5-7 in each) (Detante et al., 2004; Katsakiori et al., 2009; Thobois et al., 2008; Yianni et al., 2005). These mixed results could be related to small sample sizes including heterogenous forms of dystonia, but also variable and early PET imaging analysis methods.

These results support the hypothesis that dystonia is a network-wide brain dysfunction rather than only basal ganglia dysfunction (Jinnah et al., 2017). A stimulation induced increased glucose metabolism was also seen in the stimulation site, globus pallidus interna and also in the other basal ganglia structures such as putamen and STN and it also extended to cortical areas in S1/M1 cortex. The stimulation of GPi also activates the STN, which are both parts of the indirect pathway of basal ganglia (Albin et al., 1989; DeLong, 1990). The local increase at the stimulation site was associated with the stimulation amplitude but not with the acute motor symptom improvement or the best treatment response, which could also be explained by a network wide effect of GPi-DBS(Corp et al., 2019). This is the first study to investigate if these local changes correlate to therapeutic responses, but no correlation was found in the present study.

In line with motor network model in dystonia suggesting that different forms of dystonia may involve different brain regions (Jinnah et al., 2017), an acute motor

symptom improvement was coupled in this study with stimulation-induced increased glucose metabolism in S1/M1 in the face/neck representation region (Penfield & Boldrey, 1937). A normalized function in the primary motor and premotor cortex has also been recently shown by a sensory trick in dystonia, supporting the hypothesis that this region has an impact on the acute symptom improvement (Shin et al., 2021). A long-term therapeutic efficacy correlated with stimulation-induced metabolism in SMA, which is known to play a major role in initiation of movements (Shibasaki, 2012). Several previous studies have shown abnormalities in SMA in dystonia (Ceballos-Baumann, Passingham, Marsden, et al., 1995; Ceballos-Baumann, Passingham, Warner, et al., 1995; Eidelberg et al., 1998; Jiang et al., 2019; Naumann et al., 2000; Pan et al., 2019). Recently, connectivity from the GPi to the S1/M1 cortex and the SMA/premotor cortex was related to motor symptom improvement in generalized dystonia (Okromelidze et al., 2020) suggesting that these brain regions may play a critical role in a motor symptom improvement in dystonia.

### 6.2.3 Limitations

The sample size of this study was relatively small, although it was comparable to previous studies of motor symptoms reappearance after DBS discontinuation(Cif et al., 2013; Grabli et al., 2009; Grips et al., 2007; Ruge et al., 2014) and largest of the current dystonia DBS-PET imaging studies (Detante et al., 2004; Greuel et al., 2020; Katsakiori et al., 2009; Thobois et al., 2008; Yianni et al., 2005). However, it might have prevented this study from having sufficient statistical power to detect subtle changes in TWSTRS scales, associations between the symptoms change and clinical parameters or metabolism changes induced by GPi-DBS. In addition, two days without stimulation might not be long time enough to detect changes in TWSTRS disability or pain scales.

The study design did not allow for blinding the patients or investigator, but the order of ON and OFF visits was pseudorandomized. Counterbalancing of the visits were not equal (8 patients were studied first ON, 4 patients OFF) due to logistic issues of the imaging center. However, motor symptom scores or changes in regional glucose metabolism were not affected by the order of the visits. All the study evaluations were performed by one clinical investigator (EA Honkanen) while the preoperative and postoperative TWSTRS severity scales were extracted from the hospital records retrospectively. Best postoperative TWSTRS severity score did not differ from ON scores which suggests there were no systematic difference between the ratings.

The implantations were performed months to years prior the study, so all patients were at the stable stage of DBS treatment. All the patients had also achieved at least

a 25% treatment response. This was planned to avoid the confounding effects related to surgery and lesion effects, so it enabled this study to identify immediate stimulation effects in clinically ineffective stimulation.

## 6.3 Future directions

In terms of DAT imaging and parkinsonism, there are still several uncertainties and cofounding factors that may affect the imaging results and the interpretation of the results. As the imaging strongly directs the clinical diagnosis (Catafau et al., 2004), investigating these factors becomes more important. For example, there has been evidence of DAT availability differences between women and men (Eusebio et al., 2012; Lavalaye et al., 2000; Matsuda et al., 2018; Nobili et al., 2013; Varrone et al., 2013; Yokoyama et al., 2017), although the studies are not consistent (Jakobson Mo et al., 2013; Nam et al., 2018; Pak et al., 2018; Werner et al., 2019). The need of sex correction still remains debatable (Schmitz-Steinkrüger et al., 2020).

DBS offers great possibilities to investigate the basal ganglia function with brain imaging. Fulfilling our data with similar brain FDG imaging of healthy controls and DBS-naive dystonia patients would broaden the opportunities to investigate the metabolic effects of dystonia together with the effects of DBS. Perhaps in the future, the role of SMA could also be studied using non-invasive neuromodulation techniques, such as transcranial magnetic stimulation (TMS). Furthermore, studying the local effects to basal ganglia by different DBS targets would expand our understanding of basal ganglia circuits and be of a great interest.

# 7 Summary/Conclusions

The aim of this thesis was to investigate the basal ganglia function in parkinsonism and dystonia using striatal DAT imaging in parkinsonism and FDG-PET in GPi-targeted deep brain stimulation for dystonia.

DAT imaging was not found to correlate with the number of dopaminergic axons in the putamen, suggesting that the DAT imaging may reflect more dopaminergic activity or dopamine level rather than the number of viable neurons. Another study showed that DAT imaging result was compromised by bupropion even after a sufficient and recommended wash-out period of the medication. A third study that compared healthy subjects and symptomatic but dopaminergically healthy patients showed that symptomatic patients had a higher putaminal DAT binding. This paradoxical difference may be explained by the selection bias of symptomatic patients or the self-selection bias of healthy controls and should be taken into consideration when the neuroimaging trials are executed and interpreted. These studies of DAT imaging show that although DAT imaging appears to be an excellent tool for differential diagnosis of neurodegenerative parkinsonism, there are still several factors that should be carefully evaluated when the results are interpreted.

In dystonia, GPi-DBS was shown to be associated with good therapeutic response that was partially lost immediately after the stimulation was switched off. Moreover, there was also a slower component of symptom worsening, and preoperative level was reached by the two days follow-up visit. Brain glucose metabolism was increased at the stimulation sites, in other basal ganglia structures such as STN and putamen and also in the S1/M1 cortex due to stimulation. This local change bilaterally in the GPi was coupled up with the stimulation amplitude but not with therapeutic responses. However, the acute motor symptom improvement was related to stimulation-induced increase in glucose metabolism in S1/M1 and best long-term therapeutic response in SMA. These findings provide novel information about the motor symptom reappearance and the brain network associated with GPi-stimulation and therapeutic responses in cervical dystonia. The pathophysiology of dystonia still remains insufficiently understood and further research is needed to improve the understanding, diagnosis and treatment of these patients.

To conclude, this thesis emphasizes that further investigation is needed to fully characterize the precise cellular counterparts and interfering factors in DAT binding to achieve reliable results. Regarding the basal ganglia-targeted treatments, GPi-DBS induced metabolic changes in dystonia expanded to the sensorimotor cortices that may play an important role in symptom improvement. However, further research is still needed to utilize these results in clinical practice when treating patients suffering from parkinsonian disorders and dystonia.

# Acknowledgements

This thesis was conducted at Clinical Neurosciences of the University of Turku, Neurocenter of Turku University Hospital and Turku PET Centre during 2016–2022. This thesis was funded by the Finnish Parkinson Foundation, Turku University Foundation, Finnish Neurological Society, Finnish Medical Foundation, and Turku University Hospital (VTR-funds).

I would like to express my greatest gratitude and respect to my supervisors associate professor Juho Joutsa and professor Valtteri Kaasinen. I cannot describe how fortunate I feel to have been able to work with you, learn from you, and be supervised by you. Your dedication to the research is contagious. Although you both are highly respected experts in the field, you have always made me feel more like a co-worker. I would also like to thank you for your endless time, continuous support, and the patience you have put up with me although I doubt it has not always been so easy. I admire you greatly.

I must also thank Jaana Korpela. Without you, this thesis would probably not have been started. At the time of my first steps in the world of neurology, you showed me the enthusiasm and expertise which helped me to find my medical path in addition to my PhD supervisors. To date, you are a member of my supervisory committee, my co-author, and mentoring my residency in neurology. I can only owe my wholehearted gratitude to you for all your guidance and support.

I have had the honor to work with amazing co-authors. I want to thank Juho Aaltonen, Hazem Eldebakey, Mikael Eklund, Olli Eskola, Maria Gardberg, Risto Hirvilammi, Elina Jaakkola, Nina Kemppainen, Maija Koivu, Kari Lindholm, Elina Mäkinen, Tommi Noponen, Simo Nuuttila, Katri Orte, Riitta Parkkola, Eero Pekkonen, Martin Reich, Laura Saari, Filip Scheperjans, Marko Seppänen and Andrea Varrone. Thank you for your collaboration. I extend my thanks to Lauri Tuominen, a member of my supervisory committee, for your valuable help during this project. I have had the privilege to conduct this thesis under the excellent facilities in the Turku University Hospital and Turku PET Centre, which I want to thank professors Risto O. Roine, Jaakko Rinne, and Juhani Knuuti. I want to express my great gratitude to associate professor Harith Akram and adjunct professor Mikko Kuoppamäki for their careful and skilled review of this thesis.

I want to thank all my colleagues in our research groups sincerely. Thank you, Elina Jaakkola, Elina Mäkinen, Joonas Majuri, and Tomi Kuusimäki, for all the peer support and especially for being the best company in learning the secrets of the congress life. Laura Saari, Aleksi Kokkonen, Mikael Eklund, and Simo Nuuttila, it has been an honor to walk this research path with you. I want to express my deepest gratitude to research nurses Kari Lindholm and Leena Lauos for your help. The staff in the Department of Nuclear Medicine and in Turku PET Centre are greatly acknowledged for their endless help during the data collection.

I want to thank all my colleagues and the staff in the Department of Neurology in Satasairaala for all the support during 2018–2021. I am most grateful to the former head of the Department, neurologist Juha-Matti Seppä, who made it possible for me to combine clinical work with research during my residency in Pori. Currently I have the privilege to work with colleagues at the Neurocenter in Turku University hospital, and I want to thank you for all the support.

I want to express my wholehearted gratitude to my best friends for always being there for me. I am truly blessed to have so many amazing people around me. Emmi, Marjukka and Tiia, thank you for the friendship since the high school. Karoliina, Heini, Ina, Lara, Anna, Toni, Jukka, Aapo and Touko, thank you for being the best medical school peer support and for taking me on the cottage trips every now and then. Mari, I am thankful for the friendship we created in Pori. I would also like to thank the Ottela family for all your support and love. Jukka, Elina, Emilia, Vilppu, Jussi and Viivi, I feel fortunate to be part of your family. I appreciate all the interest you have shown in my research during all these years.

There are no words to describe my gratitude for my family. My father Aki, mother Tiina, and brother Manu; we all know that there would not be this thesis without you. You have always believed in me, and your endless support has taught me that everything can be achieved. Thank you for showing me the importance and power of loving family. I could not thank or love you enough.

Last and most importantly, I would like to thank Joonas for sharing this life with me. This thesis is dedicated to you. You mean the world to me.

Turku, January 2022
*Emma Honkanen*

# References


Akram, H., Dayal, V., Mahlknecht, P., Georgiev, D., Hyam, J., Foltynie, T., . . . Zrinzo, L. (2018). Connectivity derived thalamic segmentation in deep brain stimulation for tremor. *Neuroimage Clin*, *18*, 130–142. https://doi.org/10.1016/j.nicl.2018.01.008

Akram, H., Sotiropoulos, S. N., Jbabdi, S., Georgiev, D., Mahlknecht, P., Hyam, J., . . . Zrinzo, L. (2017). Subthalamic deep brain stimulation sweet spots and hyperdirect cortical connectivity in Parkinson's disease. *Neuroimage*, *158*, 332–345. https://doi.org/10.1016/j.neuroimage.2017.07.012

Albanese, A., Bhatia, K., Bressman, S. B., Delong, M. R., Fahn, S., Fung, V. S., . . . Teller, J. K. (2013). Phenomenology and classification of dystonia: a consensus update. *Mov Disord*, *28*(7), 863–873. https://doi.org/10.1002/mds.25475

Albanese, A., Di Giovanni, M., & Lalli, S. (2019). Dystonia: diagnosis and management. *Eur J Neurol*, *26*(1), 5–17. https://doi.org/10.1111/ene.13762

Albin, R. L., Young, A. B., & Penney, J. B. (1989). The functional anatomy of basal ganglia disorders. *Trends Neurosci*, *12*(10), 366–375. https://doi.org/10.1016/0166-2236(89)90074-x

Armstrong, M. J., Litvan, I., Lang, A. E., Bak, T. H., Bhatia, K. P., Borroni, B., . . . Weiner, W. J. (2013). Criteria for the diagnosis of corticobasal degeneration. *Neurology*, *80*(5), 496–503. https://doi.org/10.1212/WNL.0b013e31827f0fd1

Asanuma, K., Tang, C., Ma, Y., Dhawan, V., Mattis, P., Edwards, C., . . . Eidelberg, D. (2006). Network modulation in the treatment of Parkinson's disease. *Brain*, *129*(Pt 10), 2667–2678. https://doi.org/10.1093/brain/awl162

Azar, J., Elinav, H., Safadi, R., & Soliman, M. (2019). Malignant deep brain stimulator withdrawal syndrome. *BMJ Case Rep*, *12*(5). https://doi.org/10.1136/bcr-2018-229122

Balestrino, R., & Schapira, A. H. V. (2020). Parkinson disease. *Eur J Neurol*, *27*(1), 27–42. https://doi.org/10.1111/ene.14108

Beck, A. T., Epstein, N., Brown, G., & Steer, R. A. (1988). An inventory for measuring clinical anxiety: psychometric properties. *J Consult Clin Psychol*, *56*(6), 893–897. https://doi.org/10.1037//0022-006x.56.6.893

BECK, A. T., WARD, C. H., MENDELSON, M., MOCK, J., & ERBAUGH, J. (1961). An inventory for measuring depression. *Arch Gen Psychiatry*, *4*, 561–571. https://doi.org/10.1001/archpsyc.1961.01710120031004

Benamer, H. T., Patterson, J., Wyper, D. J., Hadley, D. M., Macphee, G. J., & Grosset, D. G. (2000). Correlation of Parkinson's disease severity and duration with 123I-FP-CIT SPECT striatal uptake. *Mov Disord*, *15*(4), 692–698. https://doi.org/10.1002/1531-8257(200007)15:4<692::aid-mds1014>3.0.co;2-v

Benamer, T. S., Patterson, J., Grosset, D. G., Booij, J., de Bruin, K., van Royen, E., . . . Ries, V. (2000). Accurate differentiation of parkinsonism and essential tremor using visual assessment of [123I]-FP-CIT SPECT imaging: the [123I]-FP-CIT study group. *Mov Disord*, *15*(3), 503–510.

Benítez-Rivero, S., Marín-Oyaga, V. A., García-Solís, D., Huertas-Fernández, I., García-Gómez, F. J., Jesús, S., . . . Mir, P. (2013). Clinical features and 123I-FP-CIT SPECT imaging in vascular

parkinsonism and Parkinson's disease. *J Neurol Neurosurg Psychiatry*, *84*(2), 122–129. https://doi.org/10.1136/jnnp-2012-302618

Berg, D., Postuma, R. B., Adler, C. H., Bloem, B. R., Chan, P., Dubois, B., . . . Deuschl, G. (2015). MDS research criteria for prodromal Parkinson's disease. *Mov Disord*, *30*(12), 1600–1611. https://doi.org/10.1002/mds.26431

Berman, B. D., Groth, C. L., Sillau, S. H., Pirio Richardson, S., Norris, S. A., Junker, J., . . . Perlmutter, J. S. (2020). Risk of spread in adult-onset isolated focal dystonia: a prospective international cohort study. *J Neurol Neurosurg Psychiatry*, *91*(3), 314–320. https://doi.org/10.1136/jnnp-2019-321794

Boes, A. D., Prasad, S., Liu, H., Liu, Q., Pascual-Leone, A., Caviness, V. S., & Fox, M. D. (2015). Network localization of neurological symptoms from focal brain lesions. *Brain*, *138*(Pt 10), 3061–3075. https://doi.org/10.1093/brain/awv228

Booij, J., & Kemp, P. (2008). Dopamine transporter imaging with [(123)I]FP-CIT SPECT: potential effects of drugs. *Eur J Nucl Med Mol Imaging*, *35*(2), 424–438. https://doi.org/10.1007/s00259-007-0621-0

Bostan, A. C., Dum, R. P., & Strick, P. L. (2013). Cerebellar networks with the cerebral cortex and basal ganglia. *Trends Cogn Sci*, *17*(5), 241–254. https://doi.org/10.1016/j.tics.2013.03.003

Bot, M., Schuurman, P. R., Odekerken, V. J. J., Verhagen, R., Contarino, F. M., De Bie, R. M. A., & van den Munckhof, P. (2018). Deep brain stimulation for Parkinson's disease: defining the optimal location within the subthalamic nucleus. *J Neurol Neurosurg Psychiatry*, *89*(5), 493–498. https://doi.org/10.1136/jnnp-2017-316907

Braak, H., Ghebremedhin, E., Rüb, U., Bratzke, H., & Del Tredici, K. (2004). Stages in the development of Parkinson's disease-related pathology. *Cell Tissue Res*, *318*(1), 121–134. https://doi.org/10.1007/s00441-004-0956-9

Bradberry, T. J., Metman, L. V., Contreras-Vidal, J. L., van den Munckhof, P., Hosey, L. A., Thompson, J. L., . . . Braun, A. R. (2012). Common and unique responses to dopamine agonist therapy and deep brain stimulation in Parkinson's disease: an H(2)(15)O PET study. *Brain Stimul*, *5*(4), 605–615. https://doi.org/10.1016/j.brs.2011.09.002

Burke, R. E., Fahn, S., Marsden, C. D., Bressman, S. B., Moskowitz, C., & Friedman, J. (1985). Validity and reliability of a rating scale for the primary torsion dystonias. *Neurology*, *35*(1), 73–77. https://doi.org/10.1212/wnl.35.1.73

Carbon, M., Raymond, D., Ozelius, L., Saunders-Pullman, R., Frucht, S., Dhawan, V., . . . Eidelberg, D. (2013). Metabolic changes in DYT11 myoclonus-dystonia. *Neurology*, *80*(4), 385–391. https://doi.org/10.1212/WNL.0b013e31827f0798

Carbon, M., Su, S., Dhawan, V., Raymond, D., Bressman, S., & Eidelberg, D. (2004). Regional metabolism in primary torsion dystonia: effects of penetrance and genotype. *Neurology*, *62*(8), 1384–1390. https://doi.org/10.1212/01.wnl.0000120541.97467.fe

Catafau, A. M., Tolosa, E., & Group, D. C. U. P. S. S. (2004). Impact of dopamine transporter SPECT using 123I-Ioflupane on diagnosis and management of patients with clinically uncertain Parkinsonian syndromes. *Mov Disord*, *19*(10), 1175–1182. https://doi.org/10.1002/mds.20112

Ceballos-Baumann, A. O., Boecker, H., Bartenstein, P., von Falkenhayn, I., Riescher, H., Conrad, B., . . . Alesch, F. (1999). A positron emission tomographic study of subthalamic nucleus stimulation in Parkinson disease: enhanced movement-related activity of motor-association cortex and decreased motor cortex resting activity. *Arch Neurol*, *56*(8), 997–1003. https://doi.org/10.1001/archneur.56.8.997

Ceballos-Baumann, A. O., Passingham, R. E., Marsden, C. D., & Brooks, D. J. (1995). Motor reorganization in acquired hemidystonia. *Ann Neurol*, *37*(6), 746–757. https://doi.org/10.1002/ana.410370608

Ceballos-Baumann, A. O., Passingham, R. E., Warner, T., Playford, E. D., Marsden, C. D., & Brooks, D. J. (1995). Overactive prefrontal and underactive motor cortical areas in idiopathic dystonia. *Ann Neurol*, *37*(3), 363–372. https://doi.org/10.1002/ana.410370313

Chaudhuri, K. R., Martinez-Martin, P., Brown, R. G., Sethi, K., Stocchi, F., Odin, P., . . . Schapira, A. H. (2007). The metric properties of a novel non-motor symptoms scale for Parkinson's disease: Results from an international pilot study. *Mov Disord*, *22*(13), 1901–1911. https://doi.org/10.1002/mds.21596

Chen, Y., Gong, C., Tian, Y., Orlov, N., Zhang, J., Guo, Y., . . . Li, L. (2020). Neuromodulation effects of deep brain stimulation on beta rhythm: A longitudinal local field potential study. *Brain Stimul*, *13*(6), 1784–1792. https://doi.org/10.1016/j.brs.2020.09.027

Cheung, T., Zhang, C., Rudolph, J., Alterman, R. L., & Tagliati, M. (2013). Sustained relief of generalized dystonia despite prolonged interruption of deep brain stimulation. *Mov Disord*, *28*(10), 1431–1434. https://doi.org/10.1002/mds.25353

Cif, L., Ruge, D., Gonzalez, V., Limousin, P., Vasques, X., Hariz, M. I., . . . Coubes, P. (2013). The influence of deep brain stimulation intensity and duration on symptoms evolution in an OFF stimulation dystonia study. *Brain Stimul*, *6*(4), 500–505. https://doi.org/10.1016/j.brs.2012.09.005

Colloby, S. J., McParland, S., O'Brien, J. T., & Attems, J. (2012). Neuropathological correlates of dopaminergic imaging in Alzheimer's disease and Lewy body dementias. *Brain*, *135*(Pt 9), 2798–2808. https://doi.org/10.1093/brain/aws211

Comella, C. L., Stebbins, G. T., Goetz, C. G., Chmura, T. A., Bressman, S. B., & Lang, A. E. (1997). Teaching tape for the motor section of the Toronto Western Spasmodic Torticollis Scale. *Mov Disord*, *12*(4), 570–575. https://doi.org/10.1002/mds.870120414

Conte, A., Rocchi, L., Latorre, A., Belvisi, D., Rothwell, J. C., & Berardelli, A. (2019). Ten-Year Reflections on the Neurophysiological Abnormalities of Focal Dystonias in Humans. *Mov Disord*. https://doi.org/10.1002/mds.27859

Corp, D. T., Joutsa, J., Darby, R. R., Delnooz, C. C. S., van de Warrenburg, B. P. C., Cooke, D., . . . Fox, M. D. (2019). Network localization of cervical dystonia based on causal brain lesions. *Brain*, *142*(6), 1660–1674. https://doi.org/10.1093/brain/awz112

Crossman, A., & D, N. (2010). *Neuroanatomy: an Illustrated Colour Text* (Vol. 4th edition). Elsevier Limited.

Cury, R. G., Fraix, V., Castrioto, A., Pérez Fernández, M. A., Krack, P., Chabardes, S., . . . Moro, E. (2017). Thalamic deep brain stimulation for tremor in Parkinson disease, essential tremor, and dystonia. *Neurology*, *89*(13), 1416–1423. https://doi.org/10.1212/WNL.0000000000004295

Cury, R. G., Kalia, S. K., Shah, B. B., Jimenez-Shahed, J., Prashanth, L. K., & Moro, E. (2018). Surgical treatment of dystonia. *Expert Rev Neurother*, *18*(6), 477–492. https://doi.org/10.1080/14737175.2018.1478288

De Pablo-Fernández, E., Lees, A. J., Holton, J. L., & Warner, T. T. (2019). Prognosis and Neuropathologic Correlation of Clinical Subtypes of Parkinson Disease. *JAMA Neurol*, *76*(4), 470–479. https://doi.org/10.1001/jamaneurol.2018.4377

Defazio, G., Albanese, A., Pellicciari, R., Scaglione, C. L., Esposito, M., Morgante, F., . . . Berardelli, A. (2019). Expert recommendations for diagnosing cervical, oromandibular, and limb dystonia. *Neurol Sci*, *40*(1), 89–95. https://doi.org/10.1007/s10072-018-3586-9

DeLong, M. R. (1990). Primate models of movement disorders of basal ganglia origin. *Trends Neurosci*, *13*(7), 281–285. https://doi.org/10.1016/0166-2236(90)90110-v

Deniau, J. M., Degos, B., Bosch, C., & Maurice, N. (2010). Deep brain stimulation mechanisms: beyond the concept of local functional inhibition. *Eur J Neurosci*, *32*(7), 1080–1091. https://doi.org/10.1111/j.1460-9568.2010.07413.x

Detante, O., Vercueil, L., Thobois, S., Broussolle, E., Costes, N., Lavenne, F., . . . Pollak, P. (2004). Globus pallidus internus stimulation in primary generalized dystonia: a H215O PET study. *Brain*, *127*(Pt 8), 1899–1908. https://doi.org/10.1093/brain/awh213

Dickson, D. W. (2012). Parkinson's disease and parkinsonism: neuropathology. *Cold Spring Harb Perspect Med*, *2*(8). https://doi.org/10.1101/cshperspect.a009258

Dickson, D. W. (2018). Neuropathology of Parkinson disease. *Parkinsonism Relat Disord*, *46 Suppl 1*, S30–S33. https://doi.org/10.1016/j.parkreldis.2017.07.033

Eidelberg, D., Moeller, J. R., Antonini, A., Kazumata, K., Nakamura, T., Dhawan, V., . . . Fahn, S. (1998). Functional brain networks in DYT1 dystonia. *Ann Neurol*, *44*(3), 303–312. https://doi.org/10.1002/ana.410440304

Eusebio, A., Azulay, J. P., Ceccaldi, M., Girard, N., Mundler, O., & Guedj, E. (2012). Voxel-based analysis of whole-brain effects of age and gender on dopamine transporter SPECT imaging in healthy subjects. *Eur J Nucl Med Mol Imaging*, *39*(11), 1778–1783. https://doi.org/10.1007/s00259-012-2207-8

Ewert, S., Plettig, P., Li, N., Chakravarty, M. M., Collins, D. L., Herrington, T. M., . . . Horn, A. (2018). Toward defining deep brain stimulation targets in MNI space: A subcortical atlas based on multimodal MRI, histology and structural connectivity. *Neuroimage*, *170*, 271–282. https://doi.org/10.1016/j.neuroimage.2017.05.015

Fazl, A., & Fleisher, J. (2018). Anatomy, Physiology, and Clinical Syndromes of the Basal Ganglia: A Brief Review. *Semin Pediatr Neurol*, *25*, 2–9. https://doi.org/10.1016/j.spen.2017.12.005

Fereshtehnejad, S. M., Zeighami, Y., Dagher, A., & Postuma, R. B. (2017). Clinical criteria for subtyping Parkinson's disease: biomarkers and longitudinal progression. *Brain*, *140*(7), 1959–1976. https://doi.org/10.1093/brain/awx118

Foley, K. F., DeSanty, K. P., & Kast, R. E. (2006). Bupropion: pharmacology and therapeutic applications. *Expert Rev Neurother*, *6*(9), 1249–1265. https://doi.org/10.1586/14737175.6.9.1249

Folstein, M. F., Folstein, S. E., & McHugh, P. R. (1975). "Mini-mental state". A practical method for grading the cognitive state of patients for the clinician. *J Psychiatr Res*, *12*(3), 189–198. https://doi.org/10.1016/0022-3956(75)90026-6

Fox, M. D. (2018). Mapping Symptoms to Brain Networks with the Human Connectome. *N Engl J Med*, *379*(23), 2237–2245. https://doi.org/10.1056/NEJMra1706158

Fox, S. H., Katzenschlager, R., Lim, S. Y., Barton, B., de Bie, R. M. A., Seppi, K., . . . Committee, M. D. S. E.-B. M. (2018). International Parkinson and movement disorder society evidence-based medicine review: Update on treatments for the motor symptoms of Parkinson's disease. *Mov Disord*, *33*(8), 1248–1266. https://doi.org/10.1002/mds.27372

Fukuda, M., Barnes, A., Simon, E. S., Holmes, A., Dhawan, V., Giladi, N., . . . Eidelberg, D. (2004). Thalamic stimulation for parkinsonian tremor: correlation between regional cerebral blood flow and physiological tremor characteristics. *Neuroimage*, *21*(2), 608–615. https://doi.org/10.1016/j.neuroimage.2003.09.068

Fukuda, M., Mentis, M., Ghilardi, M. F., Dhawan, V., Antonini, A., Hammerstad, J., . . . Eidelberg, D. (2001). Functional correlates of pallidal stimulation for Parkinson's disease. *Ann Neurol*, *49*(2), 155–164. https://doi.org/10.1002/1531-8249(20010201)49:2<155::aid-ana35>3.0.co;2–9

Ganguli, M., Lee, C. W., Hughes, T., Snitz, B. E., Jakubcak, J., Duara, R., & Chang, C. C. (2015). Who wants a free brain scan? Assessing and correcting for recruitment biases in a population-based sMRI pilot study. *Brain Imaging Behav*, *9*(2), 204–212. https://doi.org/10.1007/s11682-014-9297-9

Ganguli, M., Lytle, M. E., Reynolds, M. D., & Dodge, H. H. (1998). Random versus volunteer selection for a community-based study. *J Gerontol A Biol Sci Med Sci*, *53*(1), M39–46. https://doi.org/10.1093/gerona/53a.1.m39

Garraux, G., Bahri, M. A., Lemaire, C., Degueldre, C., Salmon, E., & Kaschten, B. (2011). Brain energization in response to deep brain stimulation of subthalamic nuclei in Parkinson's disease. *J Cereb Blood Flow Metab*, *31*(7), 1612–1622. https://doi.org/10.1038/jcbfm.2011.41

Geday, J., Østergaard, K., Johnsen, E., & Gjedde, A. (2009). STN-stimulation in Parkinson's disease restores striatal inhibition of thalamocortical projection. *Hum Brain Mapp*, *30*(1), 112–121. https://doi.org/10.1002/hbm.20486

Gerschlager, W., Bencsits, G., Pirker, W., Bloem, B. R., Asenbaum, S., Prayer, D., . . . Brücke, T. (2002). [123I]beta-CIT SPECT distinguishes vascular parkinsonism from Parkinson's disease. *Mov Disord*, *17*(3), 518–523. https://doi.org/10.1002/mds.10092

Gilman, S., Wenning, G. K., Low, P. A., Brooks, D. J., Mathias, C. J., Trojanowski, J. Q., . . . Vidailhet, M. (2008). Second consensus statement on the diagnosis of multiple system atrophy. *Neurology*, *71*(9), 670–676. https://doi.org/10.1212/01.wnl.0000324625.00404.15

Glass, P. G., Lees, A. J., Bacellar, A., Zijlmans, J., Katzenschlager, R., & Silveira-Moriyama, L. (2012). The clinical features of pathologically confirmed vascular parkinsonism. *J Neurol Neurosurg Psychiatry*, *83*(10), 1027–1029. https://doi.org/10.1136/jnnp-2012-302828

Goetz, C. G., Tilley, B. C., Shaftman, S. R., Stebbins, G. T., Fahn, S., Martinez-Martin, P., . . . Force, M. D. S. U. R. T. (2008). Movement Disorder Society-sponsored revision of the Unified Parkinson's Disease Rating Scale (MDS-UPDRS): scale presentation and clinimetric testing results. *Mov Disord*, *23*(15), 2129–2170. https://doi.org/10.1002/mds.22340

Gonzalez-Escamilla, G., Muthuraman, M., Ciolac, D., Coenen, V. A., Schnitzler, A., & Groppa, S. (2020). Neuroimaging and electrophysiology meet invasive neurostimulation for causal interrogations and modulations of brain states. *Neuroimage*, *220*, 117144. https://doi.org/10.1016/j.neuroimage.2020.117144

Gonzalez-Escamilla, G., Muthuraman, M., Reich, M. M., Koirala, N., Riedel, C., Glaser, M., . . . Groppa, S. (2019). Cortical network fingerprints predict deep brain stimulation outcome in dystonia. *Mov Disord*, *34*(10), 1537–1546. https://doi.org/10.1002/mds.27808

Grabli, D., Ewenczyk, C., Coelho-Braga, M. C., Lagrange, C., Fraix, V., Cornu, P., . . . Pollak, P. (2009). Interruption of deep brain stimulation of the globus pallidus in primary generalized dystonia. *Mov Disord*, *24*(16), 2363–2369. https://doi.org/10.1002/mds.22827

Greuel, A., Pauls, K. A. M., Koy, A., Südmeyer, M., Schnitzler, A., Timmermann, L., . . . Eggers, C. (2020). Pallidal Deep Brain Stimulation Reduces Sensorimotor Cortex Activation in Focal/Segmental Dystonia. *Mov Disord*. https://doi.org/10.1002/mds.27970

Grips, E., Blahak, C., Capelle, H. H., Bäzner, H., Weigel, R., Sedlaczek, O., . . . Wöhrle, J. C. (2007). Patterns of reoccurrence of segmental dystonia after discontinuation of deep brain stimulation. *J Neurol Neurosurg Psychiatry*, *78*(3), 318–320. https://doi.org/10.1136/jnnp.2006.089409

Group, E. S. o. D. i. E. E. C. (2000). A prevalence study of primary dystonia in eight European countries. *J Neurol*, *247*(10), 787–792. https://doi.org/10.1007/s004150070094

Han, V., Skorvanek, M., Smit, M., Turcanova Koprusakova, M., Hoekstra, T., van Dijk, J. P., . . . Reijneveld, S. A. (2020). Prevalence of non-motor symptoms and their association with quality of life in cervical dystonia. *Acta Neurol Scand*, *142*(6), 613–622. https://doi.org/10.1111/ane.13304

Haslinger, B., Kalteis, K., Boecker, H., Alesch, F., & Ceballos-Baumann, A. O. (2005). Frequency-correlated decreases of motor cortex activity associated with subthalamic nucleus stimulation in Parkinson's disease. *Neuroimage*, *28*(3), 598–606. https://doi.org/10.1016/j.neuroimage.2005.06.034

Hassin-Baer, S., Sirota, P., Korczyn, A. D., Treves, T. A., Epstein, B., Shabtai, H., . . . Giladi, N. (2001). Clinical characteristics of neuroleptic-induced parkinsonism. *J Neural Transm (Vienna)*, *108*(11), 1299–1308. https://doi.org/10.1007/s007020100006

Heinzel, S., Berg, D., Gasser, T., Chen, H., Yao, C., Postuma, R. B., & Disease, M. T. F. o. t. D. o. P. s. (2019). Update of the MDS research criteria for prodromal Parkinson's disease. *Mov Disord*, *34*(10), 1464–1470. https://doi.org/10.1002/mds.27802

Hernán, M. A., Hernández-Díaz, S., & Robins, J. M. (2004). A structural approach to selection bias. *Epidemiology*, *15*(5), 615–625. https://doi.org/10.1097/01.ede.0000135174.63482.43

Herrington, T. M., Cheng, J. J., & Eskandar, E. N. (2016). Mechanisms of deep brain stimulation. *J Neurophysiol*, *115*(1), 19–38. https://doi.org/10.1152/jn.00281.2015

Hershey, T., Revilla, F. J., Wernle, A. R., McGee-Minnich, L., Antenor, J. V., Videen, T. O., . . . Perlmutter, J. S. (2003). Cortical and subcortical blood flow effects of subthalamic nucleus stimulation in PD. *Neurology*, *61*(6), 816–821. https://doi.org/10.1212/01.wnl.0000083991.81859.73

Herzog, J., Weiss, P. H., Assmus, A., Wefer, B., Seif, C., Braun, P. M., . . . Fink, G. R. (2006). Subthalamic stimulation modulates cortical control of urinary bladder in Parkinson's disease. *Brain*, *129*(Pt 12), 3366–3375. https://doi.org/10.1093/brain/awl302

Herzog, J., Weiss, P. H., Assmus, A., Wefer, B., Seif, C., Braun, P. M., . . . Fink, G. R. (2008). Improved sensory gating of urinary bladder afferents in Parkinson's disease following subthalamic stimulation. *Brain*, *131*(Pt 1), 132–145. https://doi.org/10.1093/brain/awm254

*Highlights of prescribing information for DatScan ioflupane I 123 injection*. (Revised 2015). Food and Drug

Administration (FDA), USA.

Hilker, R., Voges, J., Ghaemi, M., Lehrke, R., Rudolf, J., Koulousakis, A., . . . Heiss, W. D. (2003). Deep brain stimulation of the subthalamic nucleus does not increase the striatal dopamine concentration in parkinsonian humans. *Mov Disord*, *18*(1), 41–48. https://doi.org/10.1002/mds.10297

Hilker, R., Voges, J., Weisenbach, S., Kalbe, E., Burghaus, L., Ghaemi, M., . . . Heiss, W. D. (2004). Subthalamic nucleus stimulation restores glucose metabolism in associative and limbic cortices and in cerebellum: evidence from a FDG-PET study in advanced Parkinson's disease. *J Cereb Blood Flow Metab*, *24*(1), 7–16. https://doi.org/10.1097/01.WCB.0000092831.44769.09

Horn, A. (2019). The impact of modern-day neuroimaging on the field of deep brain stimulation. *Curr Opin Neurol*, *32*(4), 511–520. https://doi.org/10.1097/WCO.0000000000000679

Horn, A., Li, N., Dembek, T. A., Kappel, A., Boulay, C., Ewert, S., . . . Kühn, A. A. (2019). Lead-DBS v2: Towards a comprehensive pipeline for deep brain stimulation imaging. *Neuroimage*, *184*, 293–316. https://doi.org/10.1016/j.neuroimage.2018.08.068

Horn, A., Reich, M., Vorwerk, J., Li, N., Wenzel, G., Fang, Q., . . . Fox, M. D. (2017). Connectivity Predicts deep brain stimulation outcome in Parkinson disease. *Ann Neurol*, *82*(1), 67–78. https://doi.org/10.1002/ana.24974

Höglinger, G. U., Respondek, G., Stamelou, M., Kurz, C., Josephs, K. A., Lang, A. E., . . . Group, M. D. S.-e. P. S. (2017). Clinical diagnosis of progressive supranuclear palsy: The movement disorder society criteria. *Mov Disord*, *32*(6), 853–864. https://doi.org/10.1002/mds.26987

Jaakkola, E., Joutsa, J., Mäkinen, E., Johansson, J., & Kaasinen, V. (2017). Ventral striatal dopaminergic defect is associated with hallucinations in Parkinson's disease. *Eur J Neurol*, *24*(11), 1341–1347. https://doi.org/10.1111/ene.13390

Jaakkola, E., Joutsa, J., Mäkinen, E., Noponen, T., Pitkonen, M., Levo, R., . . . Kaasinen, V. (2019). Burden of non-motor symptoms in unclear parkinsonism and tremor: A study with [*J Neurol Sci*, *404*, 124–127. https://doi.org/10.1016/j.jns.2019.07.025

Jakobs, M., Fomenko, A., Lozano, A. M., & Kiening, K. L. (2019). Cellular, molecular, and clinical mechanisms of action of deep brain stimulation-a systematic review on established indications and outlook on future developments. *EMBO Mol Med*, *11*(4). https://doi.org/10.15252/emmm.201809575

Jakobson Mo, S., Larsson, A., Linder, J., Birgander, R., Edenbrandt, L., Stenlund, H., . . . Riklund, K. (2013). $^{123}$I-FP-Cit and 123I-IBZM SPECT uptake in a prospective normal material analysed with two different semiquantitative image evaluation tools. *Nucl Med Commun*, *34*(10), 978–989. https://doi.org/10.1097/MNM.0b013e328364aa2e

Jamwal, S., & Kumar, P. (2019). Insight Into the Emerging Role of Striatal Neurotransmitters in the Pathophysiology of Parkinson's Disease and Huntington's Disease: A Review. *Curr Neuropharmacol*, *17*(2), 165–175. https://doi.org/10.2174/1570159X16666180302115032

Jankovic, J. (2006). Treatment of dystonia. *Lancet Neurol*, *5*(10), 864–872. https://doi.org/10.1016/S1474-4422(06)70574-9

Jankovic, J. (2013). Medical treatment of dystonia. *Mov Disord*, *28*(7), 1001–1012. https://doi.org/10.1002/mds.25552

Jankovic, J., & Tan, E. K. (2020). Parkinson's disease: etiopathogenesis and treatment. *J Neurol Neurosurg Psychiatry*, *91*(8), 795–808. https://doi.org/10.1136/jnnp-2019-322338

Jiang, W., Lei, Y., Wei, J., Yang, L., Wei, S., Yin, Q., . . . Guo, W. (2019). Alterations of Interhemispheric Functional Connectivity and Degree Centrality in Cervical Dystonia: A Resting-State fMRI Study. *Neural Plast*, *2019*, 7349894. https://doi.org/10.1155/2019/7349894

Jinnah, H. A., Neychev, V., & Hess, E. J. (2017). The Anatomical Basis for Dystonia: The Motor Network Model. *Tremor Other Hyperkinet Mov (N Y)*, *7*, 506. https://doi.org/10.7916/D8V69X3S

Joutsa, J., Gardberg, M., Röyttä, M., & Kaasinen, V. (2014). Diagnostic accuracy of parkinsonism syndromes by general neurologists. *Parkinsonism Relat Disord*, *20*(8), 840–844. https://doi.org/10.1016/j.parkreldis.2014.04.019

Joutsa, J., Rinne, J. O., Karrasch, M., Hermann, B., Johansson, J., Anttinen, A., . . . group, T. s. (2017). Brain glucose metabolism and its relation to amyloid load in middle-aged adults with childhood-onset epilepsy. *Epilepsy Res*, *137*, 69–72. https://doi.org/10.1016/j.eplepsyres.2017.09.006

Kaasinen, V., Kankare, T., Joutsa, J., & Vahlberg, T. (2019). Presynaptic Striatal Dopaminergic Function in Atypical Parkinsonism: A Metaanalysis of Imaging Studies. *J Nucl Med*, *60*(12), 1757–1763. https://doi.org/10.2967/jnumed.119.227140

Kaasinen, V., Kinos, M., Joutsa, J., Seppänen, M., & Noponen, T. (2014). Differences in striatal dopamine transporter density between tremor dominant and non-tremor Parkinson's disease. *Eur J Nucl Med Mol Imaging*, *41*(10), 1931–1937. https://doi.org/10.1007/s00259-014-2796-5

Kaasinen, V., & Vahlberg, T. (2017). Striatal dopamine in Parkinson disease: A meta-analysis of imaging studies. *Ann Neurol*, *82*(6), 873–882. https://doi.org/10.1002/ana.25103

Kalia, L. V., & Lang, A. E. (2015). Parkinson's disease. *Lancet*, *386*(9996), 896–912. https://doi.org/10.1016/S0140-6736(14)61393-3

Karimi, M., Golchin, N., Tabbal, S. D., Hershey, T., Videen, T. O., Wu, J., . . . Perlmutter, J. S. (2008). Subthalamic nucleus stimulation-induced regional blood flow responses correlate with improvement of motor signs in Parkinson disease. *Brain*, *131*(Pt 10), 2710–2719. https://doi.org/10.1093/brain/awn179

Karimi, M., Tian, L., Brown, C. A., Flores, H. P., Loftin, S. K., Videen, T. O., . . . Perlmutter, J. S. (2013). Validation of nigrostriatal positron emission tomography measures: critical limits. *Ann Neurol*, *73*(3), 390–396. https://doi.org/10.1002/ana.23798

Katsakiori, P. F., Kefalopoulou, Z., Markaki, E., Paschali, A., Ellul, J., Kagadis, G. C., . . . Constantoyannis, C. (2009). Deep brain stimulation for secondary dystonia: results in 8 patients. *Acta Neurochir (Wien)*, *151*(5), 473–478; discussion 478. https://doi.org/10.1007/s00701-009-0281-x

Kordower, J. H., Olanow, C. W., Dodiya, H. B., Chu, Y., Beach, T. G., Adler, C. H., . . . Bartus, R. T. (2013). Disease duration and the integrity of the nigrostriatal system in Parkinson's disease. *Brain*, *136*(Pt 8), 2419–2431. https://doi.org/10.1093/brain/awt192

Kraemmer, J., Kovacs, G. G., Perju-Dumbrava, L., Pirker, S., Traub-Weidinger, T., & Pirker, W. (2014). Correlation of striatal dopamine transporter imaging with post mortem substantia nigra cell counts. *Mov Disord*, *29*(14), 1767–1773. https://doi.org/10.1002/mds.25975

Kroneberg, D., Plettig, P., Schneider, G. H., & Kühn, A. A. (2018). Motor Cortical Plasticity Relates to Symptom Severity and Clinical Benefit From Deep Brain Stimulation in Cervical Dystonia. *Neuromodulation*, *21*(8), 735–740. https://doi.org/10.1111/ner.12690

Kuyper, D. J., Parra, V., Aerts, S., Okun, M. S., & Kluger, B. M. (2011). Nonmotor manifestations of dystonia: a systematic review. *Mov Disord*, *26*(7), 1206–1217. https://doi.org/10.1002/mds.23709

Kühn, A. A., Kempf, F., Brücke, C., Gaynor Doyle, L., Martinez-Torres, I., Pogosyan, A., . . . Brown, P. (2008). High-frequency stimulation of the subthalamic nucleus suppresses oscillatory beta activity in patients with Parkinson's disease in parallel with improvement in motor performance. *J Neurosci*, *28*(24), 6165–6173. https://doi.org/10.1523/JNEUROSCI.0282-08.2008

LaHue, S. C., Albers, K., Goldman, S., Lo, R. Y., Gu, Z., Leimpeter, A., . . . Tanner, C. M. (2020). Cervical dystonia incidence and diagnostic delay in a multiethnic population. *Mov Disord*, *35*(3), 450–456. https://doi.org/10.1002/mds.27927

Lanciego, J. L., Luquin, N., & Obeso, J. A. (2012). Functional neuroanatomy of the basal ganglia. *Cold Spring Harb Perspect Med*, *2*(12), a009621. https://doi.org/10.1101/cshperspect.a009621

Lanska, D. J. (2010). Chapter 33: the history of movement disorders. *Handb Clin Neurol*, *95*, 501–546. https://doi.org/10.1016/S0072-9752(08)02133-7

Lavalaye, J., Booij, J., Reneman, L., Habraken, J. B., & van Royen, E. A. (2000). Effect of age and gender on dopamine transporter imaging with [123I]FP-CIT SPET in healthy volunteers. *Eur J Nucl Med*, *27*(7), 867–869. https://doi.org/10.1007/s002590000279

Lee, A., & Gilbert, R. M. (2016). Epidemiology of Parkinson Disease. *Neurol Clin*, *34*(4), 955–965. https://doi.org/10.1016/j.ncl.2016.06.012

Leenders, K., Hartvig, P., Forsgren, L., Holmgren, G., Almay, B., Eckernäs, S. A., . . . Långström, B. (1993). Striatal [11C]-N-methyl-spiperone binding in patients with focal dystonia (torticollis) using positron emission tomography. *J Neural Transm Park Dis Dement Sect*, *5*(2), 79–87. https://doi.org/10.1007/BF02251198

Lehéricy, S., Tijssen, M. A., Vidailhet, M., Kaji, R., & Meunier, S. (2013). The anatomical basis of dystonia: current view using neuroimaging. *Mov Disord*, *28*(7), 944–957. https://doi.org/10.1002/mds.25527

Levin, J., Singh, A., Feddersen, B., Mehrkens, J. H., & Bötzel, K. (2014). Onset latency of segmental dystonia after deep brain stimulation cessation: a randomized, double-blind crossover trial. *Mov Disord*, *29*(7), 944–949. https://doi.org/10.1002/mds.25780

Lin, C. H., & Lane, H. Y. (2017). Bupropion interferes with the image diagnosis of Parkinson's disease. *Neuropsychiatr Dis Treat*, *13*, 2637–2639. https://doi.org/10.2147/NDT.S150912

Lorberboym, M., Treves, T. A., Melamed, E., Lampl, Y., Hellmann, M., & Djaldetti, R. (2006). [123I]-FP/CIT SPECT imaging for distinguishing drug-induced parkinsonism from Parkinson's disease. *Mov Disord*, *21*(4), 510–514. https://doi.org/10.1002/mds.20748

Lozano, A. M., & Lipsman, N. (2013). Probing and regulating dysfunctional circuits using deep brain stimulation. *Neuron*, *77*(3), 406–424. https://doi.org/10.1016/j.neuron.2013.01.020

Lumsden, D. E., King, M. D., & Allen, N. M. (2017). Status dystonicus in childhood. *Curr Opin Pediatr*, *29*(6), 674–682. https://doi.org/10.1097/MOP.0000000000000556

Macleod, A. D., Taylor, K. S., & Counsell, C. E. (2014). Mortality in Parkinson's disease: a systematic review and meta-analysis. *Mov Disord*, *29*(13), 1615–1622. https://doi.org/10.1002/mds.25898

Magyar-Lehmann, S., Antonini, A., Roelcke, U., Maguire, R. P., Missimer, J., Meyer, M., & Leenders, K. L. (1997). Cerebral glucose metabolism in patients with spasmodic torticollis. *Mov Disord*, *12*(5), 704–708. https://doi.org/10.1002/mds.870120513

Mansouri, A., Taslimi, S., Badhiwala, J. H., Witiw, C. D., Nassiri, F., Odekerken, V. J. J., . . . Lozano, A. M. (2018). Deep brain stimulation for Parkinson's disease: meta-analysis of results of randomized trials at varying lengths of follow-up. *J Neurosurg*, *128*(4), 1199–1213. https://doi.org/10.3171/2016.11.JNS16715

Matsuda, H., Murata, M., Mukai, Y., Sako, K., Ono, H., Toyama, H., . . . Takahashi, R. (2018). Japanese multicenter database of healthy controls for [*Eur J Nucl Med Mol Imaging*, *45*(8), 1405–1416. https://doi.org/10.1007/s00259-018-3976-5

McKeith, I., O'Brien, J., Walker, Z., Tatsch, K., Booij, J., Darcourt, J., . . . Group, D. S. (2007). Sensitivity and specificity of dopamine transporter imaging with 123I-FP-CIT SPECT in dementia with Lewy bodies: a phase III, multicentre study. *Lancet Neurol*, *6*(4), 305–313. https://doi.org/10.1016/S1474-4422(07)70057-1

McKeith, I. G., Boeve, B. F., Dickson, D. W., Halliday, G., Taylor, J. P., Weintraub, D., . . . Kosaka, K. (2017). Diagnosis and management of dementia with Lewy bodies: Fourth consensus report of the DLB Consortium. *Neurology*, *89*(1), 88–100. https://doi.org/10.1212/WNL.0000000000004058

Milenkovic, I., Bartova, L., Papageorgiou, K., Kasper, S., Traub-Weidinger, T., & Winkler, D. (2021). Case Report: Bupropion Reduces the [*Front Psychiatry*, *12*, 631357. https://doi.org/10.3389/fpsyt.2021.631357

Mirpour, S., Turkbey, E. B., Marashdeh, W., El Khouli, R., & Subramaniam, R. M. (2018). Impact of DAT-SPECT on Management of Patients Suspected of Parkinsonism. *Clin Nucl Med*, *43*(10), 710–714. https://doi.org/10.1097/RLU.0000000000002240

Monchi, O., Petrides, M., Strafella, A. P., Worsley, K. J., & Doyon, J. (2006). Functional role of the basal ganglia in the planning and execution of actions. *Ann Neurol*, *59*(2), 257–264. https://doi.org/10.1002/ana.20742

Moro, E., LeReun, C., Krauss, J. K., Albanese, A., Lin, J. P., Walleser Autiero, S., . . . Vidailhet, M. (2017). Efficacy of pallidal stimulation in isolated dystonia: a systematic review and meta-analysis. *Eur J Neurol*, *24*(4), 552–560. https://doi.org/10.1111/ene.13255

Mäkinen, E., Joutsa, J., Jaakkola, E., Noponen, T., Johansson, J., Pitkonen, M., . . . Kaasinen, V. (2019). Individual parkinsonian motor signs and striatal dopamine transporter deficiency: a study with [I-123]FP-CIT SPECT. *J Neurol*, *266*(4), 826–834. https://doi.org/10.1007/s00415-019-09202-6

Mäkinen, E., Joutsa, J., Johansson, J., Mäki, M., Seppänen, M., & Kaasinen, V. (2016). Visual versus automated analysis of [I-123]FP-CIT SPECT scans in parkinsonism. *J Neural Transm (Vienna)*, *123*(11), 1309–1318. https://doi.org/10.1007/s00702-016-1586-6

Müller, J., Kiechl, S., Wenning, G. K., Seppi, K., Willeit, J., Gasperi, A., . . . Poewe, W. (2002). The prevalence of primary dystonia in the general community. *Neurology*, *59*(6), 941–943. https://doi.org/10.1212/01.wnl.0000026474.12594.0d

Nagaoka, T., Katayama, Y., Kano, T., Kobayashi, K., Oshima, H., Fukaya, C., & Yamamoto, T. (2007). Changes in glucose metabolism in cerebral cortex and cerebellum correlate with tremor and rigidity control by subthalamic nucleus stimulation in Parkinson's disease: a positron emission tomography study. *Neuromodulation*, *10*(3), 206–215. https://doi.org/10.1111/j.1525-1403.2007.00110.x

Nam, S. B., Kim, K., Kim, B. S., Im, H. J., Lee, S. H., Kim, S. J., . . . Pak, K. (2018). The Effect of Obesity on the Availabilities of Dopamine and Serotonin Transporters. *Sci Rep*, *8*(1), 4924. https://doi.org/10.1038/s41598-018-22814-8

Nambu, A., Tokuno, H., & Takada, M. (2002). Functional significance of the cortico-subthalamo-pallidal 'hyperdirect' pathway. *Neurosci Res*, *43*(2), 111–117. https://doi.org/10.1016/s0168-0102(02)00027-5

Naumann, M., Magyar-Lehmann, S., Reiners, K., Erbguth, F., & Leenders, K. L. (2000). Sensory tricks in cervical dystonia: perceptual dysbalance of parietal cortex modulates frontal motor programming. *Ann Neurol*, *47*(3), 322–328.

Neychev, V. K., Gross, R. E., Lehéricy, S., Hess, E. J., & Jinnah, H. A. (2011). The functional neuroanatomy of dystonia. *Neurobiol Dis*, *42*(2), 185–201. https://doi.org/10.1016/j.nbd.2011.01.026

Ni, Z., Kim, S. J., Phielipp, N., Ghosh, S., Udupa, K., Gunraj, C. A., . . . Chen, R. (2018). Pallidal deep brain stimulation modulates cortical excitability and plasticity. *Ann Neurol*, *83*(2), 352–362. https://doi.org/10.1002/ana.25156

Nobili, F., Naseri, M., De Carli, F., Asenbaum, S., Booij, J., Darcourt, J., . . . Varrone, A. (2013). Automatic semi-quantification of [123I]FP-CIT SPECT scans in healthy volunteers using BasGan version 2: results from the ENC-DAT database. *Eur J Nucl Med Mol Imaging*, *40*(4), 565–573. https://doi.org/10.1007/s00259-012-2304-8

Obeso, J. A., Rodríguez-Oroz, M. C., Benitez-Temino, B., Blesa, F. J., Guridi, J., Marin, C., & Rodriguez, M. (2008). Functional organization of the basal ganglia: therapeutic implications for Parkinson's disease. *Mov Disord*, *23 Suppl 3*, S548–559. https://doi.org/10.1002/mds.22062

Okromelidze, L., Tsuboi, T., Eisinger, R. S., Burns, M. R., Charbel, M., Rana, M., . . . Middlebrooks, E. H. (2020). Functional and Structural Connectivity Patterns Associated with Clinical Outcomes in Deep Brain Stimulation of the Globus Pallidus Internus for Generalized Dystonia. *AJNR Am J Neuroradiol*, *41*(3), 508–514. https://doi.org/10.3174/ajnr.A6429

Ortiz, R., Scheperjans, F., Mertsalmi, T., & Pekkonen, E. (2018). The prevalence of adult-onset isolated dystonia in Finland 2007–2016. *PLoS One*, *13*(11), e0207729. https://doi.org/10.1371/journal.pone.0207729

Ortiz, R. M., Scheperjans, F., Mertsalmi, T., & Pekkonen, E. (2019). Comorbidity and retirement in cervical dystonia. *J Neurol*, *266*(9), 2216–2223. https://doi.org/10.1007/s00415-019-09402-0

Oswald, L. M., Wand, G. S., Zhu, S., & Selby, V. (2013). Volunteerism and self-selection bias in human positron emission tomography neuroimaging research. *Brain Imaging Behav*, *7*(2), 163–176. https://doi.org/10.1007/s11682-012-9210-3

Pak, K., Kim, K., Lee, M. J., Lee, J. M., Kim, B. S., Kim, S. J., & Kim, I. J. (2018). Correlation between the availability of dopamine transporter and olfactory function in healthy subjects. *Eur Radiol*, *28*(4), 1756–1760. https://doi.org/10.1007/s00330-017-5147-7

Palermo, G., & Ceravolo, R. (2019). Molecular Imaging of the Dopamine Transporter. *Cells*, *8*(8). https://doi.org/10.3390/cells8080872

Pan, P., Wei, S., Ou, Y., Jiang, W., Li, W., Lei, Y., . . . Luo, S. (2019). Reduced Global-Brain Functional Connectivity and Its Relationship With Symptomatic Severity in Cervical Dystonia. *Front Neurol*, *10*, 1358. https://doi.org/10.3389/fneur.2019.01358

Park, H. J., Park, B., Kim, H. Y., Oh, M. K., Kim, J. I., Yoon, M., . . . Chang, J. W. (2015). A network analysis of $^{15}O$-$H_2O$ PET reveals deep brain stimulation effects on brain network of Parkinson's disease. *Yonsei Med J*, *56*(3), 726–736. https://doi.org/10.3349/ymj.2015.56.3.726

Patel, N., Jankovic, J., & Hallett, M. (2014). Sensory aspects of movement disorders. *Lancet Neurol*, *13*(1), 100–112. https://doi.org/10.1016/S1474-4422(13)70213-8

Patton, J. H., Stanford, M. S., & Barratt, E. S. (1995). Factor structure of the Barratt impulsiveness scale. *J Clin Psychol*, *51*(6), 768–774. https://doi.org/10.1002/1097-4679(199511)51:6<768::aid-jclp2270510607>3.0.co;2-1

Payoux, P., Remy, P., Miloudi, M., Houeto, J. L., Stadler, C., Bejjani, B. P., . . . Damier, P. (2009). Contrasting changes in cortical activation induced by acute high-frequency stimulation within the globus pallidus in Parkinson's disease. *J Cereb Blood Flow Metab*, *29*(2), 235–243. https://doi.org/10.1038/jcbfm.2008.107

Penfield, W., & Boldrey, E. (1937). Somatic motor and sensory representation in the cerebral cortex of man as studied by electrical stimulation1. *Brain*, *60*(4), 389–443. https://doi.org/10.1093/brain/60.4.389

Perlmutter, J. S., Stambuk, M. K., Markham, J., Black, K. J., McGee-Minnich, L., Jankovic, J., & Moerlein, S. M. (1997). Decreased [18F]spiperone binding in putamen in idiopathic focal dystonia. *J Neurosci*, *17*(2), 843–850.

Playford, E. D., Fletcher, N. A., Sawle, G. V., Marsden, C. D., & Brooks, D. J. (1993). Striatal [18F]dopa uptake in familial idiopathic dystonia. *Brain*, *116 ( Pt 5)*, 1191–1199. https://doi.org/10.1093/brain/116.5.1191

Postuma, R. B., Arnulf, I., Hogl, B., Iranzo, A., Miyamoto, T., Dauvilliers, Y., . . . Montplaisir, J. Y. (2012). A single-question screen for rapid eye movement sleep behavior disorder: a multicenter validation study. *Mov Disord*, *27*(7), 913–916. https://doi.org/10.1002/mds.25037

Postuma, R. B., Berg, D., Stern, M., Poewe, W., Olanow, C. W., Oertel, W., . . . Deuschl, G. (2015). MDS clinical diagnostic criteria for Parkinson's disease. *Mov Disord*, *30*(12), 1591–1601. https://doi.org/10.1002/mds.26424

*Product information for DatScan ioflupane I 123 injection.* . (Updated 2017). European Medicines Agency (EMA).

Ramirez-Zamora, A., & Ostrem, J. L. (2018). Globus Pallidus Interna or Subthalamic Nucleus Deep Brain Stimulation for Parkinson Disease: A Review. *JAMA Neurol*, *75*(3), 367–372. https://doi.org/10.1001/jamaneurol.2017.4321

Ramos, V. F., Karp, B. I., & Hallett, M. (2014). Tricks in dystonia: ordering the complexity. *J Neurol Neurosurg Psychiatry*, *85*(9), 987–993. https://doi.org/10.1136/jnnp-2013-306971

Reich, M. M., Horn, A., Lange, F., Roothans, J., Paschen, S., Runge, J., . . . Volkmann, J. (2019). Probabilistic mapping of the antidystonic effect of pallidal neurostimulation: a multicentre imaging study. *Brain*, *142*(5), 1386–1398. https://doi.org/10.1093/brain/awz046

Rizzo, G., Copetti, M., Arcuti, S., Martino, D., Fontana, A., & Logroscino, G. (2016). Accuracy of clinical diagnosis of Parkinson disease: A systematic review and meta-analysis. *Neurology*, *86*(6), 566–576. https://doi.org/10.1212/WNL.0000000000002350

Rossi, C., Frosini, D., Volterrani, D., De Feo, P., Unti, E., Nicoletti, V., . . . Ceravolo, R. (2010). Differences in nigro-striatal impairment in clinical variants of early Parkinson's disease: evidence from a FP-CIT SPECT study. *Eur J Neurol*, *17*(4), 626–630. https://doi.org/10.1111/j.1468-1331.2009.02898.x

Rossi, P. J., Gunduz, A., & Okun, M. S. (2015). The Subthalamic Nucleus, Limbic Function, and Impulse Control. *Neuropsychol Rev*, *25*(4), 398–410. https://doi.org/10.1007/s11065-015-9306-9

Ruge, D., Cif, L., Limousin, P., Gonzalez, V., Vasques, X., Coubes, P., & Rothwell, J. C. (2014). Longterm deep brain stimulation withdrawal: clinical stability despite electrophysiological instability. *J Neurol Sci*, *342*(1–2), 197–199. https://doi.org/10.1016/j.jns.2014.05.011

Ruge, D., Cif, L., Limousin, P., Gonzalez, V., Vasques, X., Hariz, M. I., . . . Rothwell, J. C. (2011). Shaping reversibility? Long-term deep brain stimulation in dystonia: the relationship between effects on electrophysiology and clinical symptoms. *Brain*, *134*(Pt 7), 2106–2115. https://doi.org/10.1093/brain/awr122

Saari, L., Kivinen, K., Gardberg, M., Joutsa, J., Noponen, T., & Kaasinen, V. (2017). Dopamine transporter imaging does not predict the number of nigral neurons in Parkinson disease. *Neurology*, *88*(15), 1461–1467. https://doi.org/10.1212/WNL.0000000000003810

Schapira, A. H. V., Chaudhuri, K. R., & Jenner, P. (2017). Non-motor features of Parkinson disease. *Nat Rev Neurosci*, *18*(8), 509. https://doi.org/10.1038/nrn.2017.91

Schmitz-Steinkrüger, H., Lange, C., Apostolova, I., Mathies, F. L., Frings, L., Klutmann, S., . . . Buchert, R. (2020). Impact of age and sex correction on the diagnostic performance of dopamine transporter SPECT. *Eur J Nucl Med Mol Imaging*. https://doi.org/10.1007/s00259-020-05085-2

Sharma, N. (2019). Neuropathology of Dystonia. *Tremor Other Hyperkinet Mov (N Y)*, *9*, 569. https://doi.org/10.7916/d8-j6sx-b156

Shen, L., Jiang, C., Hubbard, C. S., Ren, J., He, C., Wang, D., . . . Li, L. (2020). Subthalamic Nucleus Deep Brain Stimulation Modulates 2 Distinct Neurocircuits. *Ann Neurol*, *88*(6), 1178–1193. https://doi.org/10.1002/ana.25906

Shibasaki, H. (2012). Cortical activities associated with voluntary movements and involuntary movements. *Clin Neurophysiol*, *123*(2), 229–243. https://doi.org/10.1016/j.clinph.2011.07.042

Shimony, J. S., Rutlin, J., Karimi, M., Tian, L., Snyder, A. Z., Loftin, S. K., . . . Perlmutter, J. S. (2018). Validation of diffusion tensor imaging measures of nigrostriatal neurons in macaques. *PLoS One*, *13*(9), e0202201. https://doi.org/10.1371/journal.pone.0202201

Shin, H. W., Cho, H. J., Lee, S. W., Shitara, H., & Hallett, M. (2021). Sensory tricks in cervical dystonia correlate with enhanced brain activity during motor preparation. *Parkinsonism Relat Disord*, *84*, 135–138. https://doi.org/10.1016/j.parkreldis.2021.02.005

Snow, B. J., Tooyama, I., McGeer, E. G., Yamada, T., Calne, D. B., Takahashi, H., & Kimura, H. (1993). Human positron emission tomographic [18F]fluorodopa studies correlate with dopamine cell counts and levels. *Ann Neurol*, *34*(3), 324–330. https://doi.org/10.1002/ana.410340304

Soland, V. L., Bhatia, K. P., & Marsden, C. D. (1996). Sex prevalence of focal dystonias. *J Neurol Neurosurg Psychiatry*, *60*(2), 204–205. https://doi.org/10.1136/jnnp.60.2.204

Speranza, L., di Porzio, U., Viggiano, D., de Donato, A., & Volpicelli, F. (2021). Dopamine: The Neuromodulator of Long-Term Synaptic Plasticity, Reward and Movement Control. *Cells*, *10*(4). https://doi.org/10.3390/cells10040735

Starr, P. A., Rau, G. M., Davis, V., Marks, W. J., Ostrem, J. L., Simmons, D., . . . Turner, R. S. (2005). Spontaneous pallidal neuronal activity in human dystonia: comparison with Parkinson's disease and normal macaque. *J Neurophysiol*, *93*(6), 3165–3176. https://doi.org/10.1152/jn.00971.2004

Steeves, T. D., Day, L., Dykeman, J., Jette, N., & Pringsheim, T. (2012). The prevalence of primary dystonia: a systematic review and meta-analysis. *Mov Disord*, *27*(14), 1789–1796. https://doi.org/10.1002/mds.25244

Stoker, T. B., & Greenland, J. C. (2018). Parkinson's Disease: Pathogenesis and Clinical Aspects. In. https://doi.org/NBK536715

Strafella, A. P., Bohnen, N. I., Perlmutter, J. S., Eidelberg, D., Pavese, N., Van Eimeren, T., . . . Group, I.-N. S. (2017). Molecular imaging to track Parkinson's disease and atypical parkinsonisms: New imaging frontiers. *Mov Disord*, *32*(2), 181–192. https://doi.org/10.1002/mds.26907

Strafella, A. P., Sadikot, A. F., & Dagher, A. (2003). Subthalamic deep brain stimulation does not induce striatal dopamine release in Parkinson's disease. *Neuroreport*, *14*(9), 1287–1289. https://doi.org/10.1097/00001756-200307010-00020

Strange, P. G. (1993). Dopamine receptors in the basal ganglia: relevance to Parkinson's disease. *Mov Disord*, *8*(3), 263–270. https://doi.org/10.1002/mds.870080303

Tagliaferro, P., & Burke, R. E. (2016). Retrograde Axonal Degeneration in Parkinson Disease. *J Parkinsons Dis*, *6*(1), 1–15. https://doi.org/10.3233/JPD-150769

Thobois, S., Ballanger, B., Xie-Brustolin, J., Damier, P., Durif, F., Azulay, J. P., . . . Broussolle, E. (2008). Globus pallidus stimulation reduces frontal hyperactivity in tardive dystonia. *J Cereb Blood Flow Metab*, *28*(6), 1127–1138. https://doi.org/10.1038/sj.jcbfm.9600610

Tian, L., Karimi, M., Brown, C. A., Loftin, S. K., & Perlmutter, J. S. (2014). In vivo measures of nigrostriatal neuronal response to unilateral MPTP treatment. *Brain Res*, *1571*, 49–60. https://doi.org/10.1016/j.brainres.2014.05.009

Tolosa, E., Coelho, M., & Gallardo, M. (2003). DAT imaging in drug-induced and psychogenic parkinsonism. *Mov Disord*, *18 Suppl 7*, S28–33. https://doi.org/10.1002/mds.10575

Trost, M., Carbon, M., Edwards, C., Ma, Y., Raymond, D., Mentis, M. J., . . . Eidelberg, D. (2002). Primary dystonia: is abnormal functional brain architecture linked to genotype? *Ann Neurol*, *52*(6), 853–856. https://doi.org/10.1002/ana.10418

Trost, M., Su, S., Su, P., Yen, R. F., Tseng, H. M., Barnes, A., . . . Eidelberg, D. (2006). Network modulation by the subthalamic nucleus in the treatment of Parkinson's disease. *Neuroimage*, *31*(1), 301–307. https://doi.org/10.1016/j.neuroimage.2005.12.024

Tsuboi, T., Wong, J. K., Almeida, L., Hess, C. W., Wagle Shukla, A., Foote, K. D., . . . Ramirez-Zamora, A. (2020). A pooled meta-analysis of GPi and STN deep brain stimulation outcomes for cervical dystonia. *J Neurol*, *267*(5), 1278–1290. https://doi.org/10.1007/s00415-020-09703-9

Varrone, A., Dickson, J. C., Tossici-Bolt, L., Sera, T., Asenbaum, S., Booij, J., . . . Tatsch, K. (2013). European multicentre database of healthy controls for [123I]FP-CIT SPECT (ENC-DAT): age-related effects, gender differences and evaluation of different methods of analysis. *Eur J Nucl Med Mol Imaging*, *40*(2), 213–227. https://doi.org/10.1007/s00259-012-2276-8

Vaughan, R. A., & Foster, J. D. (2013). Mechanisms of dopamine transporter regulation in normal and disease states. *Trends Pharmacol Sci*, *34*(9), 489–496. https://doi.org/10.1016/j.tips.2013.07.005

Vedam-Mai, V., Deisseroth, K., Giordano, J., Lazaro-Munoz, G., Chiong, W., Suthana, N., . . . Okun, M. S. (2021). Proceedings of the Eighth Annual Deep Brain Stimulation Think Tank: Advances in Optogenetics, Ethical Issues Affecting DBS Research, Neuromodulatory Approaches for Depression, Adaptive Neurostimulation, and Emerging DBS Technologies. *Front Hum Neurosci*, *15*, 644593. https://doi.org/10.3389/fnhum.2021.644593

Vidailhet, M., Vercueil, L., Houeto, J. L., Krystkowiak, P., Benabid, A. L., Cornu, P., . . . Group, F. S. d. P. I. d. l. D. S. S. (2005). Bilateral deep-brain stimulation of the globus pallidus in primary generalized dystonia. *N Engl J Med*, *352*(5), 459–467. https://doi.org/10.1056/NEJMoa042187

von Campenhausen, S., Bornschein, B., Wick, R., Bötzel, K., Sampaio, C., Poewe, W., . . . Dodel, R. (2005). Prevalence and incidence of Parkinson's disease in Europe. *Eur Neuropsychopharmacol*, *15*(4), 473–490. https://doi.org/10.1016/j.euroneuro.2005.04.007

Waln, O., Wu, Y., Perlman, R., Wendt, J., Van, A. K., & Jankovic, J. (2015). Dopamine transporter imaging in essential tremor with and without parkinsonian features. *J Neural Transm (Vienna)*, *122*(11), 1515–1521. https://doi.org/10.1007/s00702-015-1419-z

Wang, J., Ma, Y., Huang, Z., Sun, B., Guan, Y., & Zuo, C. (2010). Modulation of metabolic brain function by bilateral subthalamic nucleus stimulation in the treatment of Parkinson's disease. *J Neurol*, *257*(1), 72–78. https://doi.org/10.1007/s00415-009-5267-3

Werner, R. A., Lapa, C., Sheikhbahaei, S., Marcus, C., Solnes, L. B., Du, Y., . . . Javadi, M. S. (2019). Impact of aging on semiquantitative uptake parameters in normal rated clinical baseline [123I]Ioflupane single photon emission computed tomography/computed tomography. *Nucl Med Commun*, *40*(10), 1001–1004. https://doi.org/10.1097/MNM.0000000000001061

Wielepp, J. P., Burgunder, J. M., Pohle, T., Ritter, E. P., Kinser, J. A., & Krauss, J. K. (2001). Deactivation of thalamocortical activity is responsible for suppression of parkinsonian tremor by thalamic stimulation: a 99mTc-ECD SPECT study. *Clin Neurol Neurosurg*, *103*(4), 228–231. https://doi.org/10.1016/s0303-8467(01)00165-2

Wisidagama, S., Selladurai, A., Wu, P., Isetta, M., & Serra-Mestres, J. (2021). Recognition and Management of Antipsychotic-Induced Parkinsonism in Older Adults: A Narrative Review. *Medicines (Basel)*, *8*(6). https://doi.org/10.3390/medicines8060024

Wong, J. K., Cauraugh, J. H., Ho, K. W. D., Broderick, M., Ramirez-Zamora, A., Almeida, L., . . . Okun, M. S. (2019). STN vs. GPi deep brain stimulation for tremor suppression in Parkinson disease: A systematic review and meta-analysis. *Parkinsonism Relat Disord*, *58*, 56–62. https://doi.org/10.1016/j.parkreldis.2018.08.017

Wu, Y. S., Ni, L. H., Fan, R. M., & Yao, M. Y. (2019). Meta-Regression Analysis of the Long-Term Effects of Pallidal and Subthalamic Deep Brain Stimulation for the Treatment of Isolated Dystonia. *World Neurosurg*, *129*, e409–e416. https://doi.org/10.1016/j.wneu.2019.05.165

Yianni, J., Bradley, K., Soper, N., O'Sullivan, V., Nandi, D., Gregory, R., . . . Aziz, T. (2005). Effect of GPi DBS on functional imaging of the brain in dystonia. *J Clin Neurosci*, *12*(2), 137–141. https://doi.org/10.1016/j.jocn.2004.05.010

Yokoyama, K., Imabayashi, E., Sumida, K., Sone, D., Kimura, Y., Sato, N., . . . Matsuda, H. (2017). Computed-tomography-guided anatomic standardization for quantitative assessment of dopamine transporter SPECT. *Eur J Nucl Med Mol Imaging*, *44*(3), 366–372. https://doi.org/10.1007/s00259-016-3496-0

Zoons, E., Booij, J., Nederveen, A. J., Dijk, J. M., & Tijssen, M. A. (2011). Structural, functional and molecular imaging of the brain in primary focal dystonia--a review. *Neuroimage*, *56*(3), 1011–1020. https://doi.org/10.1016/j.neuroimage.2011.02.045

TURUN
YLIOPISTO
UNIVERSITY
OF TURKU

Painosalama, Turku, Finland 2022

ISBN 978-951-29-8777-1 (PRINT)
ISBN 978-951-29-8778-8 (PDF)
ISSN 0355-9483 (Print)
ISSN 2343-3213 (Online)